Principles of HEAT TRANSFER

third edition

Frank Kreith
University of Colorado

INTEXT EDUCATIONAL PUBLISHERS
New York and London

Library of Congress Cataloging in Publication Data

Kreith, Frank.
Principles of heat transfer.

(Series in mechanical engineering)
Includes bibliographical references.
1. Heat—Transmission. I. Title.
QC320.K7 1973 536'.2 73-1784
ISBN 0-7002-2422-X

Intext Educational Publishers
257 Park Avenue South
New York, New York 10010

Contents

Preface to the third edition ix

Preface to the second edition xi

Preface to the first edition xiii

1 *Introduction* 1

1-1. The relation of heat transfer to thermodynamics 1
1-2. Modes of heat flow 4
1-3. Basic laws of heat transfer 7
1-4. Combined heat-transfer mechanisms 14
1-5. Analogy between heat flow and electrical flow 18
1-6. Units and dimensions 20

Problems—23

2 *Steady one-dimensional heat conduction* 29

2-1. Walls of simple geometrical configuration 29
2-2. Composite structures 37
2-3. Systems with heat sources* 46

*Sections marked with an asterisk can be omitted in an undergraduate course without interrupting the continuity of the presentation.

2-4. Heat transfer from extended surfaces 56

Problems—67 References—79

3 Two- and three-dimensional steady-state conduction *81*

3-1. Methods of analysis 81
3-2. Derivation of the heat-conduction equation 82
3-3. Analytical solution* 85
3-4. Graphical method 90
3-5. Analogical method* 95
3-6. Numerical method* 97
3-7. Closure 126

Problems—126 References—137

4 Conduction of heat in the unsteady state *139*

4-1. Transient and periodic heat flow 139
4-2. Transient heat flow in systems with neglible internal resistance. 140
4-3. Periodic heat flow in systems with neglible internal resistance* 148
4-4. Transient heat flow in an infinite plate* 154
4-5. Charts for transient heat conduction. 165
4-6. Numerical method 182

Problems—208 References—216

5 Heat transfer by radiation *219*

5-1. Thermal radiation 219
5-2. Blackbody radiation 220
5-3. Radiation properties 231
5-4. The radiation shape factor. 243
5-5. Radiation in enclosures with black surfaces 251
5-6. Radiation in enclosures with gray surfaces 255
5-7. Radiation in gas-filled enclosures. 271
5-8. Radiation properties of gases and vapors 273
5-9. Radiation combined with convection and conduction . . . 281
5-10. Solar radiation 286

Problems—294 References—306

6 *Fundamentals of convection* 309

6-1. The convective-heat-transfer coefficient 309
6-2. Energy transport mechanism and fluid flow 310
6-3. Boundary-layer fundamentals 311
6-4. The Nusselt modulus 315
6-5. Evaluation of convection heat-transfer coefficients 318
6-6. Dimensional analysis 320
6-7. Laminar boundary layer on a flat plate* 327
6-8. Approximate boundary-layer analysis 343
6-9. Analogy between heat and momentum transfer in turbulent flow 352
6-10. Reynolds analogy for turbulent flow over a flat plate 358
6-11. Turbulent flow over plane surfaces 360
6-12. Heat transfer in high-speed flow 365
6-13. Closure 370

Problems—372 References—381

7 *Free convection* 383

7-1. Introduction 383
7-2. Similarity parameters for free convection 385
7-3. Evaluation of unit-surface conductance 395
7-4. Convection from rotating cylinders, disks, and spheres* . . 403
7-5. Combined forced and free convection* 405

Problems—407 References—411

8 *Forced convection inside tubes and ducts* 415

8-1. Introduction 415
8-2. Analogy between heat and momentum transfer 425
8-3. Heat-transfer coefficients for turbulent flow 431
8-4. Forced convection in laminar flow 438
8-5. Forced convection in transition flow 445
8-6. Closure 445

Problems—447 References—454

9 *Forced convection over exterior surfaces* 457

9-1. Flow over bluff bodies 457
9-2. Cylinder and sphere in crossflow 459
9-3. Tube bundles in crossflow 473

9-4. Application to heat-exchanger design 483
9-5. Summary 487

Problems—488 References—491

10 Heat transfer with change in phase *495*

10-1. Fundamentals of boiling heat transfer 495
10-2. Correlation of boiling-heat-transfer data 501
10-3. Heat transfer in condensation 524
10-4. Freezing and melting* 534

Problems—539 References—542

11 Heat exchangers *547*

11-1. Design and selection 547
11-2. Basic types of heat exchangers 548
11-3. Mean temperature difference 553
11-4. Heat-exchanger effectiveness 562
11-5. Fouling factors 571
11-6. Analysis for variable heat-transfer coefficient 573
11-7. Closure 575

Problems—576 References—585

*12 Mass transfer** *587*

12-1. Introduction 587
12-2. Mass transfer by molecular diffusion 588
12-3. Mass transfer by convection 594
12-4. Evaluation of mass-transfer coefficients 596
12-5. Interphase mass transfer 600
12-6. Simultaneous heat and mass transfer 605
12-7. Mass-transfer equipment 615

Problems—619 References—620

Appendix I. Nomenclature *621*

Appendix II. Units, dimensions, and conversion factors *627*

Appendix III. Tables *633*

Index *647*

6
Fundamentals of convection

6-1. The convective-heat-transfer coefficient

In the preceding chapters, attention has been focused on heat transfer by conduction and radiation. In an effort to simplify the work and to emphasize the methods for calculating heat transfer by conduction and radiation, an effort has been made to eliminate, as much as possible, problems related to heat transfer by convection. However, from the illustrative examples it has probably become apparent already that there are hardly any practical problems which can be solved without a knowledge of the mechanisms by which heat is transferred between the surface of a solid conductor and the surrounding medium. In our work so far we simply specified the unit convective surface conductance at the solid fluid interface and did not investigate the details of the transfer mechanism. We evaluated the rate of heat transfer by convection between a solid boundary and a fluid by means of the equation

$$q_{\text{surface to fluid}} = A\,\bar{h}_c(T_s - T_\infty) \tag{1-13}$$

The convection equation in this form seems quite simple. The simplicity is misleading, however, because Eq. 1-13 is a definition of the average unit thermal convective conductance $\bar{h}_c$ rather than a law of heat transfer by convection. The convective-heat-transfer coefficient is actually a complicated function of the fluid flow, the thermal properties of the fluid

medium, and the geometry of the system. Its numerical value is in general not uniform over a surface, and depends also on the location where the fluid temperature T_∞ is measured.

Although Eq. 1-13 is generally used to determine the rate of heat flow by convection between a surface and the fluid in contact with it, this relation is inadequate to explain the convective heat-flow mechanism. A meaningful analysis which will eventually lead to a quantitative evaluation of the convective heat-transfer coefficient must start with a study of the dynamics of the fluid flow. In this and the following chapters we shall follow this line of approach and investigate the influence of flow conditions, fluid properties, and boundary shapes on the convective-heat-transfer coefficient.

6-2. *Energy transport mechanism and fluid flow*

The transfer of heat between a solid boundary and a fluid takes place by a combination of conduction and mass transport. If the boundary is at a higher temperature than the fluid, heat flows first by conduction from the solid to fluid particles in the neighborhood of the wall. The energy thus transmitted increases the internal energy of the fluid and is carried away by the motion of the fluid. When the heated fluid particles reach a region at a lower temperature, heat is again transferred by conduction from warmer to cooler fluid.

Since the convective mode of energy transfer is so closely linked to the fluid motion, it is necessary to know something about the mechanism of fluid flow before the mechanism of heat flow can be investigated. One of the most important aspects of the hydrodynamic analysis is to establish whether the motion of the fluid is *laminar* or *turbulent*.

In laminar, or streamline, flow, the fluid moves in layers, each fluid particle following a smooth and continuous path. The fluid particles in each layer remain in an orderly sequence without passing one another. Soldiers on parade provide a somewhat crude analogy to laminar flow. They march along well-defined lines, one behind the other, and maintain their order even when they turn a corner or pass an obstacle.

In contrast to the orderly motion of laminar flow, the motion of fluid particles in turbulent flow rather resembles a crowd of commuters in a railroad station during the rush hour. The general trend of the motion is from the gate toward the train, but superimposed upon this motion are the deviations of individuals according to their instantaneous direction and their ability to pass the less agile members of the crowd. Yet if one could obtain a statistical average of the motion of a large number of individuals, it would be steady and regular. The same applies to fluid particles in turbulent flow. The path of any individual particle is zigzag and

irregular, but on a statistical basis the overall motion of the aggregate of fluid particles is regular and predictable.

When a fluid flows in laminar motion along a surface at a temperature different from that of the fluid, heat is transferred only by molecular conduction within the fluid as well as at the interface between the fluid and the surface. There exist no turbulent mixing currents or eddies by which energy stored in fluid particles is transported across streamlines. Heat is transferred between fluid layers by molecular motion on a submicroscopic scale.

In turbulent flow, on the other hand, the conduction mechanism is modified and aided by innumerable eddies which carry lumps of fluid across the streamlines. These fluid particles act as carriers of energy and transfer energy by mixing with other particles of the fluid. An increase in the rate of mixing (or turbulence) will therefore also increase the rate of heat flow by convection.

The fluid motion can be induced by two processes. The fluid may be set in motion as a result of density differences due to a temperature variation in the fluid. This mechanism is called *free*, or *natural, convection.* The motion observed when a pot of water is heated on a stove or the motion of air in the desert on a calm day after sunset are examples of free convection. When the motion is caused by some external energy, such as a pump or a blower, we speak of *forced convection.* The cooling of an automobile radiator by the air blown over it by the fan is an example of forced convection. (The term *radiator* is obviously poorly chosen because the heat flow is *not* primarily by radiation; *convector* would be a more appropriate term.)

6-3. Boundary-layer fundamentals

When a fluid flows along a surface, irrespective of whether the flow is laminar or turbulent, the particles in the vicinity of the surface are slowed down by virtue of viscous forces. The fluid particles adjacent to the surface stick to it and have zero velocity relative to the boundary.[1] Other fluid particles attempting to slide over them are retarded as a result of an interaction between faster- and slower-moving fluid, a phenomenon which gives rise to shearing forces. In laminar flow the interaction, called viscous shear, takes place between molecules on a submicroscopic scale. In turbulent flow an interaction between lumps of fluid on a macroscopic scale, called turbulent shear, is superimposed on the viscous shear.

---

[1] This is strictly true only when the mean free path of the molecules is small compared to the boundary-layer thickness. In rarefied gases the molecules may slide or slip along a surface.

The effects of the viscous forces originating at the boundary extend into the body of the fluid, but a short distance from the surface the velocity of the fluid particles approaches that of the undisturbed free stream. The fluid contained in the region of substantial velocity change is called the *hydrodynamic boundary layer*. The thickness of the boundary layer has been defined as the distance from the surface at which the local velocity reaches 99 percent of the external velocity u_∞.

The concept of a boundary layer was introduced by the German scientist, Prandtl, in 1904. The boundary layer essentially divides the flow field around a body into two domains: a thin layer covering the surface of the body where the velocity gradient is great and the viscous forces are large, and a region outside this layer where the velocity is nearly equal to the free-stream value and the effects of viscosity are negligible. By means of the boundary-layer concept, the equations of motion, usually called the Navier-Stokes equations, can be reduced to a form in which they can be solved; the effects of viscosity on the flow can be determined; and the frictional drag along a surface can be calculated. The boundary-layer concept is also of great importance, as we shall see, to an understanding of convective heat transfer.

The shape of the velocity profile within the boundary layer depends on the nature of the flow. Consider, for example, the flow of air over a flat plate, placed with its surface parallel to the stream. At the leading edge of the plate ($x = 0$ in Fig. 6-1), only the fluid particles in immediate contact with the surface are slowed down, while the remaining fluid continues at the velocity of the undisturbed free stream in front of the plate. As the fluid proceeds along the plate, the shearing forces cause more and more of the fluid to be retarded, and the thickness of the boundary layer increases. The growth of the boundary layer and typical velocity profiles at various stations along the plate are shown in Fig. 6-1.

The velocity profiles near the leading edge are representative of laminar boundary layers. However, the flow within the boundary layer remains laminar only for a certain distance from the leading edge and then

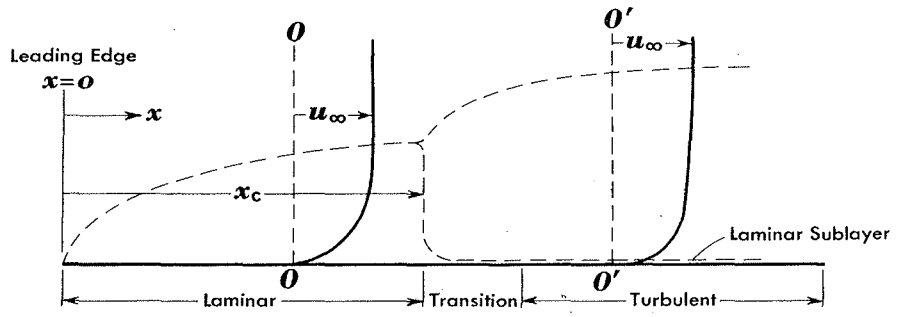

Fig. 6-1. Velocity profiles for laminar and turbulent boundary layers in flow over a field plate. (Vertical scale enlarged for clarity.)

becomes turbulent. We do not know enough about the mechanism of transition to predict precisely when the transition will occur, but the phenomenon leading to the growth of disturbances in a laminar boundary layer can be described (see Reference 1 for details). There are always small disturbances and waves in a flowing fluid, but as long as the viscous forces are large they will prevent disturbances from growing. As the laminar boundary layer thickens, the ratio of viscous forces to inertia forces decreases, and eventually a point is reached at which disturbances will no longer decay, but will grow with time. Then the boundary layer becomes unstable and the transition from laminar to turbulent flow begins. Eddies and vortexes form and destroy the laminar regularity of the boundary-layer motion. Quasi-laminar motion persists only in a thin layer in the immediate vicinity of the surface. This portion of a generally turbulent boundary layer is called the *laminar sublayer.* The region between the laminar sublayer and the completely turbulent portion of the boundary layer is called the *buffer layer.* The structure of the flow in a turbulent boundary layer is shown schematically on an enlarged scale in Fig. 6-2.

The distance from the leading edge at which the boundary layer becomes turbulent is called the *critical length* x_c (Fig. 6-1). This distance is usually specified in terms of a dimensionless quantity called the local critical Reynolds number $u_\infty \rho x_c/\mu$, which is an indication of the ratio of inertial to viscous forces at which disturbances begin to grow. Experimental results have shown that the point of transition depends on the surface contour, the surface roughness, the disturbance level, and even on the heat transfer. When the flow is calm and no disturbances occur, laminar flow can persist in the boundary layer at Reynolds numbers as high as 5×10^6. If the surface is rough, or disturbances are intentionally introduced into the flow, as for example by means of a grid, the flow may become turbulent at Reynolds numbers as low as 8×10^4. Under average conditions, the flow over a flat plate becomes turbulent at a distance from the leading edge x_c where the local Reynolds number $u\rho x_c/\mu$ is approximately equal to 5×10^5.

In view of the difference in the flow characteristics, the frictional

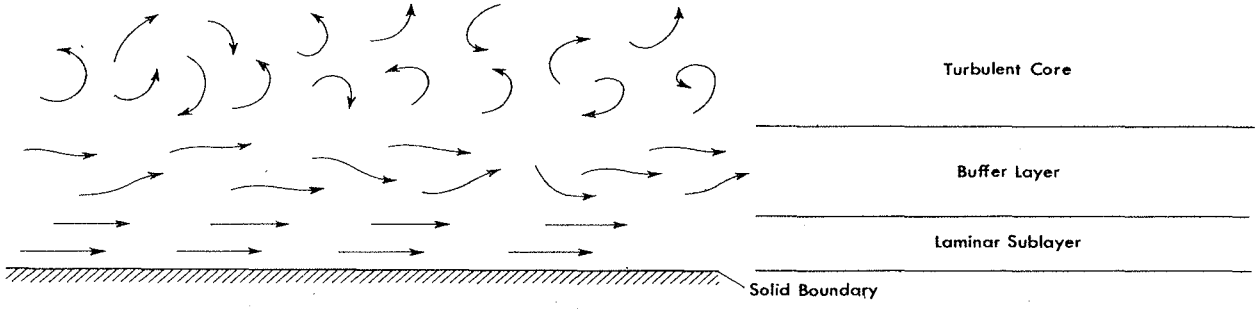

Fig. 6-2. Structure of a turbulent flow field near a solid boundary.

forces as well as the heat transfer are governed by different relations in laminar and turbulent boundary layers. Also the limiting conditions under which the flow will follow a given contour, and the boundary-layer theory can be applied, depends on whether the flow is laminar or turbulent.

Even when the contour of the surface over which the fluid flows is curved, the flow in the boundary layer is, at least qualitatively, similar to the flow in the boundary layer on a flat plate. The contour of the body becomes very important, however, in the determination of the point at which the boundary layer separates from the surface. The separation of flow occurs mainly because the kinetic energy of the fluid in the boundary layer is dissipated by viscosity within the layer. As long as the main stream is accelerating, the external pressure is decreasing along the direction of flow and the forces at the edge of the boundary layer oppose the retardation of the fluid by the wall shear. On the other hand, when the flow is decelerating, as for example in a low-speed diffuser, the external pressure as well as the shearing forces tend to decelerate the fluid. A local reversal of the flow in the boundary layer will then occur when the kinetic energy of the fluid in the boundary layer can no longer overcome the adverse pressure gradient. Near this point the boundary layer separates as shown in Fig. 6-3. Beyond the point of separation, the flow near

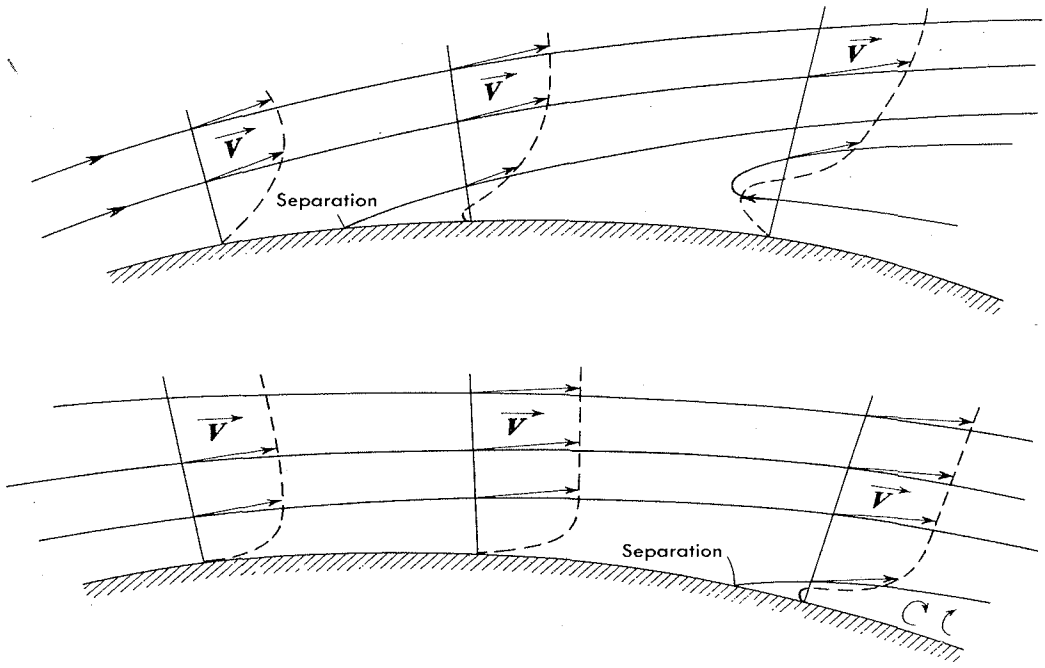

Fig. 6-3. Sketches illustrating separation of boundary layer. Top: streamlines and flow pattern near separation point of laminar boundary layer. Bottom: streamlines and flow pattern near separation point of turbulent boundary layer.

the surface consists of highly irregular eddies and vortexes and cannot be treated by boundary-layer theory.

A more advanced boundary-layer theory allows us to calculate the point at which the flow separates from the surface (1). Generally speaking, a turbulent boundary layer will not separate as easily as a laminar boundary layer because the kinetic energy of the fluid particles is larger in a turbulent layer. In flow over a streamlined object, separation takes place near the rear, if it occurs at all. In flow over bluff objects, on the other hand, separation occurs nearer to the front. The problem of separation is too complicated to be taken up in detail here, and the reader interested in additional information on this subject should consult References 1, 27, and 28 of the bibliography at the end of this chapter.

6-4. *The Nusselt modulus*

From the description of the mechanism of convective energy transport, we recall that both conduction and mass transport play a role. Since the thermal conductivity of fluids, except for liquid metals, is relatively small, the rapidity of the energy transfer depends largely on the mixing motion of the fluid particles.

When the fluid velocity and the turbulence are small, the transport of energy is not aided materially by mixing currents on a macroscopic scale. On the other hand, when the velocity is large and the mixing between warmer and colder fluid contributes substantially to the energy transfer, the conduction mechanism becomes less important. Consequently, to transfer heat by convection through a fluid at a given rate, a larger temperature gradient is required in a region of low velocity than in a region of high velocity.

Applying these qualitative observations to heat transfer from a solid wall to a fluid in turbulent flow, we can roughly sketch the temperature profile. In the immediate vicinity of the wall, heat can only flow by conduction because the fluid particles are stationary relative to the boundary. We naturally expect a large temperature drop in this layer. As we move further away from the wall, the movement of the fluid aids in the energy transport and the temperature gradient will be less steep, eventually, leveling out in the main stream. For air flowing turbulently over a flat plate, the temperature distribution shown in Fig. 6-4 illustrates these ideas qualitatively.

The foregoing discussion suggests a method for evaluating the rate of heat transfer between a solid wall and a fluid. Since at the interface (i.e., at $y = 0$) heat flows only by conduction, the rate of heat flow can be calculated from the equation

$$q_{\text{surface}\rightarrow\text{fluid}} = -k_f A \left.\frac{\partial T}{\partial y}\right|_{y=0} \tag{6-1}$$

This approach has indeed been used, but for engineering purposes the concept of the convective-heat-transfer coefficient is much more convenient. In order not to lose sight of the physical picture, we shall relate the heat-transfer coefficient defined by Eq. 1-13 to the temperature gradient at the wall. Equating Eqs. 6-1 and 1-13 we obtain

$$q_{\text{surface}\rightarrow\text{fluid}} = -k_f A \left.\frac{\partial T}{\partial y}\right|_{y=0} = \bar{h}_c A (T_s - T_\infty) \tag{6-2}$$

Since the magnitude of the temperature gradient in the fluid will be the same regardless of the reference temperature, we can write $\partial T = \partial (T - T_s)$. Introducing a significant length dimension of the system L to specify the geometry of the object from which heat flows, we can write Eq. 6-2 in dimensionless form as

$$\frac{\bar{h}_c L}{k_f} = \frac{-\left.\dfrac{\partial T}{\partial y}\right|_{y=0}}{\dfrac{T_s - T_\infty}{L}} = \left.\frac{\partial\left(\dfrac{T_s - T}{T_s - T_\infty}\right)}{\partial\left(\dfrac{y}{L}\right)}\right|_{y=0} \tag{6-3}$$

The combination of the convective heat-transfer coefficient $\bar{h}_c$, the significant length L, and the thermal conductivity of the fluid k_f in the form $\bar{h}_c L/k_f$ is called the Nusselt modulus, or *Nusselt number*, $\overline{\text{Nu}}$. The Nusselt number is a dimensionless quantity.

Inspection of Eq. 6-3 shows that the Nusselt number could be in-

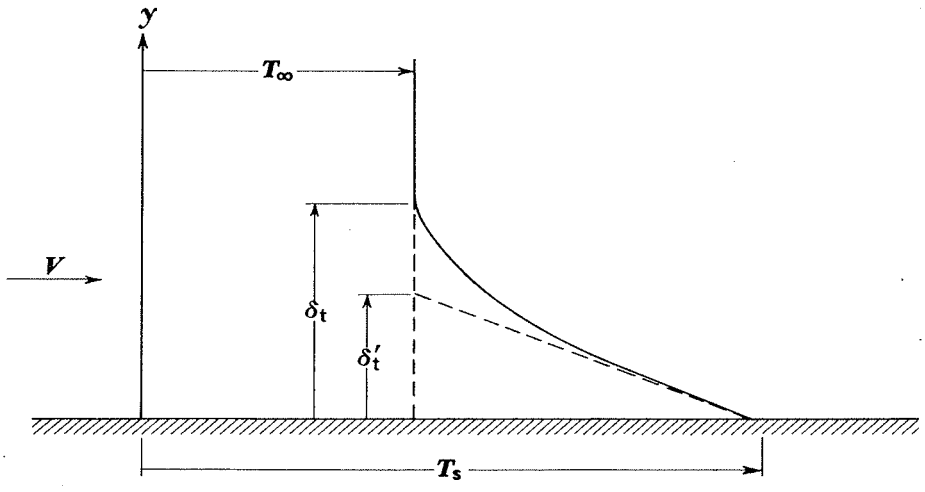

Fig. 6-4. Temperature distribution in a turbulent boundary layer for a fluid flowing over a heated plate.

terpreted physically as the ratio of the temperature gradient in the fluid immediately in contact with the surface to a reference temperature gradient $(T_s - T_\infty)/L$. In practice the Nusselt number is a convenient measure of the convective heat-transfer coefficient because, once its value is known, the convective heat-transfer coefficient can be calculated from the relation

$$\bar{h}_c = \overline{\mathrm{Nu}} \frac{k_f}{L} \tag{6-4}$$

We observe that, for a given value of the Nusselt number, the convective heat-transfer coefficient is directly proportional to the thermal conductivity of the fluid but inversely proportional to the significant length dimension describing the system.

The temperature distribution for a fluid flowing past a hot wall, as sketched by the solid line in Fig. 6-4, shows that the temperature gradient in the fluid is confined to a relatively thin layer, δ_t, in the vicinity of the surface. We shall now simplify the true picture by replacing the actual temperature distribution by the dashed straight line shown in Fig. 6-4. The dashed line is tangent to the actual temperature curve at the wall and physically represents the temperature distribution in a hypothetical layer of fluid of thickness δ_t' which, if completely stagnant, offers the same thermal resistance to the flow of heat as the actual boundary layer. In this stagnant layer, heat can flow only by conduction and the rate of heat transfer per unit area is

$$\frac{q}{A} = k_f \frac{T_s - T_\infty}{\delta_t'} = \bar{h}_c (T_s - T_\infty) \tag{6-5}$$

An inspection of Eq. 6-5 shows that $\bar{h}_c$ may be expressed as

$$\bar{h}_c = \frac{k_f}{\delta_t'} \tag{6-6}$$

and the Nusselt number as

$$\overline{\mathrm{Nu}} = \bar{h}_c \frac{L}{k_f} = \frac{L}{\delta_t'} \tag{6-7}$$

While this picture is considerably oversimplified, it does illustrate the fact that the thinner the boundary layer δ_t', the larger will be the convective conductance. To transfer large quantities of heat rapidly, one attempts to reduce the boundary-layer thickness as much as possible. This can be accomplished by increasing the velocity and/or the turbulence of the fluid. If insulation of the surface is the desired aim, a thick

stagnant layer is beneficial. In fact, most commercial insulating materials simply trap air in small spaces to eliminate its mixing motion while at the same time taking advantage of its low thermal conductivity to reduce the transfer of heat.

6-5. *Evaluation of convection heat-transfer coefficients*

There are four general methods available for the evaluation of convection heat-transfer coefficients:

1. Dimensional analysis combined with experiments.
2. Exact mathematical solutions of the boundary-layer equations.
3. Approximate analyses of the boundary layer by integral methods.
4. The analogy between heat, mass, and momentum transfer.

All four of these techniques have contributed to our understanding of convective heat-transfer. Yet, no single method can solve all the problems because each one has limitations which restrict its scope of application.

Dimensional analysis is mathematically simple and has found a wide range of application. The chief limitation of this method is that results obtained by it are incomplete and quite useless without experimental data. It contributes little to our understanding of the transfer process, but facilitates the interpretation and extends the range of application of experimental data by correlating them in terms of dimensionless groups.

There are two different methods for determining dimensionless groups suitable to correlate experimental data. The first of these methods, discussed in the following section, requires only the listing of the variables pertinent to a phenomenon. This technique is simple to use, but if a pertinent variable is omitted, erroneous results ensue. In the second method the dimensionless groups and similarity conditions are deduced from the differential equations describing the phenomenon. This method is preferable when the phenomena can be described mathematically, but the solution of the resulting equations is too involved to be practical. An illustration of this technique is presented in Sec. 7-2.

Exact mathematical analyses require the simultaneous solution of the equations describing the fluid motion and the transfer of energy in the moving fluid. The method presupposes that the physical mechanisms are sufficiently well understood to be described in mathematical language. This preliminary requirement limits the scope of exact solutions because complete mathematical equations describing the fluid flow and the heat-transfer mechanisms can be written only for laminar flow. Even for laminar flow the equations are quite complicated, but solutions have been

obtained for a number of simple systems such as flow over a flat plate or a circular cylinder.

Exact solutions are important because the assumptions made in the course of the analysis can be specified accurately and their validity can be checked by experiment. They also serve as a basis of comparison and as a check on simpler, but approximate methods. Furthermore, the development of electronic computers has increased the range of problems amenable to mathematical solution, and results of computations for different systems are continually being published in the literature.

The details of the mathematical solution are quite complicated. They are, however, not essential to a correct application of the results. We shall here only derive the boundary-layer equations to introduce the fundamental concepts, indicate how they can be solved, and finally illustrate the application of the results for the simple case of flow over a flat plate. For details regarding the methods of solution of the boundary-layer equations in geometrically more complex systems, the reader is referred to the translation of Schlichting's treatise on boundary-layer theory (1).

The approximate analysis of the boundary layer avoids the detailed mathematical description of the flow in the boundary layer. Instead, a plausible but simple equation is used to describe the velocity and temperature distributions in the boundary layer. The problem is then analyzed on a macroscopic basis by applying the equation of motion and the energy equation to the aggregate of the fluid particles contained within the boundary layer. This method is relatively simple; moreover, it yields solutions to problems which can not be treated by an exact mathematical analysis. In those instances where other solutions are available, they agree within engineering accuracy with the solutions obtained by this approximate method. The technique is not limited to laminar flow, but can also be applied to turbulent flow.

The analogy between heat, mass, and momentum transfer is a useful tool for analyzing turbulent transfer processes. Our knowledge of turbulent-exchange mechanisms is insufficient to write mathematical equations describing the temperature distribution directly, but the transfer mechanism can be described in terms of a simplified model. According to one such model which has been widely accepted, a mixing motion in a direction perpendicular to the mean flow accounts for the transfer of momentum as well as energy. The mixing motion can be described on a statistical basis by a method similar to that used to picture the motion of gas molecules in the kinetic theory. There is by no means general agreement that this model corresponds to conditions actually existing in nature, but for practical purposes its use can be justified by the fact that experimental results are substantially in agreement with analytical predictions based on the hypothetical model.

6-6. Dimensional analysis

Dimensional analysis differs from other methods of approach in that it does not yield equations which can be solved. Instead, it combines several variables into dimensionless groups, such as the Nusselt number, which facilitate the interpretation and extend the range of application of experimental data. In practice, convective heat-transfer coefficients are generally calculated from empirical equations obtained by correlating experimental data with the aid of dimensional analysis.

The most serious limitation of dimensional analysis is that it gives no information about the nature of a phenomenon. In fact, to apply dimensional analysis it is necessary to know beforehand what variables influence the phenomenon, and the success or failure of the method depends on the proper selection of these variables. It is therefore important to have at least a preliminary theory or a thorough physical understanding of a phenomenon before a dimensional analysis can be performed. However, once the pertinent variables are known, dimensional analysis can be applied to most problems by a routine procedure which is outlined below.[2]

Primary dimensions and dimensional formulas. The first step is to select a system of primary dimensions. The choice of the primary dimensions is arbitrary, but the dimensional formulas of all pertinent variables must be expressible in terms of them. We shall use the primary dimensions of length L, time θ, temperature T, and mass M.

The dimensional formula of a physical quantity follows from definitions or physical laws. For instance, the dimensional formula for the length of a bar is $[L]$ by definition.[3] The average velocity of a fluid particle is equal to a distance divided by the time interval taken to traverse it. The dimensional formula of velocity is therefore $[L/\theta]$, or $[L\theta^{-1}]$, i.e., a distance or length divided by a time. The units of velocity could be expressed in feet per second, miles per hour, or knots, since they all are a length divided by a time.

The dimensional formulas and the symbols of physical quantities occurring frequently in heat-transfer problems are given in Table 6-1. The primary dimensions in the $ML\theta T$ column of Table 6-1 avoid the use of dimensional constants such as g_c or J. This standardizes the method, but conversion factors may have to be inserted in the final results (i.e., the dimensionless quantities) to comply with the system of units used (see Appendix II for conversion factors). For convenience the dimensional

---

[2]The algebraic theory of dimensional analysis will not be developed here. For a rigorous and comprehensive treatment of the mathematical background, Chapters 3 and 4 of Reference 2 are recommended.

[3]A square bracket [ ] denotes that the quantity has the dimensional formula stated within the bracket.

Table 6-1. Some physical quantities with associated symbols, dimensions, and units.

Quantity	Symbol	Dimensions		Units in the Engineering System
		$ML\theta T$ System	$ML\theta TFQ$ System	
Length	L, x	L	L	ft
Time	θ	θ	θ	sec or hr
Mass	M	M	M	lb_m
Force	F	ML/θ^2	F	lb_f
Temperature	T	T	T	F
Heat	Q	ML^2/θ^2	Q	Btu
Velocity	V	L/θ	L/θ	ft/sec
Acceleration	a, g	L/θ^2	L/θ^2	ft/sec^2
Dimensional conversion factor	g_c	None	ML/θ^2F	32.2 lb_m ft/sec^2 lb_f
Energy conversion factor	J	None	FL/Q	778 ft-lb_f/Btu
Work	W	ML^2/θ^2	FL	ft-lb_f
Pressure	p	M/θ^2L	F/L^2	lb_f/sq ft
Density	ρ	M/L^3	M/L^3	lb_m/cu ft
Internal energy	u	L^2/θ^2	Q/M	Btu/lb_m
Enthalpy	h	L^2/θ^2	Q/M	Btu/lb_m
Specific heat	c	L^2/θ^2T	Q/MT	Btu/lb_m F
Dynamic viscosity	μ_f	$M/L\theta$	$F\theta/L^2$	lb_f-sec/sq ft
Absolute viscosity	μ	$M/L\theta$	$M/L\theta$	lb_m/ft-sec
Kinematic viscosity	$\nu = \mu/\rho$	L^2/θ	L^2/θ	sq ft/sec
Thermal conductivity	k	ML/θ^3T	$Q/LT\theta$	Btu/hr ft F
Thermal diffusivity	a	L^2/θ	L^2/θ	sq ft/hr
Thermal resistance	R	$T\theta^3/ML^2$	$T\theta/Q$	F hr/Btu
Coefficient of expansion	β	$1/T$	$1/T$	$1/F$
Surface tension	σ	M/θ^2	F/L	lb_f/ft
Shear per unit area	τ	$M/L\theta^2$	F/L^2	lb_f/sq ft
Unit surface conductance	h	M/θ^3T	$Q/\theta L^2T$	Btu/hr sq ft F
Mass flow rate	m	M/θ	M/θ	lb_m/sec

formulas are also listed in the $ML\theta TFQ$ system. In this system, sometimes called the engineering system, there are six primary dimensions.[4]

Buckingham π-theorem. To determine the number of independent dimensionless groups required to obtain a relation describing a physical phenomenon, the Buckingham π (pi) theorem may be used.[5] According to this rule, the required number of independent dimensionless groups which can be formed by combining the physical variables pertinent to a

[4] Since the number of primary quantities is increased by two, the conversion constants g_c and J, whose dimensional formulas can be derived from the primary dimensions, must be included among the physical quantities.

[5] A more rigorous rule, proposed by van Driest (3), shows that the π-theorem holds as long as the set of simultaneous equations formed by equating the exponents of each primary dimension to zero is linearly independent. If one equation in the set is a linear combination of one or more of the other equations, i.e., if the equations are linearly dependent, then the number of dimensionless groups is equal to the total number of variables n minus the number of independent equations.

problem is equal to the total number of these physical quantities n (for example, density, viscosity, heat-transfer coefficient, etc.) minus the number of primary dimensions m required to express the dimensional formulas of the n physical quantities. If we call these groups π_1, π_2, etc., the equation expressing the relationship among the variables has a solution of the form

$$F(\pi_1, \pi_2, \pi_3, \cdots) = 0 \tag{6-8}$$

In a problem involving five physical quantities and three primary dimensions, $n - m$ is equal to two and the solution either has the form

$$F(\pi_1, \pi_2) = 0 \tag{6-9}$$

or the form

$$\pi_1 = f(\pi_2)$$

Experimental data for such a case can be presented conveniently by plotting π_1 against π_2. The resulting empirical curve reveals the functional relationship between π_1 and π_2 which can not be deduced from dimensional analysis.

For a phenomenon which can be described in terms of three dimensionless groups (i.e., if $n - m = 3$), Eq. 6-8 has the form

$$F(\pi_1, \pi_2, \pi_3) = 0 \tag{6-10}$$

but can also be written as

$$\pi_1 = f(\pi_2, \pi_3)$$

For such a case, experimental data can be correlated by plotting π_1 against π_2 for various values of π_3. Sometimes it is possible to combine two of the π's in some manner and to plot this parameter against the remaining π on a single curve.

Determination of dimensionless groups. A simple method for determining dimensionless groups will now be illustrated by applying it to the problem of correlating experimental convection heat-transfer data for a fluid flowing across a heated tube. Exactly the same approach could be used for heat transfer in flow through a heated tube.

From the description of the convective heat-transfer process, it is reasonable to expect that the physical quantities listed in Table 6-2 are pertinent to the problem.

There are seven physical quantities and four primary dimensions.

Table 6-2

Variable	Symbol	Dimensional Equation
Tube diameter	D	$[L]$
Thermal conductivity of the fluid	k	$[ML/\theta^3\ T]$
Velocity of the fluid	V	$[L/\theta]$
Density of the fluid	ρ	$[M/L^3]$
Viscosity of the fluid	μ	$[M/L\theta]$
Specific heat at constant pressure	c_p	$[L^2/\theta^2\ T]$
Heat-transfer coefficient	$\bar{h}_c$	$[M/\theta^3\ T]$

We therefore expect that three dimensionless groups will be required to correlate the data. To find these dimensionless groups, we write π as a product of the variables, each raised to an unknown power

$$\pi = D^a k^b V^c \rho^d \mu^e c_p{}^f \bar{h}_c{}^g \tag{6-11}$$

and substitute the dimensional formulas

$$\pi = [L]^a[ML/\theta^3 T]^b[L/\theta]^c[M/L^3]^d\ [M/L\theta]^e[L^2/\theta^2 T]^f[M/\theta^3 T]^g \tag{6-12}$$

For π to be dimensionless, the exponents of each primary dimension must separately add up to zero. Equating the sum of the exponents of each primary dimension to zero, we obtain the set of equations

$$\begin{aligned} b + d + e + g &= 0 \quad \text{for } M \\ a + b + c - 3d - e + 2f &= 0 \quad \text{for } L \\ -3b - c - e - 2f - 3g &= 0 \quad \text{for } \theta \\ -b - f - g &= 0 \quad \text{for } T \end{aligned}$$

Evidently any set of values of a, b, c, d, and e that simultaneously satisfies this set of equations will make π dimensionless. There are seven unknowns, but only four equations. We can therefore choose values for three of the exponents in each of the dimensionless groups. The only restriction on the choice of the exponents is that each of the selected exponents be independent of the others. An exponent is independent if the determinant formed with the coefficients of the remaining terms does not vanish (i.e., is not equal to zero).

Since $\bar{h}_c$, the convective heat-transfer coefficient, is the variable we eventually want to evaluate, it is convenient to set its exponent g equal to unity. At the same time we let $c = d = 0$ to simplify the algebraic manipulations. Solving the equations simultaneously, we obtain $a = 1$, $b = -1$, $e = f = 0$, and the first dimensionless group is

$$\pi_1 = \frac{\bar{h}_c D}{k}$$

which we recognize as the *Nusselt number*, $\overline{\mathrm{Nu}}$.

For π_2 we select g equal to zero, so that $\bar{h}_c$ will not appear again, and let $a = 1$ and $f = 0$. Simultaneous solution of the equations with these choices yields $b = 0$, $c = d = 1$, $e = -1$, and

$$\pi_2 = \frac{VD\rho}{\mu}$$

This dimensionless group is a *Reynolds number*, Re_D, with the tube diameter as the length parameter.

If we let $e = 1$ and $c = g = 0$, we obtain the third dimensionless group

$$\pi_3 = \frac{c_p \mu}{k}$$

which is known as the *Prandtl number*, Pr.

We observe that, although the heat-transfer coefficient is a function of six variables, with the aid of dimensional analysis, the seven original variables have been combined into three dimensionless groups. According to Eq. 6-10, the functional relationship can be written

$$\overline{\mathrm{Nu}} = f(\mathrm{Re}_D, \mathrm{Pr})$$

and experimental data can now be correlated in terms of three variables instead of the original seven. The importance of this reduction in the variables becomes apparent when we attempt to correlate experimental data.

Correlation of experimental data. Suppose that, in a series of tests with air flowing over a 1-in.-OD pipe, the heat-transfer coefficient has been measured experimentally at velocities ranging from 0.1 to 100 fps. This range of velocities corresponds to Reynolds numbers based on the diameter, $VD\rho/\mu$, ranging from 50 to 50,000. Since the velocity was the only variable in these tests, the results are correlated in Fig. 6-5 by plotting the heat-transfer coefficient $\bar{h}_c$ against the velocity V. The resulting curve permits a direct determination of $\bar{h}_c$ at any velocity for the system used in the tests, but it cannot be used to determine the heat-transfer coefficients for cylinders which are larger or smaller than the one used in the tests. Neither could the heat-transfer coefficient be evaluated if the air were under pressure and its density were different from that used in the

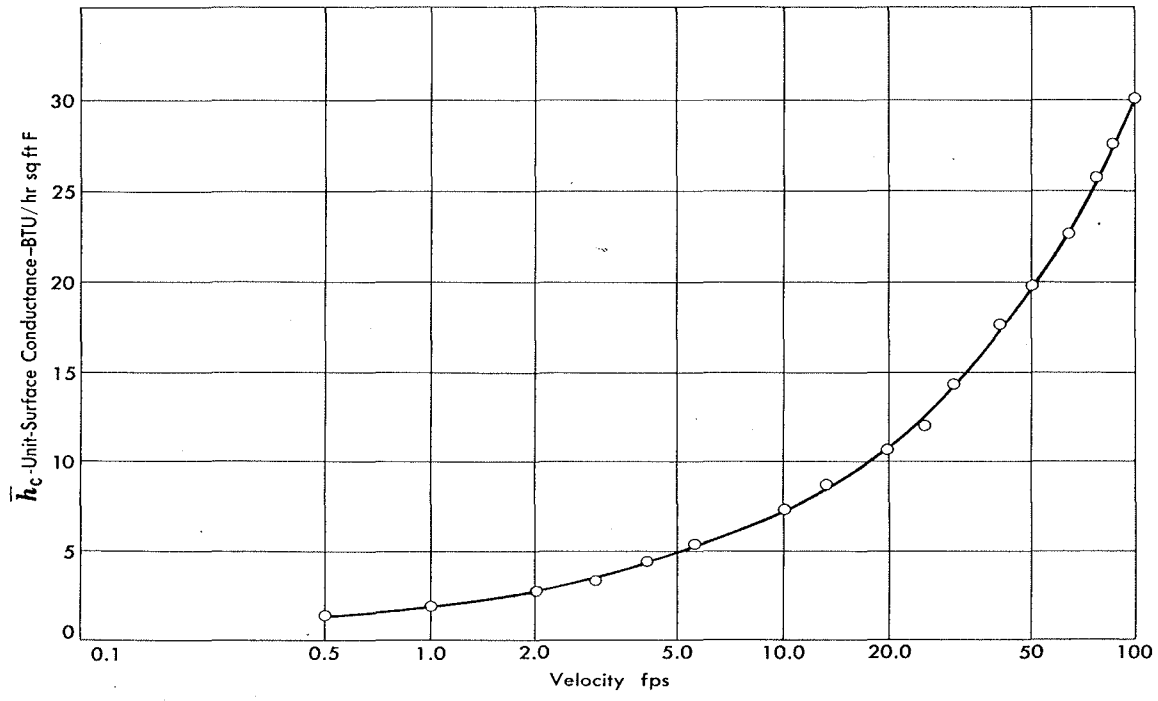

Fig. 6-5. Variation of heat-transfer coefficient with velocity for flow of air over a 1-in.-OD pipe.

tests. Unless experimental data could be correlated more effectively, it would be necessary to perform separate experiments for every cylinder diameter, every density, etc. The amount of labor would obviously be enormous.

With the aid of dimensional analysis, however, the results of one series of tests can be applied to a variety of other problems. This is illustrated by Fig. 6-6, where the data of Fig. 6-5 are replotted in terms of pertinent dimensionless groups. The abscissa in Fig. 6-6 is the Reynolds number $VD\rho/\mu$, and the ordinate is the Nusselt number $\bar{h}_c D/k$. This correlation of the data permits the evaluation of the heat-transfer coefficient for air flowing over any size of pipe or wire as long as the Reynolds number of the system falls within the range covered in the experiment.

Experimental data obtained with air alone do not reveal the dependence of the Nusselt number on the Prandtl number since the Prandtl number is a combination of physical properties whose value does not vary appreciably for gases. To determine the influence of the Prandtl number it is necessary to use different fluids. According to the preceding analysis, experimental data with several fluids whose physical properties yield a wide range of Prandtl numbers are necessary to complete the correlation (see Prob. 6-17).

In Fig. 6-7 the experimental results of several independent investigations for heat transfer between air, water, and oils in cross-flow over a tube or a wire are plotted for a wide range of temperatures, cylinder sizes,

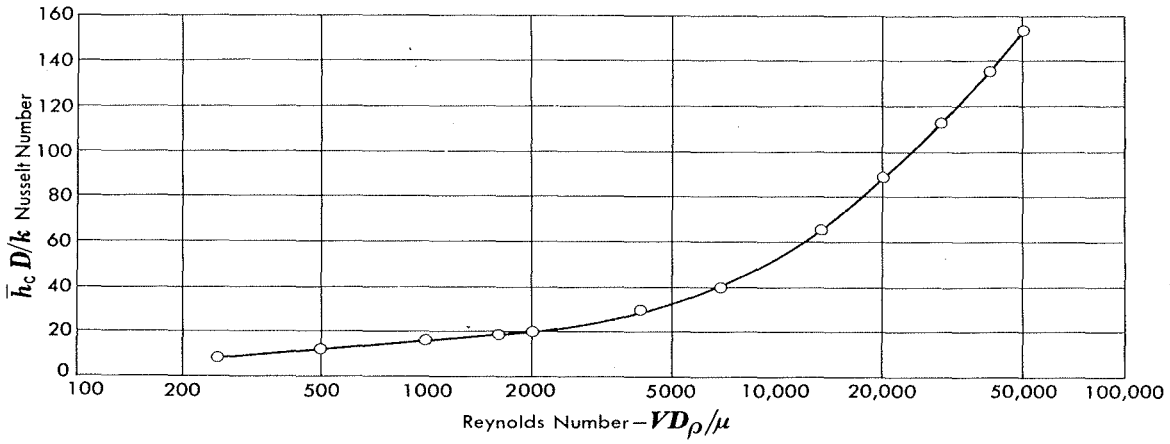

Fig. 6-6. Variation of a Nusselt number with a Reynolds number for flow of air over a 1-in.-OD pipe.

and velocities. The ordinate in Fig. 6-7 is the dimensionless quantity[6] $\overline{\mathrm{Nu}}/\mathrm{Pr}^{0.3}$ and the abscissa is Re_D. An inspection of the results shows that all of the data follow a single line reasonably well, so that they can be correlated empirically. For example, in the range of Reynolds numbers between 3 and 100 a straight line on the log-log plot is a satisfactory approximation to the best correlation, shown by a heavy dotted line in Fig. 6-7. The slope of this straight line is approximately 0.4 and its ordinate value at Re_D of unity is 0.82. The empirical correlation equation within the range of Reynolds numbers between 3 and 100 is therefore

$$\overline{\mathrm{Nu}}/\mathrm{Pr}^{0.3} = 0.82\ \mathrm{Re}_D{}^{0.4}$$

Principle of similarity. The remarkable result of Fig. 6-7 can be explained by the principle of similarity. According to this principle, often called the model law, the behavior of two systems will be similar if the ratios of their linear dimensions, forces, velocities, etc., are the same. Under conditions of forced convection in geometrically similar systems, the velocity fields will be similar provided the ratio of inertia forces to viscous forces is the same in both fluids. The Reynolds number is the ratio of these forces, and consequently we expect similar flow conditions in forced convection for a given value of the Reynolds number. The Prandtl number is the ratio of two molecular-transport properties, the kinematic viscosity $\nu = \mu/\rho$, which affects the velocity distribution, and

[6]Combining the Nusselt number with the Prandtl number for plotting the data is simply a matter of convenience. As mentioned previously, any combination of dimensionless parameters is satisfactory. The selection of the most convenient parameter is usually made on the basis of experience by trial and error with the aid of experimental results, although sometimes the characteristic groups are suggested by the results of analytical analyses.

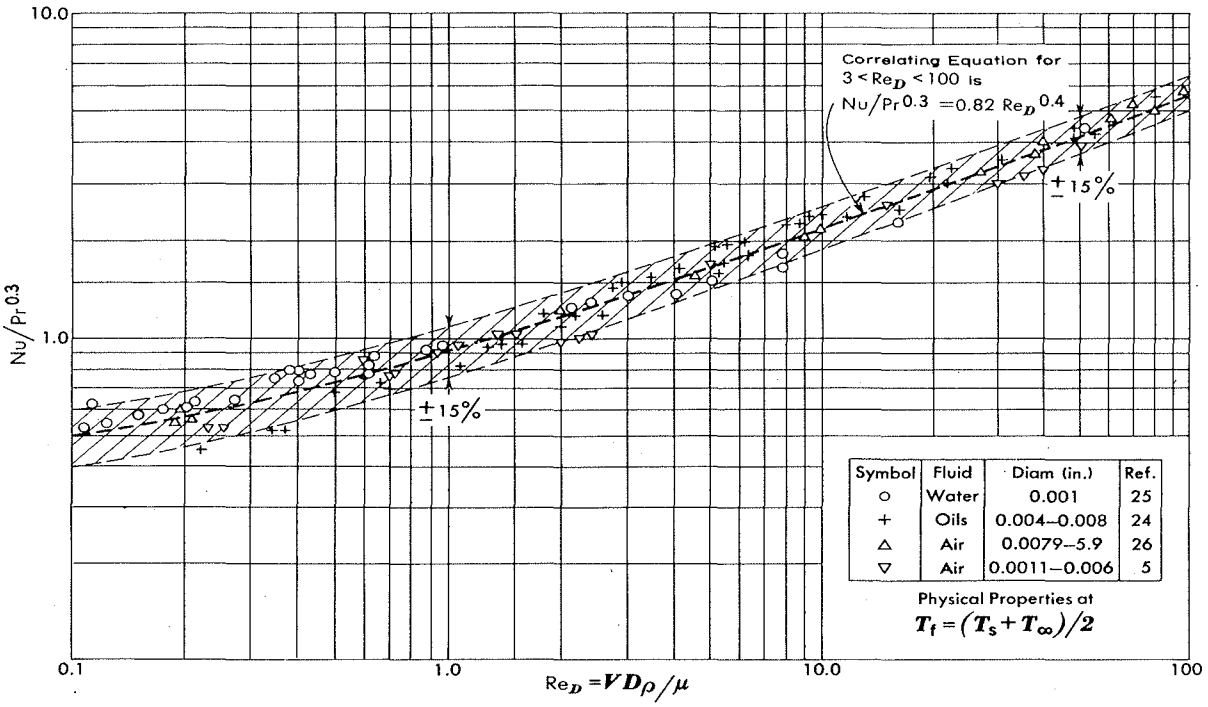

Fig. 6-7. Correlation of experimental heat-transfer data for various fluids in cross flow over cylinders of various diameters.

the thermal diffusivity $k/\rho c_p$, which affects the temperature profile. In other words, it is a dimensionless group which relates the temperature distribution to the velocity distribution. Hence, in geometrically similar systems having the same Prandtl and Reynolds numbers, the temperature distribution will be similar. According to its definition (see Eq. 6-3), the Nusselt number is numerically equal to the ratio of the temperature gradient at a fluid-to-surface interface to a reference-temperature gradient. We expect therefore that, in systems having similar geometries and similar temperature fields, the numerical values of the Nusselt numbers will be equal. This fact is borne out by the experimental results in Fig. 6-7.

6-7. *Laminar boundary layer on a flat plate*[7]

In the preceding section we determined dimensionless groups for correlating experimental data of heat transfer by forced convection. We found that the Nusselt number depends on the Reynolds number and the Prandtl number, i.e.,

[7]In the remainder of this chapter the mathematical details may be omitted in an introductory course without breaking the continuity of the presentation.

$$\mathrm{Nu} = \phi(\mathrm{Re})\,\psi(\mathrm{Pr}) \tag{6-13}$$

To determine the functional relationship in this equation it is necessary to resort either to experiments or to analytical methods.

In this and the following sections of the chapter we shall consider analytical methods of approach and apply them to the problem of heat transfer between a flat plate and an incompressible fluid flowing parallel to its surface. This system has been selected primarily because it is the simplest to analyze. However, the results obtained from this analysis have many practical applications. They are good approximations to forced convection in flow over the surfaces of streamlined bodies or in the inlet regions of pipes and ducts. In some cases appropriate transformations can reduce the equations for the flow of a compressible fluid, or the equations for the flow over wedges and cones, to the same form as those of the boundary-layer equations for the flat plate. The results for this case are therefore of considerable value; for more advanced boundary-layer problems and digital computer calculation methods, the reader should consult References 1 and 30.

In view of the difference in the flow characteristics, the frictional forces as well as the heat transfer are governed by different relations for laminar and turbulent types of boundary layers. We will first consider the laminar boundary layer, which is amenable to both an exact mathematical treatment and an approximate boundary-layer analysis. The turbulent boundary layer is taken up in Sec. 6-9.

Continuity and momentum equations. The equations of motion for boundary layer flow can be obtained by means of mass and force-and-momentum balances. As any other dynamic process, the flow of a fluid is governed by Newton's second law of motion which states that the summation of forces acting on a body in a given direction is equal to the time rate of change of its momentum in that direction, or

$$\Sigma F = \frac{1}{g_c}\,\frac{d(mV)}{d\theta}$$

In this form Newton's second law applies to a system of constant mass. In fluid dynamics, however, it is usually not convenient to deal with elements of mass; instead, one defines an elemental control volume, such as that shown in Fig. 6-8. Mass can flow in and out of this volume which is fixed in space, and a force-and-momentum balance in the x-direction for this system can be written

$$\Sigma F_x = \text{increase in momentum flux in } x\text{-direction}$$

where ΣF_x are the external forces acting on the control volume and the

momentum flux in the x-direction is the product of the mass flow rate through the control volume and the component of the velocity in the x-direction there.

To derive the equations governing the flow in the boundary layer, consider an elemental control volume having the shape of a parallelepiped with dimensions $dx \cdot dy \cdot 1$ (see Fig. 6-8) and assume

1. The flow is two-dimensional, i.e., the velocity distribution is the same in any plane perpendicular to the z axis (i.e., parallel to the surface of the paper).
2. The fluid is incompressible.
3. The flow is steady with respect to time.
4. The pressure changes in the direction perpendicular to the surface are negligible.
5. The physical properties are constant.
6. Viscous shear forces in the y-direction are negligible.

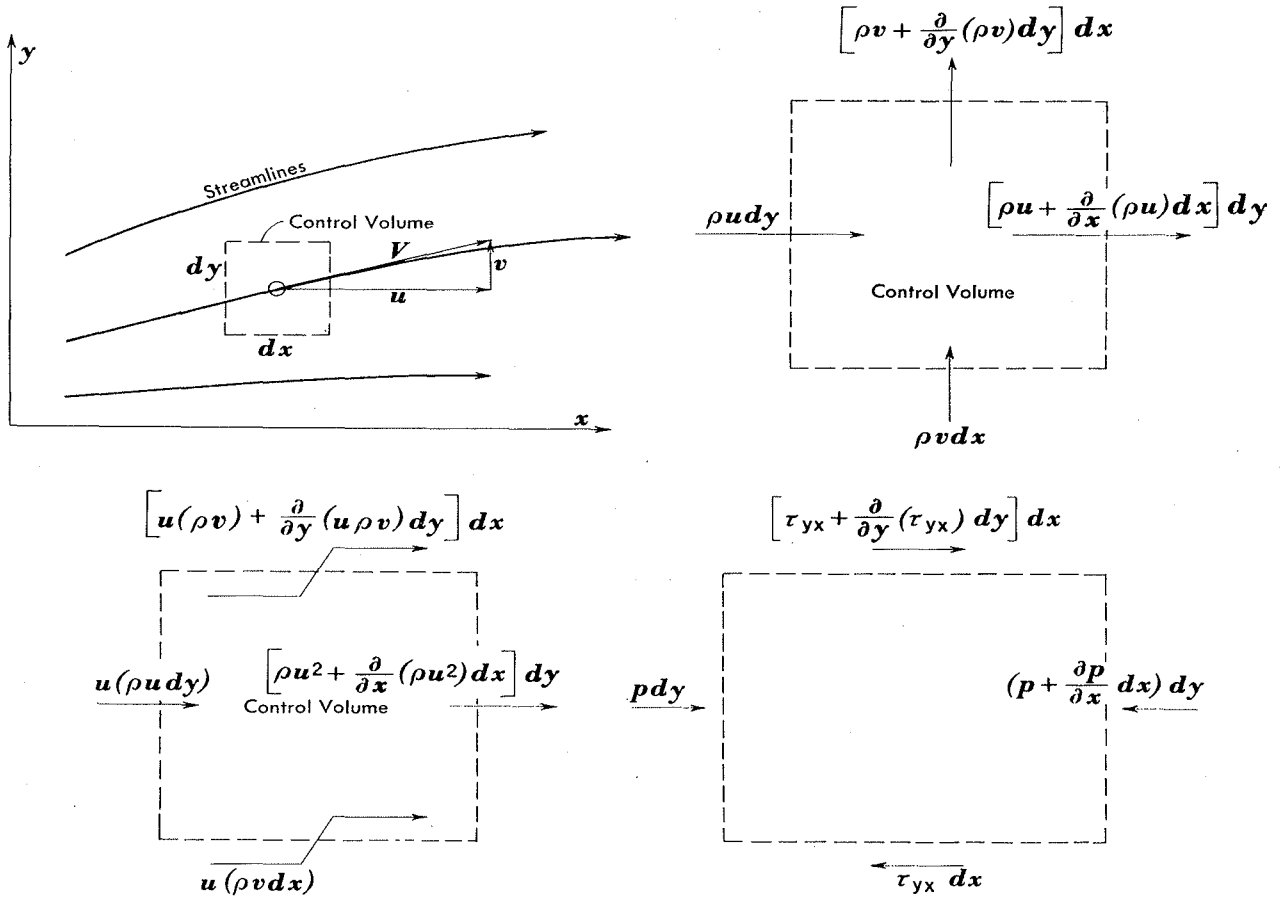

Fig. 6-8. Notation for continuity and momentum equations. Upper left: control volume in boundary layer. Upper right: mass flow through surface of control volume. Lower left: momentum fluxes in x-direction through surface of control volume. Lower right: forces acting on surface of control volume.

The mass flow rate entering through the left face is

$$\rho u dy$$

while the corresponding momentum flux is

$$(\rho u dy)u = \rho u^2 dy.$$

The mass flow rate leaving through the right face is

$$\rho\left(u + \frac{\partial u}{\partial x}\,dx\right) dy$$

and the corresponding momentum flux is

$$\rho\left(u + \frac{\partial u}{\partial x}\,dx\right)^2 dy.$$

The mass flow rate entering through the bottom face is

$$\rho v dx$$

and the mass flow rate leaving through the top is

$$\rho\left(v + \frac{\partial v}{\partial y}\,dy\right) dx.$$

A mass balance on the control volume gives

$$\rho u dy + \rho v dx = \rho\left(u + \frac{\partial u}{\partial x}\,dx\right) dy + \rho\left(v + \frac{\partial v}{\partial y}\,dy\right) dx$$

or

$$\frac{\partial u}{\partial x} + \frac{\partial v}{\partial y} = 0 \qquad (6\text{-}14)$$

Equation 6-14 is the *equation of continuity* for an incompressible two-dimensional flow.

To complete the momentum analysis, note that the momentum in the x-direction entering through the bottom face is

$$(\rho v dx) \cdot u$$

and the momentum in the x-direction leaving through the top face is

$$\rho \left(v + \frac{\partial v}{\partial y}\, dy \right) \left(u + \frac{\partial u}{\partial y}\, dy \right) dx$$

The forces in the x-direction acting on the elemental volume are due to pressure and viscous shear. The pressure force on the left face is pdy and that on the right face is $\left[p + \left(\frac{\partial p}{\partial x} \right) dx \right] dy$; thus, the net pressure force in the x-direction is

$$- \frac{\partial p}{\partial x}\, dxdy$$

Viscous shear is the result of molecular interaction between faster- and slower-moving layers of fluid. It gives rise to a frictional stress τ, which is proportional to the velocity gradient normal to the direction of flow. The factor of proportionality is a property of the fluid and is called the *dynamic viscosity* μ_f. For flow over a flat plate (Fig. 6-9) when the change of velocity occurs only in the y direction perpendicular to the surface, the shearing stress in a plane parallel to the plate is

$$\tau_{yx} = \mu_f \frac{du}{dy} = \frac{\mu}{g_c} \frac{du}{dy} \tag{6-15}$$

where τ_{yx} = shearing stress in lb_f/sq ft;
u = velocity, in ft/sec;
y = distance, in ft;
μ_f = dynamic viscosity, in lb_f sec/sq ft;
μ = absolute viscosity, in lb_m/sec ft.

The dynamic viscosity is physically the same property of the fluid as the

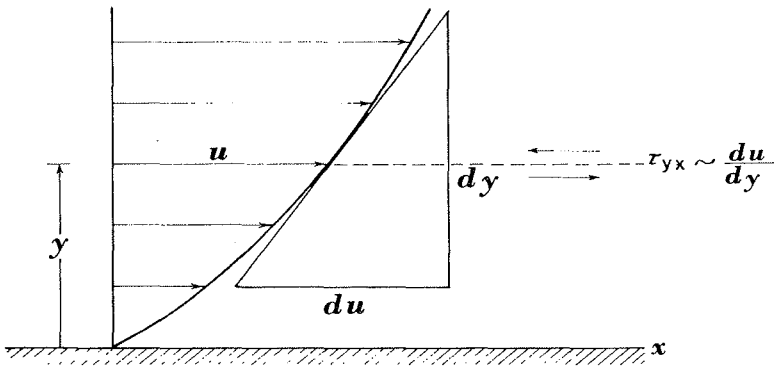

Fig. 6-9. Shearing stress in a laminar boundary layer.

absolute viscosity. The difference between them is merely the system of units used in their evaluation and the reason for distinguishing between μ_f and μ is to avoid errors in numerical computations by calling attention to the fact that some references list numerical values of viscosity in lb_f sec/sq ft, whereas this book uses the units lb_m/sec ft throughout. The subscript notation for the shearing stress τ indicates the axis to which the shear-affected area is perpendicular by the first letter and the direction of the stress by the second letter, e.g., τ_{yx} is the shear in the x direction on a plane perpendicular to the y axis.

At the lower face the shear acting on the fluid within the control volume is

$$(\tau_{yx})\,dx = \left(\frac{\mu}{g_c}\frac{\partial u}{\partial y}\right)dx$$

and at the upper face the shear is

$$\left[\tau_{yx} + \frac{\partial}{\partial y}(\tau_{yx})\,dy\right]dx = \left[\frac{\mu}{g_c}\frac{\partial u}{\partial y} + \frac{\partial}{\partial y}\left(\frac{\mu}{g_c}\frac{\partial u}{\partial y}\right)dy\right]dx$$

Since the wall is stationary, the shear on the fluid at the lower face of the control volume (Fig. 6-8) acts in a direction opposite to that of the flow (i.e., in the negative direction), while the shear on the upper face is caused by fluid tending to pull in the direction of motion. The net positive shear force is thus

$$\left[\left(\tau_{yx} + \frac{\partial \tau_{yx}}{\partial y}\,dy\right) - \tau_{yx}\right]dx = \frac{\partial}{\partial y}\left(\frac{\mu}{g_c}\frac{\partial u}{\partial y}\right)dxdy$$

Equating the sum of the viscous shear and pressure forces to the net momentum transfer in the x-direction gives

$$\mu\frac{\partial^2 u}{\partial y^2}\,dxdy - \frac{\partial p}{\partial x}\,dxdy = \rho\left(u + \frac{\partial u}{\partial x}\,dx\right)^2 - \rho u^2 dy + \rho\left(v + \frac{\partial v}{\partial y}\,dy\right)\left(u + \frac{\partial u}{\partial y}\,dy\right)dx - \rho v u dx$$

Neglecting higher order terms and simplifying the above relation with the aid of Eq. 6-14 yields

$$\rho\left(u\frac{\partial u}{\partial x} + v\frac{\partial u}{\partial y}\right) = \mu\frac{\partial^2 u}{\partial y^2} - \frac{\partial p}{\partial x} \qquad (6\text{-}16)$$

For flow over a flat plate the pressure gradient is zero.

Boundary-layer thickness and skin friction. Equation 6-16 must be solved simultaneously with the continuity equation (Eq. 6-14) in order to determine the velocity distribution, the boundary-layer thickness, and the friction force at the wall. These equations are solved by first defining a stream function, $\psi(x,y)$, which automatically satisfies the continuity equation, or

$$u = \frac{\partial \psi}{\partial y} \qquad \text{and} \qquad v = -\frac{\partial \psi}{\partial x}$$

Introducing the new variable

$$\eta = y\sqrt{u_\infty / \nu x}$$

we can let

$$\psi = \sqrt{\nu x u_\infty} f(\eta)$$

where $f(\eta)$ denotes a dimensionless stream function. In terms of $f(\eta)$, the velocity components are

$$u = \frac{\partial \psi}{\partial y} = \frac{\partial \psi}{\partial \eta}\frac{\partial \eta}{\partial y} = u_\infty \frac{d[f(\eta)]}{d\eta}$$

and

$$v = -\frac{\partial \psi}{\partial x} = \frac{1}{2}\sqrt{\frac{\nu u_\infty}{x}}\left\{\frac{d[f(\eta)]}{d\eta}\eta - f(\eta)\right\}$$

Expressing $\partial u/\partial x$, $\partial u/\partial y$, and $\partial^2 u/\partial y^2$ in terms of η and inserting the resulting expressions in the momentum equation yields the ordinary, nonlinear, third-order differential equation

$$f(\eta)\frac{d^2[f(\eta)]}{d\eta^2} + 2\frac{d^3[f(\eta)]}{d\eta^3} = 0$$

which can be solved subject to the three boundary conditions that

$$\text{at } \eta = 0, f(\eta) = 0, \frac{d[f(\eta)]}{d\eta} = 0$$

and

$$\text{at } \eta = \infty, \frac{d[f(\eta)]}{d\eta} = 1$$

The solution to this differential equation was obtained numerically by Blasius, in 1908 (6). The significant results are shown in Figs. 6-10 and 6-11.

In Fig. 6-10 the Blasius velocity profiles in the laminar boundary on a flat plate are plotted in dimensionless form together with experimental data obtained by Hansen (13). The ordinate in Fig. 6-10 is the local velocity in the x direction u divided by the free stream velocity u_∞, and the abscissa is a dimensionless distance parameter, $(y/x)\sqrt{(\rho u_\infty x)/\mu}$. We note that a single curve is sufficient to correlate the velocity distributions at all stations along the plate. The velocity u reaches 99 percent of the free-stream value u_∞ at $(y/x)\sqrt{(\rho u_\infty x)/\mu} = 5.0$. If we define the hydrodynamic boundary-layer thickness as that distance from the surface at which local velocity u reaches 99 percent of the free-stream value u_∞, the boundary-layer thickness δ becomes

$$\delta = \frac{5x}{\sqrt{\mathrm{Re}_x}} \tag{6-17}$$

where $\mathrm{Re}_x = (\rho u_\infty x)/\mu$, the local Reynolds number. Equation 6-17

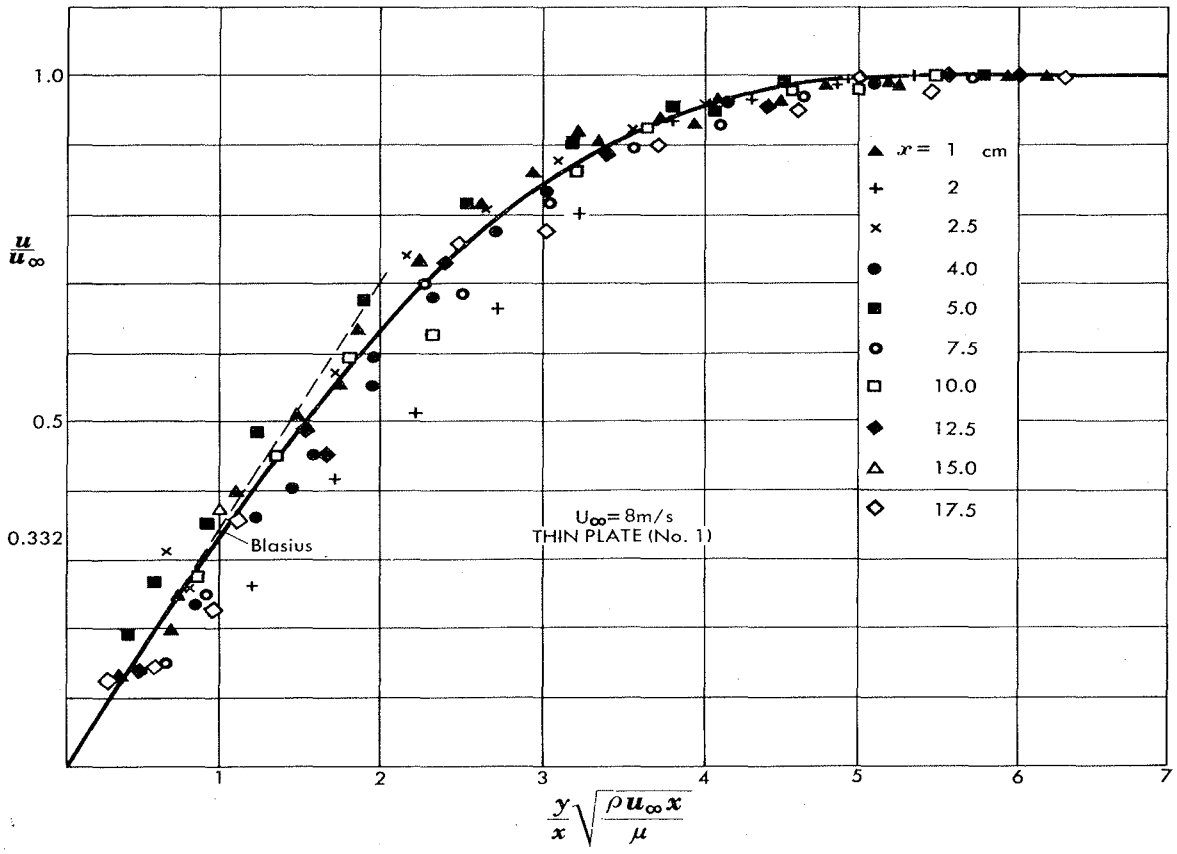

Fig. 6-10. Velocity profile in the laminar boundary layer according to Blasius with experimental data of Hansen (13). (Courtesy of National Advisory Committee for Aeronautics, NACA TM 585)

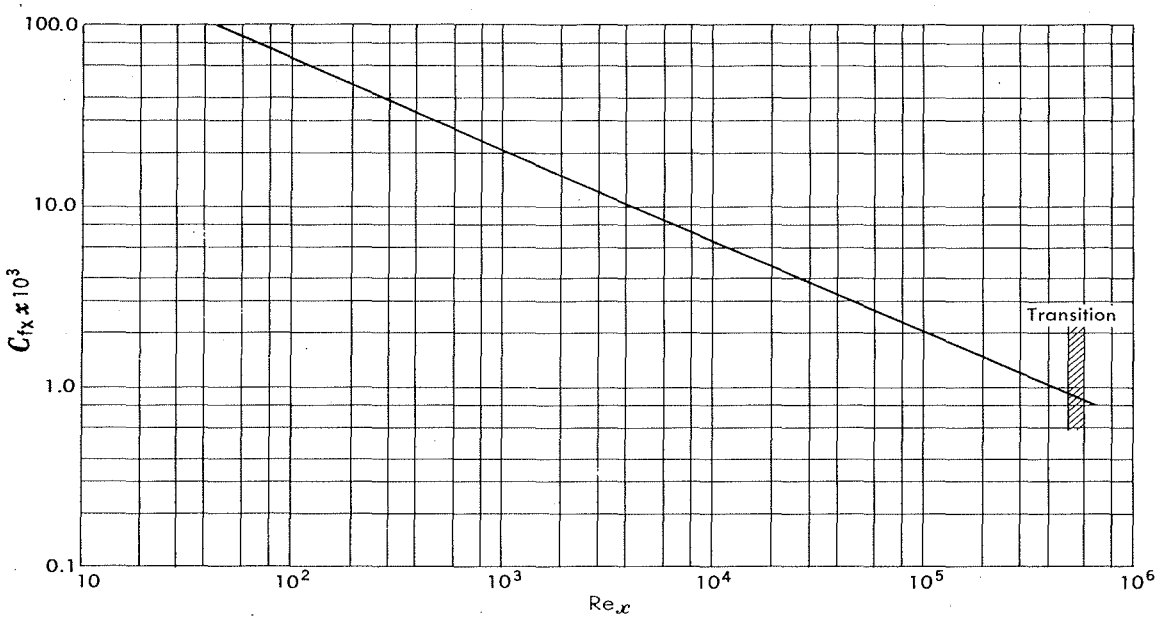

Fig. 6-11. Variation of local friction coefficient with dimensionless distance from leading edge for laminar flow over a flat plate.

satisfies the qualitative description of the boundary-layer growth, δ being zero at the leading edge ($x = 0$) and increasing with x along the plate. At any station, i.e., a given value of x, the thickness of the boundary layer is inversely proportional to the square root of the local Reynolds number. Hence, an increase in velocity will result in a decrease of the boundary-layer thickness.

The shear force at the wall can be obtained by substituting the velocity gradient at $y = 0$ into Eq. 6-15. From Fig. 6-10 we see that

$$\left.\frac{\partial (u/u_\infty)}{\partial (y/x)\sqrt{\mathrm{Re}_x}}\right|_{y=0} = 0.332$$

and thus at any specified value of x the velocity gradient at the surface is

$$\left.\frac{\partial u}{\partial y}\right|_{y=0} = 0.332 \frac{u_\infty}{x} \sqrt{\mathrm{Re}_x}$$

Substituting this velocity gradient in Eq. 6-15, the wall shear per unit area τ_s becomes

$$\tau_s = \frac{\mu}{g_c} \left.\frac{\partial u}{\partial y}\right|_{y=0} = 0.332 \frac{\mu}{g_c} \frac{u_\infty}{x} \sqrt{\mathrm{Re}_x} \qquad (6\text{-}18)$$

We note that the wall shear near the leading edge is very large and decreases with increasing distance from the leading edge.

For a graphical presentation it is more convenient to use dimensionless coordinates. Dividing both sides of Eq. 6-18 by the velocity pressure of the free stream $\rho u_\infty^2/2g_c$, we obtain

$$C_{fx} = \frac{\tau_s}{\rho u_\infty^2/2g_c} = 0.664/\sqrt{\mathrm{Re}_x} \tag{6-19}$$

where C_{fx} is a dimensionless number called the *local drag or friction coefficient*. Figure 6-11 is a plot of C_{fx} against Re_x and shows the variation of the local friction coefficient graphically.

In many practical cases the average friction coefficient for a plate of finite length L is more important than the local friction coefficient. The average friction coefficient is obtained by integrating Eq. 6-19 between the leading edge, $x = 0$, and $x = L$. For laminar flow over the flat plate we get

$$\bar{C}_f = \frac{1}{L}\int_0^L C_{fx}\,dx = 1.33/\sqrt{\frac{u_\infty \rho L}{\mu}} \tag{6-20}$$

Thus, the average friction coefficient $\bar{C}_f$ is equal to twice the value of the local friction coefficient at $x = L$.

Energy equation. To evaluate the rate of heat transfer by convection we must determine the temperature gradient at the surface. The equation governing the temperature distribution in the boundary layer is obtained with the aid of the first law of thermodynamics, the principle of

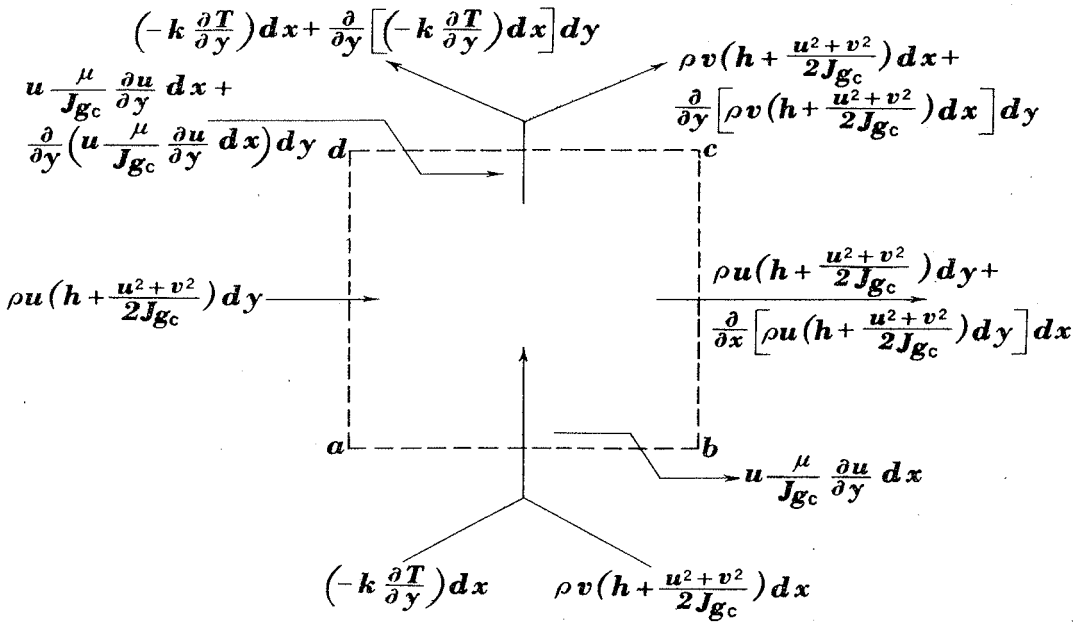

Fig. 6-12. Control volume in the boundary layer illustrating energy balance.

conservation of energy. Since we are dealing with a moving fluid, energy stored in fluid particles is transported by their motion. The rate of transport depends on the velocity of the fluid particles, and it is therefore always necessary to solve the hydrodynamic problem before the temperature distribution can be obtained.

To derive the equation governing the temperature distribution, consider the elementary control volume in the boundary layer shown in Fig. 6-12. Let the surfaces *ab*, *bc*, *cd*, and *da* define the boundaries of the system, and make an energy balance under the same assumptions used previously for the hydrodynamic equations. The energy equation for the system can be expressed semantically as

Influx of enthalpy and kinetic energy	+	rate of heat inflow by conduction	+	rate at which work is done by frictional shear *on* the fluid in control volume	=	efflux of enthalpy and kinetic energy	+	rate at heat outflow by conduction	+	rate at which work is done as a result of frictional shear *by* the fluid in control volume

or in symbolic form as

$$\rho u\left(h + \frac{u^2 + v^2}{2g_c J}\right)dy + \rho v\left(h + \frac{u^2 + v^2}{2g_c J}\right)dx$$

$$-k\left(\frac{\partial T}{\partial y}\right)dx + \frac{1}{J}\left[u\frac{\mu}{g_c}\frac{\partial u}{\partial y}dx + \frac{\partial}{\partial y}\left(u\frac{\mu}{g_c}\frac{\partial u}{\partial y}dx\right)dy\right]$$

$$= \rho u\left(h + \frac{u^2 + v^2}{2g_c J}\right)dy + \frac{\partial}{\partial x}\left[\rho u\left(h + \frac{u^2 + v^2}{2g_c J}\right)dy\right]dx$$

$$+ \rho v\left(h + \frac{u^2 + v^2}{2g_c J}\right)dx + \frac{\partial}{\partial y}\left[\rho v\left(h + \frac{u^2 + v^2}{2g_c J}\right)dx\right]dy$$

$$- k\left(\frac{\partial T}{\partial y}\right)dx + \frac{\partial}{\partial y}\left[-k\left(\frac{\partial T}{\partial y}\right)dx\right]dy + \frac{1}{J}\left(u\frac{\mu}{g_c}\frac{\partial u}{\partial y}\right)dx \qquad (6\text{-}21)$$

The frictional work terms represent the work done by shearing forces on the surface of the control volume as faster fluid particles slide over slower ones. At the lower surface, the fluid inside the control volume exerts a force on the fluid outside because the former moves faster. The force

times distance per unit time (i.e., velocity) u (μ/g_c) $(\partial u/\partial y)$ represents the rate at which work is done *by* the fluid in the control volume. Similarly, the last term in square brackets on the left-hand side of Eq. 6-21 represents the rate at which work is done *on* the fluid in the control volume.

Conduction along the x direction has been omitted because, in the boundary layer, the term $-k(\partial T/\partial x$ is negligible compared to $-k(\partial T/\partial y)$ and the convection terms.

The term $h + (u^2 + v^2)/2g_cJ$ can be written c_pT_o for fluids having a constant specific heat. T_o is the stagnation temperature, i.e., the temperature reached by the fluid when it is isentropically slowed down to zero velocity. For low-speed flow, $T \simeq T_o$ because the kinetic energy of the flow is negligible. For high-speed flow, on the other hand, especially at supersonic velocities, this simplification is not permissible (see Sec. 6-12).

Adding up the terms of Eq. 6-21 and dropping those of higher order (i.e., terms involving triple products of d quantities) we obtain after simplifying[8]

$$\rho c_p u \frac{\partial T_o}{\partial x} + \rho c_p v \frac{\partial T_o}{\partial y} = k \frac{\partial^2 T}{\partial y^2} + \frac{\partial}{\partial y}\left(u \frac{\mu}{g_c} \frac{\partial u}{\partial y}\right) \tag{6-22}$$

The last term of Eq. 6-22 represents the net rate at which shearing forces perform work *on* the fluid in the control volume. The mechanical energy or frictional power increases the internal energy of the fluid in the control volume appreciably only at high velocities, but for low subsonic flow in the main stream the frictional power term is small compared to the other terms and can be neglected. With these simplifications, Eq. 6-22 becomes

$$u \frac{\partial T}{\partial x} + v \frac{\partial T}{\partial y} = a \frac{\partial^2 T}{\partial y^2} \tag{6-23}$$

where $a = k/\rho c_p$.

The velocities in the energy equation, u and v, have the same values at any point (x, y) as in the dynamic equation. For the case of the flat plate, Pohlhausen (7) used the velocities calculated previously by Blasius to obtain the solution of the heat-transfer problem. Without considering the details of this mathematical solution, we can obtain significant results by comparing Eq. 6-23, the heat-transfer equation for the boundary layer, with Eq. 6-16, the momentum equation for the boundary layer. The two equations are similar; in fact, a solution for the velocity distribution

[8]In this and in subsequent equations the work-to-heat conversion constant J has been ommitted.

$u(x, y)$ is also a solution for the temperature distribution $T(x, y)$ if $\nu = a$ and if the temperature of the plate T_s is constant. We can easily verify this by replacing the symbol T in Eq. 6-23 by the symbol u and noting that the boundary conditions for both T and u are identical. If we use the surface temperature as our datum and let the variable in Eq. 6-23 be $(T - T_s)/(T_\infty - T_s)$, then the boundary conditions are:

$$\text{at } y = 0: \quad \frac{T - T_s}{T_\infty - T_s} = 0 \quad \text{and} \quad \frac{u}{u_\infty} = 0$$

$$\text{at } y \longrightarrow \infty: \quad \frac{T - T_s}{T_\infty - T_s} = 1 \quad \text{and} \quad \frac{u}{u_\infty} = 1$$

where T_∞ is the free-stream temperature.

The condition that $\nu = a$ corresponds to a Prandtl number of unity since

$$\text{Pr} = \frac{c_p \mu}{k} = \frac{\nu}{a}$$

For Pr = 1 the velocity distribution is therefore identical to the temperature distribution. An interpretation in terms of physical processes is that the transfer of momentum is analogous to the transfer of heat when Pr = 1. The physical properties of most gases are such that they have Prandtl numbers ranging from 0.65 to 1.0, and the analogy is therefore satisfactory. Liquids, on the other hand, have Prandtl numbers considerably different from unity, and the preceding analysis cannot be applied directly (36).

Using the analytical results of Pohlhausen's work, the temperature distribution in the laminar boundary layer for Pr = 1 can be modified empirically to include fluids having Prandtl numbers different from unity. In Fig. 6-13 theoretically calculated temperature profiles in the boundary layer are shown for values of Pr of 0.6, 0.8, 1.0, 3.0, 7.0, 15, and 50. We now define a thermal boundary-layer thickness δ_{th} as the distance from the surface at which the temperature difference between the wall and the fluid reaches 99 percent of the free-stream value. Inspection of the temperature profiles shows that the thermal boundary layer is larger than the hydrodynamic boundary layer for fluids having Pr less than unity, but smaller when Pr is larger than one. According to Pohlhausen's calculations, the relationship between the thermal and hydrodynamic boundary layer is approximately

$$\delta_{th} = \delta/\text{Pr}^{1/3} \tag{6-24}$$

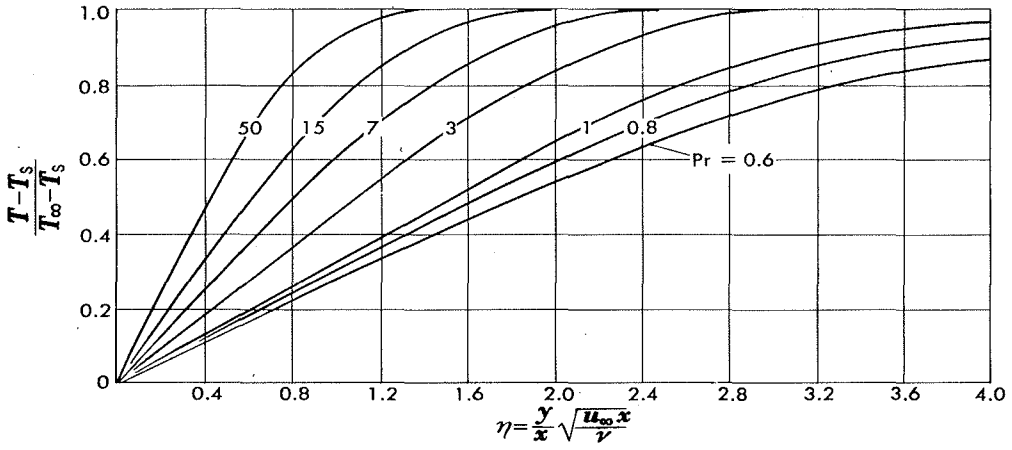

Fig. 6-13. Temperature distribution in a fluid flowing over a heated plate for various Prandtl numbers.

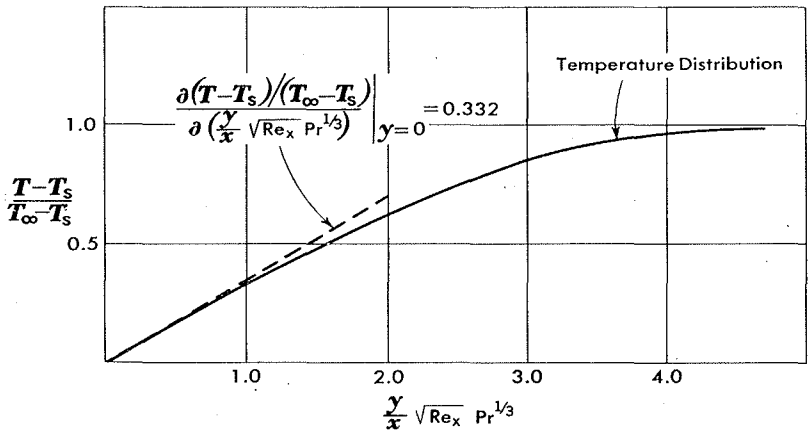

Fig. 6-14. Dimensionless correlation of temperature profiles for flow over a flat plate at constant temperature.

Using the same correction factor, i.e., $\mathrm{Pr}^{1/3}$, at any distance from the surface, the curves of Fig. 6-13 are replotted in Fig. 6-14. The new abscissa is $\mathrm{Pr}^{1/3}(y/x)\sqrt{\mathrm{Re}_x}$ and the ordinate is the dimensionless temperature $(T - T_s)/(T_\infty - T_s)$, where T is the local fluid temperature of the fluid, T_s the surface temperature of the plate, and T_∞ the free-stream temperature. This modification of the ordinate brings the temperature profiles for a wide range of Prandtl numbers together on the curve for $\mathrm{Pr} = 1$.

Evaluation of convective-heat-transfer coefficient. The rate of heat transfer by convection and the convective-heat-transfer coefficient can now be determined. The dimensionless temperature gradient at the surface (i.e., at $y = 0$) is

$$\left.\frac{\partial\left(\frac{T - T_s}{T_\infty - T_s}\right)}{\partial\left(\frac{y}{x}\sqrt{\mathrm{Re}_x}\mathrm{Pr}^{1/3}\right)}\right|_{y=0} = 0.332$$

Therefore, at any specified value of x

$$\left.\frac{\partial T}{\partial y}\right|_{y=0} = 0.332\,\frac{\mathrm{Re}_x^{1/2}\,\mathrm{Pr}^{1/3}}{x}\,(T_\infty - T_s) \tag{6-25}$$

and the local rate of heat transfer by convection per unit area becomes on substituting $\partial T/\partial y$ from Eq. 6-25 in Eq. 6-1

$$\frac{q}{A} = -k\left.\frac{\partial T}{\partial y}\right|_{y=0} = -0.332k\,\frac{\mathrm{Re}_x^{1/2}\,\mathrm{Pr}^{1/3}}{x}\,(T_\infty - T_s) \tag{6-26}$$

The total rate of heat transfer from a plate of width b and length L, obtained by integrating q from Eq. 6-26 between $x = 0$ and $x = L$, is

$$q = 0.664k\mathrm{Re}_L^{1/2}\,\mathrm{Pr}^{1/3}b\,(T_s - T_\infty) \tag{6-27}$$

where $\mathrm{Re}_L = u_\infty L/\nu$.

The local convective-heat-transfer coefficient is

$$h_{cx} = \frac{q}{A\,(T_s - T_\infty)} = 0.332\,\frac{k}{x}\,\mathrm{Re}_x^{1/2}\,\mathrm{Pr}^{1/3} \tag{6-28}$$

and the corresponding local Nusselt number is

$$\mathrm{Nu}_x = \frac{h_{cx}x}{k} = 0.332\,\mathrm{Re}_x^{1/2}\,\mathrm{Pr}^{1/3} \tag{6-29}$$

The average Nusselt number, $\bar{h}_c L/k$, is obtained by integrating the right-hand side of Eq. 6-28 between $x = 0$ and $x = L$ and dividing the result by L to obtain $\bar{h}_c$, the average value of h_{cx}; multiplying $\bar{h}_c$ by L/k gives

$$\overline{\mathrm{Nu}}_L = 0.664\,\mathrm{Re}_L^{1/2}\,\mathrm{Pr}^{1/3} \tag{6-30}$$

The average value of the Nusselt number over a length L of the plate is therefore twice the local value of Nu_x at $x = L$. It can easily be verified that the same relation between the average and local value holds also for the heat-transfer coefficient, that is,

$$\bar{h}_c = 2h_{c(x=L)} \tag{6-31}$$

In practice, the physical properties in Eqs. 6-24 to 6-30 vary with temperature, while for the purpose of analysis it was assumed that the physical properties are constant. Experimental data have been found to agree satisfactorily with the results predicted analytically if the properties are evaluated at a mean temperature halfway between that of the wall and the free-stream temperature.

EXAMPLE 6-1. Air at 60 F and at a pressure of 1 atm is flowing over a plate at a velocity of 10 fps. If the plate is 1 ft wide and at 140 F, calculate the following quantities at $x = 1$ ft and $x = x_c$.

a) Boundary-layer thickness.
b) Local friction coefficient.
c) Average friction coefficient.
d) Local drag or shearing stress due to friction.
e) Thickness of thermal boundary layer.
f) Local convective heat-transfer coefficient.
g) Average convective heat-transfer coefficient.
h) Rate of heat transfer by convection.

Solution: Properties of air at 100 F from Table A-3 are:

$$\begin{aligned} \rho &= 0.071 \text{ lb}_m/\text{cu ft} \\ c_p &= 0.240 \text{ Btu/lb}_m \text{ F} \\ \mu &= 1.285 \times 10^{-5} \text{ lb}_m/\text{ft sec} \\ k &= 0.0154 \text{ Btu/hr ft F} \\ \text{Pr} &= 0.72 \end{aligned}$$

The local Reynolds number at $x = 1$ ft is

$$\text{Re}_{x=1} = \frac{u_\infty \rho x}{\mu} = \frac{(10 \text{ ft/sec})(0.071 \text{ lb}_m/\text{cu ft})(1 \text{ ft})}{1.285 \times 10^{-5} \text{ lb}_m/\text{ft sec}} = 55{,}200$$

Assuming that the critical Reynolds number is 5×10^5, the critical distance is

$$x_c = \frac{5 \times 10^5 \mu}{u_\infty \rho} = \frac{(5 \times 10^5)(1.285 \times 10^{-5} \text{ lb}_m/\text{ft sec})}{(10 \text{ ft/sec})(0.071 \text{ lb}_m/\text{cu ft})} = 9 \text{ ft}$$

The desired quantities are determined by substituting appropriate values of the variable into the pertinent equations. The results of the calculations are shown in Table 6-3, and it is suggested that the reader verify them.

A useful relation between the local Nusselt number Nu_x and the corresponding friction coefficient C_{fx} is obtained by dividing Eq. 6-29 by $\text{Re}_x \text{Pr}^{1/3}$, or

Table 6-3

Part	Symbol	Unit	Eq. Used	Result (x = 1 ft)	Result (x = 9 ft)
a	δ	ft	6–17	0.0212	0.064
b	C_{fx}	.....	6–19	0.00282	0.00094
c	$\bar{C}_f$	.....	6–20	0.00564	0.00188
d	τ_s	lb_f/sq ft	6–18	3.12×10^{-4}	1.04×10^{-4}
e	δ_{th}	ft	6–24	0.0236	0.0715
f	h_{cx}	Btu/hr sq ft F	6–28	1.03	0.36
g	$\bar{h}_c$	Btu/hr sq ft F	6–31	2.06	0.72
h	q_c	Btu/hr	6–27	206	648

$$\left(\frac{\mathrm{Nu}_x}{\mathrm{Re}_x \mathrm{Pr}}\right)\mathrm{Pr}^{2/3} = \frac{0.322}{\mathrm{Re}_x^{1/2}} = \frac{C_{fx}}{2} \tag{6-32}$$

The dimensionless ratio $\mathrm{Nu}_x/\mathrm{Re}_x \mathrm{Pr}$ is known as the *Stanton number*, St_x. According to Eq. 6-32 the Stanton number times the Prandtl raised to the two-thirds power is equal to one-half the value of the friction coefficient. This relation between heat transfer and fluid friction was proposed by Colburn (4) and illustrates the interrelationship of the two processes.

6-8. *Approximate boundary-layer analysis*

The mathematical difficulties of an exact solution of the boundary layer equations in Sec. 6-7 can be circumvented by an approximate analysis which simplifies the mathematical manipulations and whose results agree with satisfactory accuracy with exact solutions. Instead of writing the equations of motion and heat transfer for a differential control volume, in the approximate method we write these equations for the aggregate of particles in the boundary layer. For this purpose we choose a control volume (Fig. 6-15) bounded by the two planes *ab* and *cd* which are perpendicular to the wall and a distance *dx* apart, the surface of the plate, and a parallel plane in the free stream at a distance *l* from the surface. Under steady-state conditions the mass flow rate into the control volume through the face *ab* is

$$\int_0^l \rho u dy$$

and the associated momentum flux is

$$\int_0^l \rho u^2 dy$$

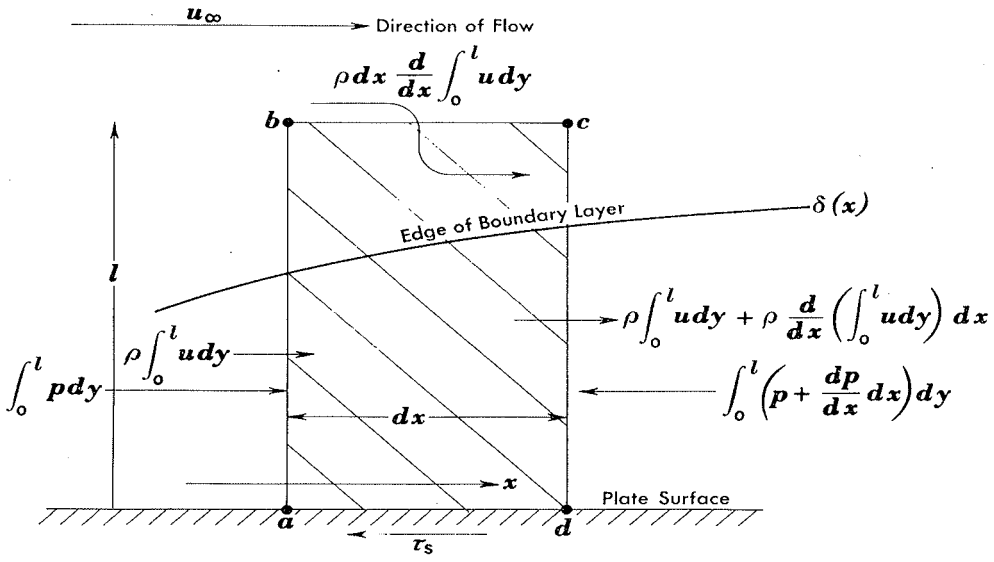

Fig. 6-15. Control volume for approximate momentum analysis of a boundary layer.

The mass flow rate out of the control volume through the face *cd* is

$$\int_0^l \rho u dy + \frac{d}{dx}\left(\int_0^l \rho u dy\right) dx$$

and the momentum flux out through *cd* is

$$\int_0^l \rho u^2 dy + \frac{d}{dx}\left(\int_0^l \rho u^2 dy\right) dx$$

No mass can enter the control volume through the plate and the difference in the mass flow out through *cd* and the mass flow in through *ab* must, therefore, enter through the upper face *bd*. Since the velocity at $y = 1$ is approximately equal to the free stream velocity u_∞, the x-momentum flux associated with the fluid entering through *bd* is

$$u_\infty \frac{d}{dx}\left(\int_0^l \rho u dy\right) dx$$

The net x-momentum flux out of the control volume is therefore

$$\frac{d}{dx}\left(\int_0^l \rho u^2 dy\right) dx - u_\infty \frac{d}{dx}\left(\int_0^l \rho u dy\right) dx$$

We can recast the second term in this expression into a more useful form by using the so-called "product formula" of integral calculus

$$d(r \cdot q) = rdq + qdr$$

or

$$rdq = d(r \cdot q) - q \cdot dr$$

If we treat the integral $\int_0^l \rho u dy$ as the q function and the free-stream velocity $u_\infty(x)$ as the r function

$$u_\infty \frac{d}{dx}\left(\int_0^l \rho u dy\right)dx = \frac{d}{dx}\left(u_\infty \int_0^l \rho u dy\right)dx - \frac{du_\infty}{dx}\left(\int_0^l \rho u dy\right)dx$$

But since $u_\infty(x)$ is not a function of y it can be placed under the integral sign and this gives

$$u_\infty \frac{d}{dx}\left(\int_0^l \rho u dy\right)dx = \frac{d}{dx}\left(\int_0^l \rho u u_\infty dy\right)dx - \frac{du_\infty}{dx}\left(\int_0^l \rho u dy\right)dx$$

The increase in x-momentum flux is equal to the summation of the forces in the x direction acting on the surface of the control volume. These forces, considered positive in the direction of flow, are

1. The shearing stress at the bottom surface, $-\tau_s dx = -\frac{\mu}{g_c} dx \left.\frac{\partial u}{\partial y}\right|_{y=0}$
2. The pressure on face ab, $\int_0^l p dy$.
3. The pressure on face cd, $-\left[\int_0^l p dy + \frac{d}{dx}\left(\int_0^l p dy\right)dx\right]$.

Since the velocities on both sides of the face bc are equal, no shearing stress exists there.

Equating the forces to the rate of momentum increase yields finally

$$\tau_s + \frac{d}{dx}\left(\int_0^l p dy\right) = \frac{d}{dx}\left(\int_0^l \frac{\rho}{g_c} u(u_\infty - u) dy\right) - \frac{du_\infty}{dx}\left(\int_0^l \frac{\rho}{g_c} u dy\right)dx \tag{6-33}$$

Equation 6-33 is the *von Karman momentum integral equation of the boundary layer for incompressible flow over a flat plate.* It applies also to flow over slightly curved boundaries if x is measured along the surface and y normal to it; but if the surface over which the fluid flows is curved, the free-stream velocity u_∞ and the pressure p_∞ vary with x. For incompres-

sible flow a relationship between u_∞ and p_∞ can be obtained from Bernouilli's equation

$$p_\infty + \frac{\rho u_\infty^2}{2g_c} = \text{constant}$$

or

$$\frac{dp_\infty}{dx} = -\frac{\rho u_\infty}{g_c}\frac{du_\infty}{dx}$$

Since the boundary layer is very thin, it may be assumed (1) that the pressure at any x location is constant throughout the boundary layer, i.e., $p(x) = p_\infty(x)$, and

$$\int_0^l \frac{dp}{dx}\,dy = \int_0^l \frac{dp_\infty}{dx}\,dy = -\frac{\rho}{g_c}\frac{du_\infty}{dx}\int_0^l u_\infty\,dy \tag{6-34}$$

Substituting Eq. 6-34 for the pressure term in Eq. 6-33 gives

$$\tau_s = \frac{d}{dx}\int_0^l \frac{\rho u}{g_c}(u_\infty - u)\,dy + \frac{\rho}{g_c}\frac{du_\infty}{dx}\int_0^l (u_\infty - u)\,dy$$

Since the integrals in both terms on the right-hand side are zero for $y > \delta$, their upper limits can be replaced by δ. For flow over a flat plate u_∞ does not vary with x and

$$\frac{du_\infty}{dx} = 0 = \int_0^l \frac{dp_\infty}{dx}\,dy$$

For the constant pressure condition, Eq. 6-33 becomes therefore simply

$$g_c\frac{\tau_s}{\rho} = \frac{d}{dx}\int_0^l u(u_\infty - u)\,dy$$

If one assumes a physically reasonable velocity distribution in the boundary layer, then the momentum integral equation can be used to determine the boundary-layer thickness and the wall friction for specified geometries and flow conditions. The results naturally become more accurate the more closely the assumed velocity distribution resembles actual conditions. It has been found, however, that even a very rough assumption for the velocity distribution will yield satisfactory results. For this reason the approximate method is a powerful tool in engineering analysis. Example 6-2 illustrates the method.

EXAMPLE 6-2. Determine the hydrodynamic boundary-layer thickness for laminar flow over a flat plate by means of the von Karman momentum equation of the boundary layer. Assume a straight-line velocity distribution in the boundary layer.

Solution: The equation describing the velocity distribution for a linear increase in velocity from $u = 0$ at $y = 0$ to $u = u_\infty$ at $y = \delta$ is $u = u_\infty y/\delta$. The shearing stress at the wall τ_s is then

$$g_c \tau_s = \mu \left.\frac{\partial u}{\partial y}\right|_{y=0} = \frac{\mu u_\infty}{\delta}$$

Substituting for u and τ_s in Eq. 6-33 yields

$$\rho u_\infty^2 \frac{d}{dx} \int_0^\delta \left(1 - \frac{y}{\delta}\right) \frac{y}{\delta} dy = \frac{\mu u_\infty}{\delta}$$

Evaluating the integral above yields

$$\int_0^\delta \frac{y}{\delta} dy - \int_0^\delta \frac{y^2}{\delta^2} dy = \frac{1}{\delta} \left.\frac{y^2}{2}\right|_0^\delta - \frac{1}{\delta^2} \left.\frac{y^3}{3}\right|_0^\delta = \frac{\delta}{6}$$

Then, we get

$$\frac{\rho u_\infty^2}{6} \frac{d\delta}{dx} = \frac{\mu u_\infty}{\delta}$$

which yields

$$\delta d\delta = d\left(\frac{\delta^2}{2}\right) = \frac{6\mu}{\rho u_\infty} dx$$

Integrating the above equation gives the boundary-layer thickness δ as

$$\delta = \sqrt{(12\mu x)/(\rho u_\infty)} = 3.46x/\sqrt{\mathrm{Re}_x} \qquad \textit{Ans.}$$

The boundary-layer thickness calculated by means of a linear approximation to the velocity distribution is about 30 percent less than the value obtained by Blasius (see Eq. 6-17). However, the approximate method can be considerably improved by taking a velocity distribution which resembles the true conditions more closely. Eckert (9) used a cubic parabola of the form

$$\frac{u}{U_\infty} = C_1 \frac{y}{\delta} - C_2 \left(\frac{y}{\delta}^3 \right) \tag{6-35}$$

and obtained, by substituting the above relation for u in Eq. 6-33,

$$\delta = 4.64x / \sqrt{\mathrm{Re}_x} \tag{6-36}$$

a value only 8 percent less than that of the exact analysis. Since most of the experimental measurements are only accurate to within 10 percent, the results of the approximate analysis are satisfactory in practice.

To determine the rate of convective heat transfer to or from a surface we make an energy balance for the aggregate of fluid particles within the control volume of Fig. 6-16. To simplify the problem we shall neglect the shear work due to the frictional forces along the wall and assume also that the physical properties are independent of the temperature.

Energy is convected into and out of the control volume as a result of the fluid motion, and there is also heat flow by conduction across the interface. The energy flow rates across the individual faces of the control volume are listed in Table 6-4. To satisfy the principle of conservation of energy in the steady state, the rate of energy influx must equal the rate of energy efflux. Equating the net rate of convective energy outflow to the net rate of heat inflow by conduction we obtain

$$\frac{\partial}{\partial x} \int_0^l (T_{o\infty} - T_o)\, u dy = \frac{k}{\rho c_p} \frac{\partial T}{\partial y}\bigg|_{y=0}$$

Since the total temperature T_o equals the free-stream total temperature

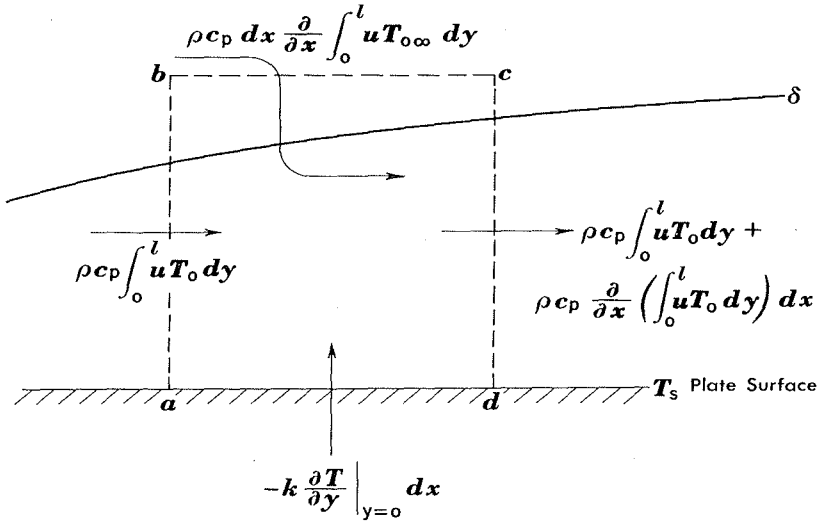

Fig. 6-16. Control volume for approximate energy balance in a boundary layer.

Table 6-4

Face	Mass-Flow Rate	Heat-Flow Rate
ab	$\rho \int_0^l u dy$	$\rho c_p \int_0^l u T_o dy$
bc	$\rho dx \frac{\partial}{\partial x} \int_0^l u dy$	$\rho c_p dx \frac{\partial}{\partial x} \int_0^l u T_{o\infty} dy$
cd	$\rho\left[\int_0^l u dy + \frac{\partial}{\partial x}\left(\int_0^l u dy\right) dx\right]$	$\rho c_p \int_0^l u T_o dy + \rho c_p \frac{\partial}{\partial x}\left(\int_0^l u T_o dy\right) dx$
da	0	$- k \frac{\partial T}{\partial y}\Big\vert_{y=0} dx$

$T_{o\infty}$ outside the thermal boundary layer (i.e., $y > \delta_{th}$), the integrand becomes zero for values of y larger than δ_{th}. We therefore replace l, the upper limit of the integral, by δ_{th}, and the heat-transfer equation of the boundary layer becomes

$$\frac{\partial}{\partial x} \int_0^{\delta_{th}} (T_{o\infty} - T_o) u dy = \frac{k}{\rho c_p} \frac{\partial T}{\partial y}\Big|_{y=0} \tag{6-37}$$

If we restrict our analysis to low-speed flow in which the kinetic energy is negligible compared with the enthalpy, the total temperatures in Eq. 6-37 are equal to the static temperatures for all practical purposes, i.e., $T_0 \cong T$ and $T_{o\infty} \cong T_\infty$.

To determine the convective heat-transfer coefficient we now select a suitable shape for the temperature distribution which meets the physical boundary conditions. Near the surface, where heat flows by conduction, the temperature gradient should be linear, and at $y = 0$, the fluid temperature should be equal to the plate temperature. At the edge of the thermal boundary layer (i.e., at $y = \delta_{th}$) the temperature should smoothly approach the free-stream temperature. Mathematically these boundary conditions are

$$\frac{\partial T}{\partial y} = C \qquad \text{and} \qquad (T - T_s) = 0 \qquad \text{at } y = 0$$

$$(T - T_s) = (T_\infty - T_s) \qquad \text{and} \qquad \frac{\partial (T - T_s)}{\partial y} = 0 \qquad \text{at } y = \delta_{th}$$

A cubic parabola of the form

$$T - T_s = C_1 y + C_2 y^3 \tag{6-38}$$

satisfies these boundary conditions if the constants C_1 and C_2 are selected

appropriately. The conditions at $y = 0$ are automatically satisfied for any value of C_1 and C_2. At $y = \delta_{th}$ we have

$$T_\infty - T_s = C_1\delta_{th} + C_2\delta_{th}^3$$

and

$$\left.\frac{\partial(T - T_s)}{\partial y}\right|_{y=\delta} = C_1 + 3C_2\delta_{th}^2 = 0$$

Solving for C_1 and C_2, and substituting these expressions in Eq. 6-38 yields

$$\frac{T - T_s}{T_\infty - T_s} = \frac{3}{2}\left(\frac{y}{\delta_{th}}\right) - \frac{1}{2}\left(\frac{y}{\delta_{th}}\right)^3 \tag{6-39}$$

Using Eqs. 6-39 and 6-35 for $(T - T_s)$ and u respectively, the integral in Eq. 6-37 can be written as

$$\int_0^{\delta_{th}} (T_\infty - T)\,u\,dy = \int_0^{\delta_{th}} [(T_\infty - T_s) - (T - T_s)]\,u\,dy$$

$$= (T_\infty - T_s)\,u_\infty \int_0^{\delta_{th}} \left[1 - \frac{3}{2}\frac{y}{\delta_{th}} + \frac{1}{2}\left(\frac{y}{\delta_{th}}\right)^3\right]\left[\frac{3}{2}\left(\frac{y}{\delta}\right) - \frac{1}{2}\left(\frac{y}{\delta}\right)^3\right] dy$$

Performing the multiplication under the integral sign we obtain

$$(T_\infty - T_s)\,u_\infty \int_0^{\delta_{th}} \left[\left(\frac{3}{2\delta}\right)y - \left(\frac{9}{4\delta\delta_{th}}\right)y^2 + \left(\frac{3}{4\delta\delta_{th}^3}\right)y^4 - \left(\frac{1}{2\delta^3}\right)y^3 + \left(\frac{3}{4\delta_{th}\delta^3}\right)y^4 - \left(\frac{1}{4\delta_{th}^3\delta^3}\right)y^6\right] dy$$

which yields after integrating

$$(T_\infty - T_s)\,u_\infty \left[\frac{3}{4}\frac{\delta_{th}^2}{\delta} - \frac{3}{4}\frac{\delta_{th}^2}{\delta} + \frac{3}{20}\frac{\delta_{th}^2}{\delta} - \frac{1}{8}\frac{\delta_{th}^4}{\delta^3} + \frac{3}{20}\frac{\delta_{th}^4}{\delta^3} - \frac{1}{28}\frac{\delta_{th}^4}{\delta^3}\right]$$

If we let $\zeta = \delta_{th}/\delta$, the above expression can be written

$$(T_\infty - T_s) u_\infty \delta \left(\frac{3}{20} \zeta^2 - \frac{3}{280} \zeta^4 \right)$$

For fluids having a Prandtl number equal to or larger than unity, ζ is equal to or less than unity and the second term in the bracket can be neglected compared to the first.[9] Substituting this approximate form for the integral in Eq. 6-37, we obtain

$$\frac{3}{20} u_\infty (T_s - T_\infty) \zeta^2 \frac{\partial \delta}{\partial x} = -a \left. \frac{\partial T}{\partial y} \right|_{y=0} = \frac{3}{2} a \frac{T_s - T_\infty}{\delta \zeta}$$

or

$$\frac{1}{10} u_\infty \zeta^3 \delta \frac{\partial \delta}{\partial x} = a$$

From Eq. 6-36 we obtain

$$\delta \frac{\partial \delta}{\partial x} = 10.75 \frac{\nu}{u_\infty}$$

and with this expression we get

$$\zeta^3 = \frac{10}{10.75} \frac{a}{\nu}$$

or

$$\delta^{th} = 0.9 \delta \mathrm{Pr}^{-1/3} \tag{6-40}$$

Except for the numerical constant (0.9 compared with 1.0) the foregoing result is in agreement with the exact calculations of Pohlhausen (Eq. 6-24).

The rate of heat flow by convection from the plate per unit area is, from Eqs. 1-1 and 6-39,

$$\frac{q}{A} = -k \left. \frac{\partial T}{\partial y} \right|_{y=0} = -\frac{3}{2} \frac{k}{\delta_{th}} (T_\infty - T_s)$$

Substituting Eqs. 6-36 and 6-40 for δ_{th} yields

---

[9] This assumption is not valid for liquid metals, which have $\mathrm{Pr} \ll 1$.

$$\frac{q}{A} = -\frac{3}{2}\frac{k}{x}\frac{\mathrm{Pr}^{1/3}\mathrm{Re}_x^{1/2}}{(0.9)(4.64)}(T_\infty - T_s) = 0.36\frac{k}{x}\mathrm{Re}_x^{1/2}\mathrm{Pr}^{1/3}(T_s - T_\infty) \tag{6-41}$$

and

$$\mathrm{Nu}_x = \frac{q}{A(T_s - T_\infty)}\frac{x}{k} = 0.36\,\mathrm{Re}_x^{1/2}\,\mathrm{Pr}^{1/3} \tag{6-42}$$

This result is in agreement with the exact analysis (Eq. 6-29) except for the numerical constant, which is about 9 percent larger.

The foregoing example illustrates the usefulness of the approximate boundary-layer analysis. Guided by a little physical insight and intuition, this technique yields satisfactory results without the mathematical complications inherent in the exact boundary-layer equations. The approximate method has been applied to many other problems, and the results are available in the literature.

6-9. *Analogy between heat and momentum transfer in turbulent flow*

In a majority of practical applications the flow in the boundary layer is turbulent rather than laminar. It is therefore not surprising that many famous scientists, such as Osborn Reynolds, G. I. Taylor, Ludwig Prandtl, and T. von Karman, have studied problems dealing with turbulent-exchange mechanisms. Although these men as well as many others have contributed considerably to our understanding of turbulent flow, so far no one has succeeded in predicting friction and heat-transfer coefficients by a direct analysis. The reason for this lack of success is the extreme complexity of turbulent motion. In turbulent flow, irregular velocity fluctuations are always superimposed upon the motion of the main stream, and the fluctuating components can not be described by simple equations. Yet, it is precisely these fluctuations which are primarily responsible for the transfer of heat as well as momentum in turbulent flow.

Qualitatively the exchange mechanism in turbulent flow can be pictured as a magnification of the molecular exchange in laminar flow. In steady laminar flow, physical properties such as temperature and pressure remain constant at any point and fluid particles follow well-defined streamlines. Heat and momentum are transferred across streamlines only by molecular diffusion. The amount of cross flow is so small that, when a colored dye is injected at some point into the fluid, it follows a streamline without appreciable diffusion. In turbulent flow, on the other hand, the color will be distributed over a wide area a short distance downstream

from the point of injection. The mixing mechanism consists of rapidly fluctuating eddies which transport blobs of fluid in an irregular manner. Groups of particles collide with each other at random, establish cross flow on a macroscopic scale, and effectively mix the fluid. Since the mixing in turbulent flow is on a macroscopic scale with groups of particles transported in a zigzag path through the fluid, the exchange mechanism is many times more effective than in laminar flow. As a result, the rates of heat and momentum transfer in turbulent flow and the associated friction and heat-transfer coefficients are many times larger than in laminar flow.

Instantaneous streamlines in turbulent flow are highly jagged, and it would be a hopelessly difficult task to trace the path of individual fluid elements. However, if the flow at a point is averaged over a period of time, long as compared with the period of a single fluctuation, the time-mean properties and the velocity of the fluid are constant if the average flow remains steady. It is therefore general practice to describe each fluid property and the velocity in turbulent flow in terms of a *mean value* which does not vary with time and a *fluctuating component* which is a function of time. To simplify the problem, consider a two-dimensional flow (Fig. 6-17) in which the mean value of velocity is parallel to the x direction. The instantaneous velocity components u and v can then be expressed in the form

$$\begin{aligned} u &= \bar{u} + u' \\ v &= v' \end{aligned} \tag{6-43}$$

where the bar over a symbol denotes the temporal mean value, and the prime denotes the instantaneous deviation from the mean value. According to the model used to describe the flow,

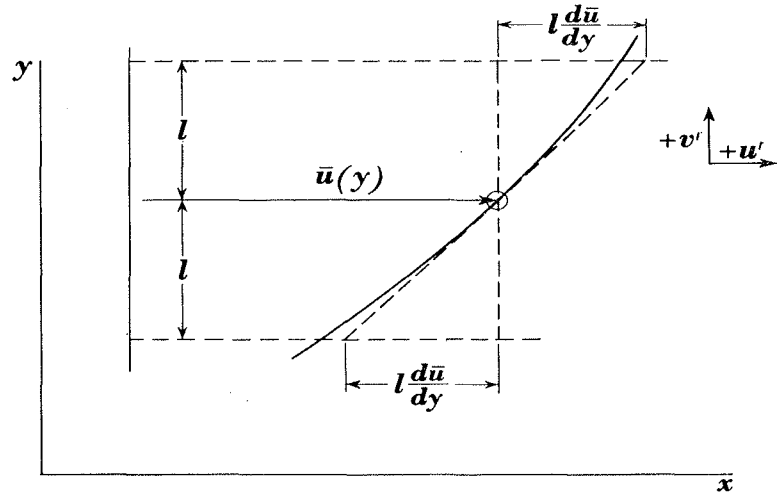

Fig. 6-17. Sketch illustrating mixing length for momentum transfer.

$$\bar{u} = \frac{1}{\theta^*} \int_0^{\theta^*} u d\theta \tag{6-44}$$

where θ^* is large compared with the period of the fluctuations. Figure 6-18 shows qualitatively the time variation of u and u'. From Eq. 6-44 or from an inspection of the graph it is apparent that the time average of u' is zero, i.e. $\bar{u}' = 0$. A similar argument shows that $\bar{v}'$ and $(\overline{\rho v})'$ are also zero.

The fluctuating velocity components continuously transport mass, and consequently momentum, across a plane normal to the y direction. The instantaneous rate of transfer in the y direction of x-momentum per unit area at any point is

$$-(\rho v)'(\bar{u} + u')$$

where the minus sign, as will be shown later, takes account of the statistical correlation between u' and v'.

The time average of the x-momentum transfer gives rise to an *apparent turbulent shear or Reynolds stress* τ_t defined by

$$g_c \tau_t = -\frac{1}{\theta^*} \int_0^{\theta^*} (\rho v)'(\bar{u} + u')\, d\theta \tag{6-45}$$

Breaking this term up into two parts, the time average of the first is zero, or

$$\frac{1}{\theta^*} \int_0^{\theta^*} (\rho v)' \bar{u} d\theta = 0$$

since $\bar{u}$ is a constant and the time average of $(\rho v)'$ is zero. Integrating the second term, Eq. 6-45 becomes

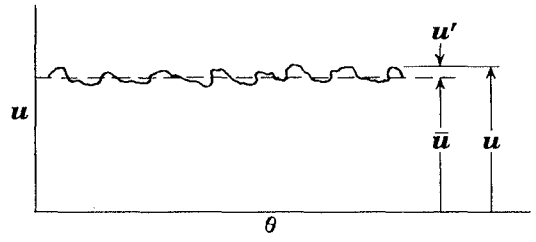

Fig. 6-18. Sketch illustrating time variation of instantaneous velocity.

$$g_c \tau_t = -\frac{1}{\theta^*} \int_0^{\theta^*} (\rho v)' u' \, d\theta = -\overline{(\rho v)' u'} \tag{6-45a}$$

or if ρ is constant

$$g_c \tau_t = -\rho(\overline{v' u'}) \tag{6-46}$$

It is not difficult to visualize that the time averages of the mixed products of velocity fluctuations, such as for example $\overline{v' u'}$, differ from zero. From Fig. 6-17 we can see that the particles which travel upward ($v' > 0$) arrive at a layer in the fluid in which the mean velocity $\bar{u}$ is larger than in the layer from which they come. Assuming that the fluid particles preserve on the average their original velocity $\bar{u}$ during their migration, they will tend to slow down other fluid particles after they have reached their destination and thereby give rise to a negative component u'. Conversely, if v' is negative, the observed value of u' at the new destination will be positive. On the average, therefore, a positive v' is associated with a negative u', and vice versa. The time average of $u'v'$ is therefore on the average not zero but a negative quantity. The turbulent shearing stress defined by Eq. 6-46 is thus positive and has the same sign as the corresponding laminar shearing stress (Eq. 6-15),

$$\tau_{yx} = \mu_f \frac{d\bar{u}}{dy} = \frac{\rho}{g_c} \nu \frac{d\bar{u}}{dy}$$

It should be noted, however, that the laminar shearing stress is a true stress, whereas the apparent turbulent shearing stress is simply a concept introduced to account for the effects of the momentum transfer by turbulent fluctuations. This concept allows us to express the total shear stress in turbulent flow as

$$\tau = \frac{\text{viscous force}}{\text{unit area}} + \frac{1}{g_c} (\text{turbulent momentum flux}) \tag{6-47}$$

To relate the turbulent momentum flux to the time-average velocity gradient, $d\bar{u}/dy$, Prandtl (10) postulated that fluctuations of macroscopic blobs of fluid in turbulent flow are, on the average, similar to the motion of molecules in a gas, i.e., they travel on the average a distance l perpendicular to $\bar{u}$ (Fig. 6-17) before coming to rest in another y plane. This distance l is known as Prandtl's mixing length and corresponds qualitatively to the mean free path of a gas molecule. Prandtl further argued that the fluid particles retain their identity and physical properties during the cross motion and that the turbulent fluctuation arises chiefly from the difference in the time-mean properties between y planes spaced a distance

l apart. According to this argument, if a fluid particle travels from the layer y to the layer $y + l$,

$$u' \simeq l \frac{d\bar{u}}{dy} \tag{6-48}$$

With this model we can write the turbulent shearing stress in a form analogous to the laminar shearing stress as

$$g_c \tau_t = -\rho \overline{v'u'} = \rho \epsilon_M \frac{d\bar{u}}{dy} \tag{6-49}$$

where the symbol ϵ_M is called the eddy viscosity or the turbulent exchange coefficient for momentum. The eddy viscosity ϵ_M is formally analogous to the kinematic viscosity ν, but whereas ν is a physical property, ϵ_M depends on the dynamics of the flow. Combining Eqs. 6-48 and 6-49 shows that $\epsilon_M = -\overline{v'l}$. Substituting Eqs. 6-15 and 6-49 in Eq. 6-47 gives the total shearing stress in the form

$$\tau = \frac{\rho}{g_c} (\nu + \epsilon_M) \frac{d\bar{u}}{dy} \tag{6-50}$$

In turbulent flow ϵ_M is much larger than ν and the viscous term may therefore be neglected.

The transfer of energy as heat in a turbulent flow can be pictured in an analogous fashion. Consider a two-dimensional time-mean temperature distribution as shown in Fig. 6-19. The fluctuating velocity components continuously transport fluid particles and the energy stored in

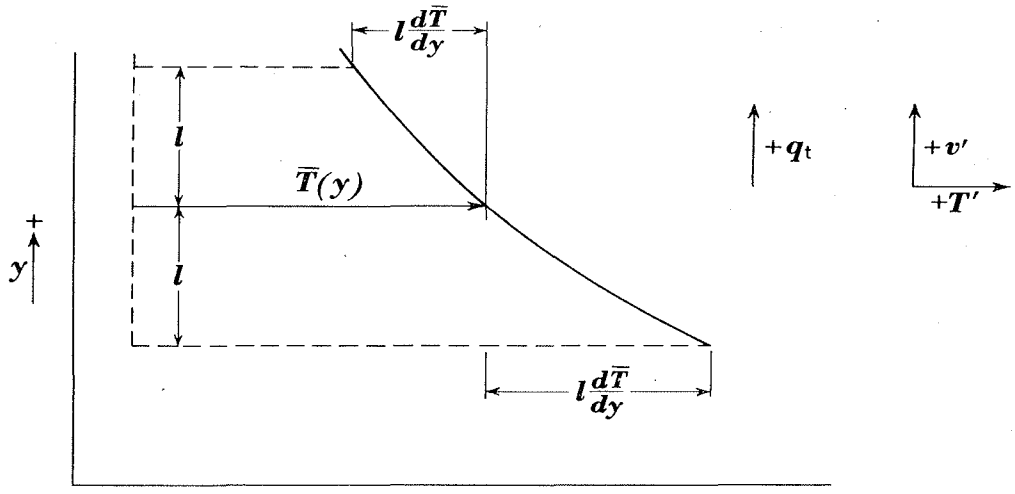

Fig. 6-19. Sketch illustrating mixing length for energy transfer.

them across a plane normal to the y direction. The instantaneous rate of energy transfer per unit area at any point in the y direction is

$$(\rho v')(c_p T) \tag{6-51}$$

where $T = \overline{T} + T'$. Following the same line of reasoning which led to Eq. 6-46, the time average of energy transfer due to the fluctuations, called the turbulent rate of heat transfer q_t, is

$$q_t = A\rho c_p \overline{v'T'} \tag{6-52}$$

Using Prandtl's concept of mixing length, we can relate the temperature fluctuation to the time-mean temperature gradient by the equation

$$T' \simeq l \frac{d\overline{T}}{dy} \tag{6-53}$$

This means physically that, when a fluid particle migrates from the layer y to another layer a distance l above or below, the resulting temperature fluctuation is caused chiefly by the difference between the time-mean temperatures in the layers. Assuming that the transport mechanisms of temperature (or energy) and velocity are similar, the mixing lengths in Eqs. 6-48 and 6-53 are equal. The product $\overline{v'T'}$, however, is positive on the average because a positive v' is accompanied by a positive T', and vice versa.

Combining Eqs. 6-52 and 6-53, the turbulent rate of heat transfer per unit area becomes

$$\frac{q_t}{A} = c_p \rho \overline{v'T'} = -c_p \rho \overline{v'l} \frac{d\overline{T}}{dy} \tag{6-54}$$

where the minus sign is a consequence of the second law of thermodynamics (see Sec. 1-3). To express the turbulent heat flux in a form analogous to the Fourier conduction equation we define ϵ_H, a quantity called the turbulent exchange coefficient for temperature, eddy diffusivity of heat, or eddy heat conductivity, by the equation $\epsilon_H = \overline{v'l}$. Substituting ϵ_H for $\overline{v'l}$ in Eq. 6-54, gives

$$\frac{q_t}{A} = -c_p \rho \epsilon_H \frac{d\overline{T}}{dy} \tag{6-55}$$

The total rate of heat transfer per unit area normal to the mean stream velocity can then be written as

$$\frac{q}{A} = \frac{\text{molecular conduction}}{\text{unit area}} + \frac{\text{turbulent transfer}}{\text{unit area}}$$

or in symbolic form as

$$\frac{q}{A} = -c_p \rho (a + \epsilon_H) \frac{d\overline{T}}{dy} \tag{6-56}$$

where $a = k/c_p\rho$, the molecular diffusivity of heat. The contribution to the heat transfer by molecular conduction is proportional to a, and the turbulent contribution is proportional to ϵ_H. For all fluids except liquid metals, ϵ_H is much larger than a in turbulent flow. The ratio of the molecular kinematic viscosity to the molecular diffusivity of heat ν/a has previously been named the Prandtl number. Similarly, the ratio of the turbulent eddy viscosity to the eddy diffusivity ϵ_M/ϵ_H could be considered a turbulent Prandtl number Pr_t. According to the Prandtl mixing-length theory, the turbulent Prandtl number is unity, since $\epsilon_M = \epsilon_H = \overline{v'l}$.

Although the model postulated by Prandtl in his treatment of turbulent flow is certainly grossly oversimplified, experimental results indicate it is at least qualitatively correct. Isakoff and Drew (11) found that Pr_t for the heating of mercury in turbulent flow inside a tube may vary from 1.0 to 1.6, and Forstall and Shapiro (12) found that Pr_t is about 0.7 for gases. The latter investigators also showed that Pr_t is substantially independent of the value of the laminar Prandtl number as well as of the type of experiment. For practical calculations it is usually satisfactory to assume that Pr_t is unity. With this simplification we can relate the turbulent heat flux to the turbulent shear stress by combining Eqs. 6-49 and 6-55 and obtain

$$\frac{q_t}{A} = -g_c \tau_t c_p \frac{d\overline{T}}{d\overline{u}} \tag{6-57}$$

This relation was originally drived in 1874 by the British scientist Osborn Reynolds and is called the *Reynolds analogy* in his honor. It is a good approximation whenever the flow is turbulent, and can be applied to turbulent boundary layers as well as to turbulent flow in pipes or ducts. However, the Reynolds analogy does not hold in the laminar sublayer. Since this layer offers a large thermal resistance to the flow of heat, Eq. 6-57 does in general not suffice for a quantitative solution. Only for fluids having a Prandtl number of unity can it be used directly to calculate the rate of heat transfer. This special case will now be considered.

6-10. *Reynolds analogy for turbulent flow over a flat plate*

In this section we shall derive for flow over a plane surface a relation between the heat transfer and the skin friction for a Prandtl number of

unity. In the following section we shall show how to calculate the skin friction and consider some improvements over the simple analogy.

In two-dimensional flow the shearing stress in the laminar sublayer τ_{yx} is (Eq. 6-15)

$$g_c \tau_{yx} = \mu \frac{du}{dy}$$

and the rate of heat flow per unit area across any plane perpendicular to the y direction is (Eq. 1-1)

$$\frac{q}{A} = -k \frac{dT}{dy}$$

Combining Eqs. 1-1 and 6-15 yields

$$\frac{q}{A} = -g_c \tau_{yx} \frac{k}{\mu} \frac{dT}{du} \tag{6-58}$$

An inspection of Eqs. 6-57 and 6-58 shows that if $c_p = k/\mu$ (i.e., for Pr = 1), the same equation of heat flow applies in the laminar and turbulent layers.

To determine the rate of heat transfer from a flat plate to a fluid with Pr = 1 flowing over it in turbulent flow, we replace k/μ by c_p and separate the variables in Eq. 6-58. Assuming that q and τ are constant, we get the equation

$$\frac{q_s}{A \tau_s c_p g_c} du = -dT \tag{6-59}$$

where the subscript s is used to indicate that both q and τ are taken at the surface of the plate. Integrating Eq. 6-59 between the limits $u = 0$ when $T = T_s$, and $u = u_\infty$ when $T = T_\infty$, yields

$$\frac{q_s}{A \tau_s c_p g_c} u_\infty = (T_s - T_\infty) \tag{6-60}$$

But since by definition

$$h_{cx} = \frac{q_s}{A (T_s - T_\infty)} \qquad \text{and} \qquad \tau_{sx} = C_{fx} \frac{\rho u_\infty^2}{2 g_c}$$

Eq. 6-60 can be written as

$$\frac{h_{cx}}{c_p \rho u_\infty} = \frac{\text{Nu}}{\text{Re}_x \text{Pr}} = \frac{C_{fx}}{2} \tag{6-61}$$

Equation 6-61 is satisfactory for gases in which Pr is approximately unity. Colburn (4) has shown that Eq. 6-61 can also be used for fluids having Prandtl numbers ranging from 0.6 to about 50 if it is modified in accordance with experimental results to read

$$\frac{\mathrm{Nu}_x}{\mathrm{Re}_x \mathrm{Pr}} \mathrm{Pr}^{2/3} = \mathrm{St}_x \mathrm{Pr}^{2/3} = \frac{C_{fx}}{2} \tag{6-62}$$

where the subscript x denotes the distance from the leading edge of the plate.

6-11. *Turbulent flow over plane surfaces*

To apply the analogy between heat transfer and momentum transfer in practice it is necessary to know the skin-friction coefficient C_{fx}. For turbulent flow over a plane surface the empirical equation for the local friction coefficient

$$C_{fx} = 0.0576 \left(\frac{u_\infty x}{\nu}\right)^{-1/5} \tag{6-63}$$

is in good agreement with experimental results (1) in the Reynolds number range between 5×10^5 and 10^7 as long as no separation occurs. Assuming that the turbulent boundary layer starts at the leading edge, the average friction coefficient over a plane surface of length L can be obtained by integrating Eq. 6-63, or

$$\bar{C}_f = \frac{1}{L} \int_0^L C_{fx}\, dx = 0.072 \left(\frac{u_\infty L}{\nu}\right)^{-1/5} \tag{6-64}$$

In reality, however, a laminar boundary layer precedes the turbulent boundary layer between $x = 0$ and $x = x_c$. Since the local frictional drag of a laminar boundary layer is less than the local frictional drag of a turbulent boundary layer at the same Reynolds number, the average drag calculated from Eq. 6-64 without correcting for the laminar portion of the boundary layer is too large. The actual drag can be closely estimated, however, by assuming that, behind the point of transition, the turbulent boundary layer behaves as though it had started at the leading edge.

Adding the laminar friction drag between $x = 0$ and $x = x_c$ to the turbulent drag between $x = x_c$ and $x = L$ gives, per unit width,

$$\bar{C}_f = [0.072\, \mathrm{Re}_L^{-1/5} L - 0.072\, \mathrm{Re}_{x_c}^{-1/5} x_c + 1.33\, \mathrm{Re}_{x_c}^{-1/2} x_c]/L$$

For a critical Reynolds number of 5×10^5 this yields

$$\bar{C}_f = 0.072\,(\mathrm{Re}_L^{-1/5} - 0.0464\,x_c/L) \tag{6-65}$$

Substituting Eq. 6-63 for C_{fx} in Eq. 6-62 yields the local Nusselt number at any value of x larger than x_c, or

$$\mathrm{Nu}_x = \frac{h_{cx}x}{k} = 0.0288\,\mathrm{Pr}^{1/3}\left(\frac{u_\infty x}{\nu}\right)^{0.8} \tag{6-66}$$

We observe that the local heat-transfer coefficient h_{cx} for heat transfer by convection through a turbulent boundary layer decreases with the distance x as $h_{cx} \propto 1/x^{0.2}$. Equation 6-66 shows that, in comparison with laminar flow where $h_{cx} \propto 1/x^{1/2}$, the heat-transfer coefficient in turbulent flow decreases less rapidly with x and that the turbulent-heat-transfer coefficient is much larger than the laminar heat-transfer coefficient at a given value of the Reynolds number.

The average conductance in turbulent flow over a plane surface of length L can be calculated to a first approximation by integrating Eq. 6-66 between $x = 0$ and $x = L$, or

$$\bar{h}_c = \frac{1}{L}\int_0^L h_{cx}dx$$

In dimensionless form we get

$$\overline{\mathrm{Nu}}_L = \frac{\bar{h}_c L}{k} = 0.036\,\mathrm{Pr}^{1/3}\,\mathrm{Re}_L^{0.8} \tag{6-67}$$

Equation 6-67 neglects the existence of the laminar boundary layer and is therefore valid only when $L \gg x_c$. The laminar boundary layer can be included in the analysis if Eq. 6-28 is used between $x = 0$ and $x = x_c$, and Eq. 6-66 between $x = x_c$ and $x = L$ for the integration of h_{cx}. This yields for $\mathrm{Re}_c = 5 \times 10^5$

$$\overline{\mathrm{Nu}}_L = 0.036\,\mathrm{Pr}^{1/3}(\mathrm{Re}_L^{0.8} - 23{,}200) \tag{6-68}$$

EXAMPLE 6-3. The crankcase of an automobile is approximately 30 in. long, 12 in. wide, and 4 in. deep. Assuming that the surface temperature of the crankcase is 160 F, estimate the rate of heat flow from the crankcase to atmospheric air at 40 F at a road speed of 60 mph. Assume that the vibration of the engine and the chassis induce the transition from laminar to turbulent flow so near to the leading edge that, for practical purposes, the boundary layer is turbulent over the entire surface. Neglect radiation and use for the front and rear surfaces the same average convective heat-transfer coefficient as for the bottom and sides.

Solution: Using physical properties of air at 100 F from Table A-3 in Appendix III, the Reynolds number is

$$\mathrm{Re}_L = \frac{u_\infty \rho L}{\mu} = \frac{(88 \text{ ft/sec})(0.071 \text{ lb}_m/\text{cu ft})(30/12 \text{ ft})}{1.285 \times 10^{-5} \text{lb}_m/\text{ft sec}}$$

$$= 1.21 \times 10^6$$

From Eq. 6-67 the average Nusselt number is

$$\overline{\mathrm{Nu}}_L = 0.036 \, \mathrm{Pr}^{1/3} \, \mathrm{Re}_L^{0.8}$$

$$= (0.036)(0.896)(73{,}480) = 2370$$

and the average convective heat-transfer coefficient becomes

$$\bar{h}_c = \overline{\mathrm{Nu}}_L \frac{k}{L} = \frac{(2370)(0.0154 \text{ Btu/hr ft F})}{30/12 \text{ ft}}$$

$$= 14.55 \text{ Btu/hr sq ft F}$$

The overall area is 4.84 sq ft and the rate of heat loss is therefore

$$q = \bar{h}_c A (T_s - T_\infty) = (14.55)(4.84)(160-40) = 8430 \text{ Btu/hr} \qquad \textit{Ans.}$$

The thickness of a turbulent boundary layer in flow over a plane surface can be calculated by means of the Karman integral relations. To improve the accuracy of the calculations, we shall use a velocity distribution determined by experiment. Figure 6-20 shows several velocity profiles measured by Van der Hegge-Zynen (14). Near the wall the velocity increases linearly with the distance from the surface. This is the region called the laminar sublayer, although some recent measurements suggest that it is not completely devoid of turbulence. In the fully turbulent portion of the boundary layer the velocity increases with the one-seventh power of distance and can be represented by the equation

$$\frac{u}{u_\infty} = \left(\frac{y}{\delta}\right)^{1/7} \tag{6-69}$$

Between the laminar sublayer and the turbulent portion of the boundary layer is a transition region where the turbulence level is variable. Because the laminar sublayer as well as the transition layer are very thin we shall, as a first approximation, neglect both of them and use Eq. 6-69 to evaluate the momentum change in the integral equations. This approximation cannot be used, however, to determine the shearing stress because, according to Eq. 6-69, the velocity gradient is

$$\frac{du}{dy} = \frac{1}{7} \frac{u_\infty}{\delta^{1/7} y^{6/7}}$$

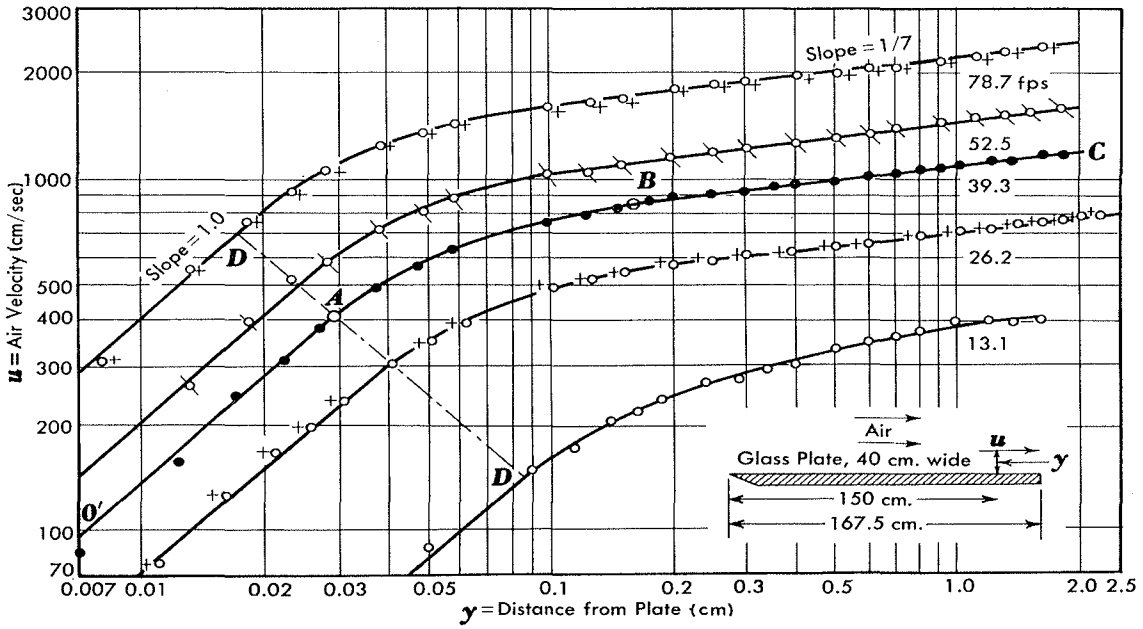

Fig. 6-20. Velocity distribution in turbulent boundary layers over plane surfaces after Van der Hegge-Zynen (14).

which would lead to infinitely large shearing stress at the wall (i.e., at $y = 0$). To overcome this difficulty we shall use an experimentally determined relation for the shearing stress.

In the Reynolds-number range between 10^5 and 10^7 the relation

$$g_c\tau_s = 0.0228\,\rho u_\infty^2 \left(\frac{\nu}{u_\infty \delta}\right)^{1/4} \tag{6-70}$$

is in good agreement with experimental results obtained by Schultz-Grunow (15). Substituting Eq. 6-70 for the shearing stress and Eq. 6-69 for the velocity distribution in the integral of Eq. 6-33 gives

$$\frac{7}{72}\,\rho u_\infty^2 \frac{d\delta}{dx} = 0.0228\,\rho u_\infty^2 \left(\frac{\nu}{u_\infty \delta}\right)^{1/4}$$

Separation of the variables yields

$$\delta^{1/4} d\delta = 0.235 \left(\frac{\nu}{u_\infty}\right)^{1/4} dx$$

from which we obtain the boundary-layer thickness in the form

$$\delta = 0.376 \left(\frac{\nu}{u_\infty}\right)^{1/5} x^{4/5}$$

or

$$\frac{\delta}{x} = 0.376\,\mathrm{Re}_x^{-1/5} \tag{6-71}$$

where $\mathrm{Re}_x = (u_\infty x/\nu)$. It can be seen from Eqs. 6-36 and 6-71 that, at any given value of x, a turbulent boundary layer increases at a faster rate than a laminar boundary layer. Despite its greater thickness, the turbulent boundary layer offers less resistance to heat flow than a laminar layer because the turbulent eddies produce continuous mixing between warmer and cooler fluids on a macroscopic scale. An inspection of the velocity profiles in Fig. 6-20 shows, however, that the eddies diminish in intensity in the buffer layer and hardly penetrate the laminar sublayer. Unless the Prandtl number equals unity, the relative magnitudes of the eddy conductivity and the molecular conductivity in the vicinity of the surface have a pronounced effect on the heat-transfer coefficient.

The effect of the diminution of the turbulent mixing near the surface on the heat-transfer coefficient for fluids having Prandtl numbers larger than unity was considered by Prandtl (16,17), von Karman (18), and most recently also by Deissler (19) in their respective improvements of the Reynolds analogy. Martinelli (20) also treated the problem of heat transfer to liquid metals, which have very small Prandtl numbers.

Prandtl divided the flow field into a laminar and a turbulent layer but neglected the buffer layer in his analysis. The relation for flow over plane surfaces, derived in detail in Ref. 21, is

$$\frac{\mathrm{Nu}_x}{\mathrm{Re}_x\mathrm{Pr}} = \frac{C_{fx}/2}{1 + 2.1\,\mathrm{Re}_x^{-0.1}(\mathrm{Pr} - 1)} \tag{6-72}$$

We observe that, for $\mathrm{Pr} = 1$, Eq. 6-72 reduces to the simple Reynolds analogy. The second term in the denominator is a measure of the thermal resistance in the laminar sublayer. We see that this portion of the total thermal resistance increases as the Prandtl number becomes larger and accounts for most of the thermal resistance when the Prandtl number is very large.

Prandtl's analysis was later refined by von Karman (18), who divided the flow field into three zones: a laminar sublayer adjacent to the surface in which the eddy diffusivity is zero and heat flows only by conduction; next to it a buffer layer in which both conduction and convection contribute the heat-transfer mechanism (i.e., $k/c\rho$ and ϵ_H are of the same order of magnitude); and, finally, a turbulent region in which conduction is negligible compared to convection, and the Reynolds analogy applies. He used experimental data for the velocity distribution and the shear stress to evaluate ϵ_M from Eq. 6-50 and assumed $\epsilon_M = \epsilon_H$ in his analysis. He also postulated that the physical properties of the fluid are indepen-

dent of the temperature. With these simplifications he determined the thermal resistances in each of the three zones. The results of von Karman's analysis are given below for flow over a flat plate:

Thermal resistance of laminar sublayer	$\dfrac{5\,\mathrm{Pr}}{c_p\sqrt{\rho g_c \tau_s}}$
Thermal resistance of buffer layer	$\dfrac{5\ln(5\,\mathrm{Pr}+1)}{c_p\sqrt{\rho g_c \tau_s}}$
Thermal resistance of the turbulent region	$\dfrac{5(1+\ln 6)+u_\infty/\sqrt{\tau_s g_c/\rho}}{c_p\sqrt{\rho g_c \tau_s}}$

Adding the thermal resistances and introducing the definitions for the Stanton number St and the local drag-friction coefficient C_{fx} yields, after some rearrangement, the expression

$$\mathrm{St}_x = \frac{\mathrm{Nu}_x}{\mathrm{Re}_x\mathrm{Pr}} = \frac{C_{fx}/2}{1+5\sqrt{C_{fx}/2}\left[(\mathrm{Pr}-1)+\ln\dfrac{5\,\mathrm{Pr}+1}{6}\right]} \tag{6-73}$$

for the local value of the Stanton number for flow over a plane surface at a given value of x. The average value of St or $\bar{h}_c$ over a surface of length L can be obtained by numerical or graphical integration.

To apply any of the equations relating the Stanton number and the friction coefficient in practice, the physical properties must be evaluated at some appropriate mean temperature. It is general practice to evaluate the physical properties at the *mean film temperature* T_f defined as $T_f = (T_s + T_\infty)/2$. This procedure is purely empirical, but has been found satisfactory for moderate-temperature ranges.

The three-distinct-layer concept is somewhat of an oversimplification of the real situation but is satisfactory for Prandtl numbers less than 25 or 30. For larger Prandtl numbers it is preferable to assume turbulent eddy generation near the outer edges of turbulent boundary layers and continuous damping of these eddies as they approach the wall. Some progress has been made recently with this approach (19,22), and the reader is referred to the original papers for details. An extensive review of the analogies is presented in Ref. 23.

6-12. *Heat transfer in high-speed flow*

Convection heat transfer in high-speed flow is important for systems such as aircraft and missiles when the velocity approaches or exceeds the velocity of sound. For a perfect gas the accoustical velocity, a, can be

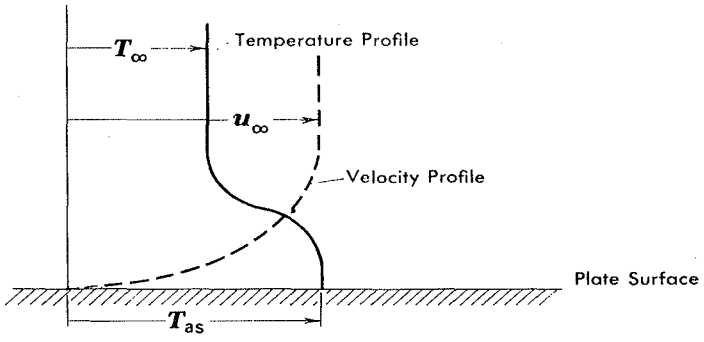

Fig. 6-21. Velocity and temperature distribution in high-speed flow over an insulated plate.

obtained from the relation

$$a = \sqrt{\gamma R T/\mathfrak{M}} \tag{6-74}$$

where γ = specific heat ratio, c_p/c_u (about 1.4 for air)
R = universal gas constant
T = absolute temperature, and
$\mathfrak{M}$ = molecular weight of the gas.

When the velocity of a gas flowing over a heated or cooled surface is of the order of the accoustical velocity or larger, the flow field can no longer be described solely in terms of the Reynolds number, but also the ratio of the gas flow-velocity to the accoustical velocity, i.e., the Mach number $M = u_\infty/a_\infty$, must be considered. When the gas velocity in a flow system reaches a value of about one-half of the speed of sound, the effects of viscous dissipation in the boundary layer become important. Under such conditions the temperature of a surface over which a gas is flowing can actually exceed the free-stream temperature. For flow over an adiabatic surface, e.g., a perfectly insulated wall, Fig. 6-21 shows the velocity and temperature distributions schematically. The high temperature at the surface is the combined result of the heating due to viscous dissipation and the temperature rise of the fluid as the kinetic energy of the flow is converted to internal energy while the flow decelerates through the boundary layer. The actual shape of the temperature profile depends on the relation between the rate at which viscous shear work increases the internal energy of the fluid and the rate at which heat is conducted towards the free stream.

Although the processes in a high-speed boundary layer are not adiabatic, it is general practice to relate them to adiabatic processes. The conversion of kinetic energy in a gas being slowed down adiabatically to zero velocity is described by the relation

$$i_0 = i_\infty + u_\infty^2/2Jg_c \tag{6-75}$$

where i_0 is the stagnation enthalpy and i_∞ is the enthalpy of the gas in the free stream. For an ideal gas Eq. 6-75 becomes

$$T_0 = T_\infty + u_\infty^2/2Jg_c c_p$$

or in terms of the Mach number

$$\frac{T_0}{T_\infty} = 1 + \frac{\gamma - 1}{2} M_\infty^2 \tag{6-76}$$

where T_0 is the stagnation temperature and T_∞ is the free-stream temperature.

In a real boundary layer the fluid is not brought to rest reversibly because the viscous shearing process is thermodynamically irreversible. To account for the irreversibility in a boundary-layer flow we define a recovery factor r as

$$r = \frac{T_{as} - T_\infty}{T_0 - T_\infty} \tag{6-77}$$

where T_{as} is the adiabatic surface temperature.

Experiments (31) have shown that in laminar flow,

$$r = \mathrm{Pr}^{1/2} \tag{6-78}$$

whereas in turbulent flow

$$r = \mathrm{Pr}^{1/3} \tag{6-79}$$

When a surface is not insulated, the rate of heat transfer by convection between a high-speed gas and that surface is governed by the relation

$$q_c/A = -k\frac{\partial T}{\partial y}\bigg|_{y=0}$$

The influence of heat transfer to and from the surface on the temperature distribution is illustrated in Fig. 6-22. We observe that in high-speed flow heat can be transferred to the surface even when the surface temperature is above the free-stream temperature. This phenomenon is the result of viscous shear, often called aerodynamic heating. The heat transfer in high-speed flow over a flat surface can be predicted (1) from the boundary-layer energy equation

$$u\frac{\partial T}{\partial x} + v\frac{\partial T}{\partial y} = a\frac{\partial^2 T}{\partial y^2} + \frac{\mu}{\rho c_p}\left(\frac{\partial u}{\partial x}\right)^2$$

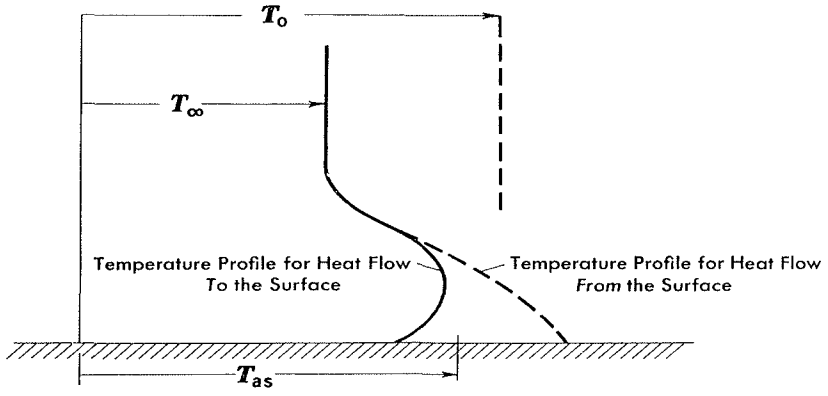

Fig. 6-22. Temperature profiles in high-speed boundary layer for heating and cooling.

where the last term accounts for the viscous dissipation. However, for most practical purposes the rate of heat transfer can be calculated with the same relations used for low speed flow, if the average convection heat-transfer coefficient is redefined by the relation

$$q_c/A = \bar{h}_c(T_s - T_{as}) \tag{6-80}$$

which will yield a zero heat flow when the surface temperature T_s equals the adiabatic surface temperature.

Since in high-speed flow the temperature gradients in a boundary layer are large, also variations in the physical properties of the fluid will be substantial. Eckert (32) has shown, however, that the constant property heat-transfer equations can still be used if all the properties are evaluated at a reference temperature T^* given by the relation

$$T^* = T_\infty + 0.5(T_s - T_\infty) + 0.22(T_{as} - T_\infty) \tag{6-81}$$

The local values of the heat-transfer coefficient, defined by the relation

$$h_{cx} = (q/A)/(T_s - T_{as})$$

can be obtained from the following equations:

Laminar Boundary Layer ($\mathrm{Re}_x^* < 10^5$):

$$\mathrm{St}_x^* = \left(\frac{h_{cx}}{c_p \rho u_\infty}\right)^* = 0.332(\mathrm{Re}_x^*)^{-1/2}(\mathrm{Pr}^*)^{-2/3} \tag{6-82}$$

Turbulent Boundary Layer ($10^5 < \mathrm{Re}_x^* < 10^7$):

$$\mathrm{St}_x^* = \left(\frac{h_{cx}}{c_p \rho u_\infty}\right)^* = 0.0288(\mathrm{Re}_x^*)^{-1/5}(\mathrm{Pr}^*)^{-2/3} \tag{6-83}$$

Turbulent Boundary Layer ($10^7 < \mathrm{Re}_x^* < 10^9$):

$$\mathrm{St}_x^* = \left(\frac{h_{cx}}{c\rho u_\infty}\right)^* = \frac{2.46}{(ln\mathrm{Re}_x^*)^{2.584}}(\mathrm{Pr}^*)^{-2/3} \tag{6-84}$$

because experimental data for local friction coefficients in high-speed gas flow (32) in the Reynolds number range between 10^7 and 10^9 are correlated by the relation

$$C_{fx} = \frac{4.92}{(ln\mathrm{Re}_x^*)^{2.584}} \tag{6-85}$$

If the average value of the heat-transfer coefficients is to be determined, the above expressions must be integrated between $x = 0$ and $x = L$ as shown in Sec. 6-7 for low-speed flow. However, the integration may have to be done numerically in most practical cases because the reference temperature T^* is not the same for the laminar and turbulent portions of the boundary layer, as shown by Eqs. 6-78 and 6-79.

When the speed of a gas is exceedingly high the boundary layer may become so hot that the gas begins to dissociate. In such situations Eckert (32) recommends that the heat-transfer coefficient be based on the enthalpy difference and be defined by the relation

$$q_c/A = h_{ci}(i_s - i_{as}) \tag{6-86}$$

If an enthalpy recovery factor is defined by

$$r_i = \frac{i_{as} - i_\infty}{i_0 - i_\infty} \tag{6-87}$$

the same relation used previously to calculate the reference temperature can be used to calculate a reference enthalpy, or

$$i^* = i_\infty + 0.5(i_s - i_\infty) + 0.22(i_{as} - i_\infty) \tag{6-88}$$

The local Stanton number is then redefined as

$$\mathrm{St}_{x,i}^* = \frac{h_{c,i}}{\rho^* u_\infty} \tag{6-89}$$

and used in Eqs. 6-83, 6-84, and 6-85 to calculate the heat-transfer coefficient. It should be noted that the enthalpies in the above relations are the total values, which include the chemical energy of dissociation as well as the internal energy. As shown in Ref. 32, this method of calculation is in excellent agreement with experimental data.

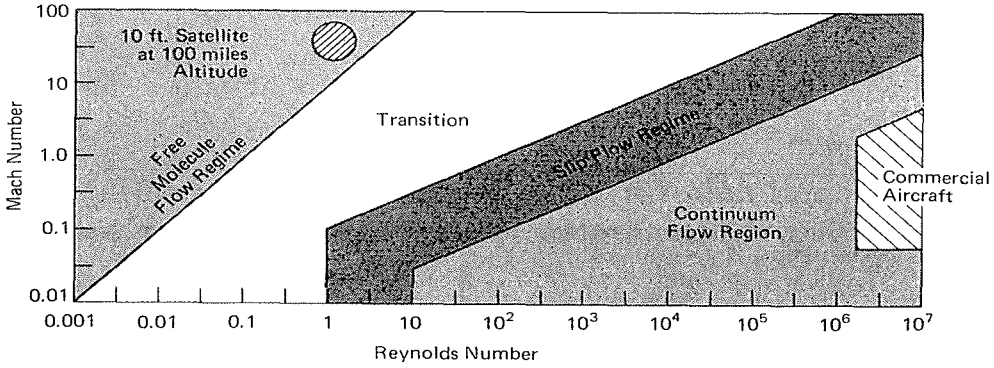

Fig. 6-23. Flow regimes.

In some situations, e.g., extremely high altitudes, the fluid density may be so small that the distance between gas molecules becomes of the same order of magnitude as the boundary layer. In such cases the fluid cannot be treated as a continuum and it is necessary to subdivide the flow processes into regimes. These flow regimes are characterized by the ratio of the molecular free path to a significant physical scale of the system, called the Knudsen number, Kn. Continuum flow corresponds to small values of Kn, while at larger values of Kn, molecular collisions occur primarily at the surface and in the main stream. Since energy transport is by free motion of molecules between the surface and the main stream, this regime is called "free-molecule." Between the free-molecule and the continuum regime is a transition range, called the "slip-flow" regime because it is treated by assuming temperature and velocity "slip" at fluid-solid interfaces. Fig. 6-23 shows a map of these flow regimes. For a treatment of heat transfer and friction in these specialized flow systems the reader is referred to Refs. 33, 34, and 35.

6-13. Closure

In this chapter we have studied the principles of heat transfer by forced convection. We have seen that the transfer of heat by convection is intimately related to the mechanics of the fluid flow, particularly to the flow in the vicinity of the heat-transfer surface. We have also observed that the nature of heat transfer as well as flow phenomena depend greatly on whether the fluid far away from the surface is in laminar or in turbulent flow.

To become familiar with the basic principles of boundary layer theory and forced-convection heat transfer, we have considered the problem of convection in flow over a flat plate in some detail. This system is geometrically very simple, but it illustrates the most important features of forced convection. In subsequent chapters we shall treat heat transfer by

Table 6-5. Summary of useful equations for calculating friction and heat-transfer coefficients in flow over flat surfaces.*

LAMINAR FLOW		
Local friction coefficient	$C_{fx} = 0.664\,\mathrm{Re}_x^{-0.5}$	$\mathrm{Re}_x < 5 \times 10^5$
Local Nusselt number at distance x from leading edge	$\mathrm{Nu}_x = 0.332\,\mathrm{Re}_x^{0.5}\,\mathrm{Pr}^{0.33}$	$\mathrm{Pr} > 0.1, \mathrm{Re}_x > 5 \times 10^5$
	$\mathrm{Nu}_x = 0.565(\mathrm{Re}_x\,\mathrm{Pr})^{0.5}$	$\mathrm{Pr} < 0.1, \mathrm{Re}_x < 5 \times 10^5$
Average friction coefficient	$\bar{C}_f = 1.33\,\mathrm{Re}_L^{-0.5}$	$\mathrm{Re}_L < 5 \times 10^5$
Average Nusselt number between $x = 0$ and $x = L$	$\overline{\mathrm{Nu}}_L = 0.664\,\mathrm{Re}_L^{0.5}\,\mathrm{Pr}^{0.33}$	$\mathrm{Pr} > 0.1, \mathrm{Re}_L < 5 \times 10^5$
	$\overline{\mathrm{Nu}}_L = 1.13(\mathrm{Re}_L\,\mathrm{Pr})^{0.5}$	$\mathrm{Pr} < 0.1, \mathrm{Re}_L < 5 \times 10^5$
TURBULENT FLOW		
Local friction coefficient	$C_{fx} = 0.0576\,\mathrm{Re}_x^{-0.2}$	$\mathrm{Re}_x > 5 \times 10^5, \mathrm{Pr} > 0.5$
Local Nusselt number at distance x from leading edge	$\mathrm{Nu}_x = 0.0288\,\mathrm{Re}_x^{0.8}\,\mathrm{Pr}^{0.3}$	$\mathrm{Re}_x > 5 \times 10^5, \mathrm{Pr} > 0.5$
	(For $\mathrm{Pr} < 0.1$ use Eq. 6-73 or see Ref. 20)	
Average friction coefficient	$\bar{C}_f = 0.072[\mathrm{Re}_L^{-0.2} - 0.0464(x_{\mathrm{crit}}/L)]$	$\mathrm{Re}_L > 5 \times 10^5, \mathrm{Pr} > 0.5$
Average Nusselt number between $x = 0$ and $x = L$ with transition at $\mathrm{Re}_{x,\mathrm{crit}} = 5 \times 10^5$	$\overline{\mathrm{Nu}}_L = 0.036\,\mathrm{Pr}^{0.33}[\mathrm{Re}_L^{0.8} - 23{,}200]$	$\mathrm{Re}_L > 5 \times 10^5, \mathrm{Pr} > 0.5$

*Applicable to low-speed flow (Mach number < 0.5) of gases and liquids if all physical properties at the mean film temperature, $T_f = (T_s + T_\infty)/2$.

$$C_{fx} = \tau_s/(\rho u_\infty^2/2g_c), \qquad \bar{C}_f = (1/L)\int_0^L C_{fx}\,dx$$

$$\mathrm{Nu}_x = h_c x/k, \qquad \overline{\mathrm{Nu}} = \bar{h}_c L/k, \qquad \bar{h}_c = (1/L)\int_0^L h_c(x)\,dx$$

$$\mathrm{Re}_x = \rho u_\infty x/\mu, \qquad \mathrm{Re}_L = \rho u_\infty L/\mu, \qquad \mathrm{Pr} = c_p\mu/k$$

convection in geometrically more complicated systems. In the next chapter we shall examine free-convection phenomena. In Chapter 8, heat transfer by convection to and from fluids flowing inside of pipes and ducts will be taken up. In Chapter 9, forced convection in flow over the exterior surfaces of bodies such as cylinders, spheres, tubes, and tube bundles will be considered. The application of the principles of forced-convection heat transfer to the selection and design of heat-transfer equipment will be taken up in Chapter 11.

For the convenience of the reader, a summary of the equations used to calculate the heat-transfer and the friction coefficients in low-speed flow of gases and liquids over flat, or only slightly curved, plane surfaces is presented in Table 6-5.

PROBLEMS

The problems below have been organized in the following manner: Problems 6-1 through 6-5 deal with the evaluation of dimensionless parameters, 6-6 through 6-17 with dimensional analysis, 6-18 through 6-33 with the evaluation of heat transfer and friction coefficients in flow over a flat plate, 6-34 through 6-40 with boundary layers, 6-41 through 6-48 with thermal design, and 6-49 through 6-54 with high-speed flow.

6-1. Evaluate the Reynolds number from the following data:

$$D = 6 \text{ in.}$$
$$u_\infty = 1.0 \text{ ft/sec.}$$
$$\rho = 30 \text{ slug/ft}^3$$
$$\mu = 90 \text{ lb}_m/\text{ft hr}$$

Ans. 19,333

6-2. Evaluate the Prandtl number from the data below:

$$c_p = 0.5 \text{ Btu/lb}_m \text{ F}$$
$$k = 2 \text{ Btu/ft hr F}$$
$$\mu = 5 \text{ dyne sec/cm}^2$$

6-3. Evaluate the Nusselt number for the following condition:

$$D = 6 \text{ in.}$$
$$k = 2 \text{ Kcal/m hr C}$$
$$h = 18 \text{ Btu/ft}^2 \text{ hr F}$$

Ans. 7.7

6-4. Evaluate the Stanton number for the data below:

$$D = 4 \text{ in.}$$
$$V = 12 \text{ ft/sec.}$$

$$\rho = 1280 \text{ lb}_m/\text{ft}^3$$
$$\mu = 30 \text{ slug}/\text{ft hr}$$
$$c_p = 0.95 \text{ Btu}/\text{lb}_m$$
$$\bar{h}_c = 3.0 \text{ Btu}/\text{hr ft}^2 \text{ F}$$

6-5. Evaluate the dimensionless groups $\bar{h}_c D/k$, $u_\infty D\rho/\mu$, $c_p\mu/k$, and $\bar{h}_c/c_p G$ for water, ethyl alcohol, mercury, hydrogen, air, and saturated steam over as wide a temperature range as possible and plot the results vs. temperature. For the purpose of these calculations let $D = 1$ ft, $V = 1$ ft/sec, and $\bar{h}_c = 1$ Btu/hr sq ft F.

6-6. Replot the data points of Fig. 6-6 on a log-log paper and find an equation approximating the best correlation line. Compare your results with Fig. 6-7. Then, suppose steam at 1 atm and 212 F is flowing across a 2-in.-OD pipe at a velocity of 20 fps. Using the data in Fig. 6-7 estimate the Nusselt number, the heat-transfer coefficient, and the rate of heat transfer per ft length of pipe if the pipe is at 400 F.

6-7. The average Reynolds number for air passing in turbulent flow over a 60-in.-long flat plate is 2.4×10^6. Under these conditions the average Nusselt number was found to be equal to 4150. Determine the average heat-transfer coefficient for an oil having a thermal conductivity of 0.11 Btu/hr sq ft F, a specific heat of 0.8 Btu/lb, and a viscosity of 22 lb/ft hr at the same Reynolds number in flow over the same plate.

6-8. A long solid cylinder of radius r_o, initially at a uniform temperature T_o, is suddenly immersed in a fluid at temperature T_∞ with a unit-surface conductance $\bar{h}$. Show by means of dimensional analysis that the temperature distribution can be expressed in terms of the following four parameters:

$$[T(r) - T_\infty]/(T_o - T_\infty), \qquad r/r_o, \qquad a\theta/r_o^2, \qquad \bar{h}r_o/k.$$

6-9. The dimensionless ratio $V/\sqrt{Lg}$, called Froude number, is a measure of similarity between the shapes of the waves produced by a ship model and by its prototype. A 500 ft long cargo ship is designed to run at 20 knots, and a 5 ft. geometrically similar model is towed in a water channel to study the wave resistance. What should be the towing speed?

6-10. The torque due to the frictional resistance of the oil film between a rotating shaft and its bearing is found to be dependent on the force F normal to the shaft, the speed of rotation N of the shaft, the dynamic viscosity μ of the oil, and the shaft diameter D. Establish a correlation between the variables by using dimensional analysis. *Ans.* $[T/(F^3/N\mu)^{1/2} = \phi(N\mu D^2/F)$

6-11. When a sphere falls freely through a homogeneous fluid, it reaches a terminal velocity at which the weight of the sphere is balanced by the buoyant force and the frictional resistance of the fluid. Make a dimensional analysis of this problem and indicate how experimental data for this problem could be correlated. Neglect compressibility effects and the influence of surface roughness.

6-12. Experiments have been performed on the temperature distribution in a homogeneous long cylinder (0.40 ft diameter, thermal conductivity of 0.12 Btu/hr ft F) with uniform internal heat generation. By dimensional analysis determine the relation between the steady-state temperature at the center of the cylinder T_c, the diameter, the thermal conductivity, and the rate of heat generation. Take the temperature at the surface as your datum. What is the equation for the center temperature if the difference between center and surface temperature is 80 F when the heat generation rate is 960 Btu/hr cu ft?

6-13. Experimental data for the transient cooling of a thick slab are to be correlated by dimensional analysis. The temperature of the slab is originally uniform at T_o. At time $\theta = 0$, the temperature at face $x = 0$ is suddenly lowered to T_s. Thermocouples are imbedded at various depths. Determine dimensionless groups relating T_x, the temperature at x, to the cooling time θ.

6-14. The convection equations relating the Nusselt, Reynolds, and Prandtl numbers can be rearranged to show that for gases the heat-transfer coefficient $\bar{h}_x$ depends on the absolute temperature T and the group $\sqrt{u_\infty/x}$. This formulation is of the form $\bar{h}_x = CT^n\sqrt{u_\infty/x}$, where n and C are constants. Indicate clearly how such a relationship could be obtained for the laminar flow case from $\mathrm{Nu}_x = 0.332\,\mathrm{Re}_x^{0.5}\,\mathrm{Pr}^{0.333}$ for the condition $0.5 < \mathrm{Pr} < 5.0$. State restrictions on method if any such restrictions are necessary.

6-15. Experimental pressure-drop data obtained in a series of tests in which water was heated while flowing through an electrically heated tube of 0.527 in. ID, 38.6 in. long, are tabulated below.

Mass Flow Rate m (lb/sec)	Fluid Bulk Temperature T_b (F)	Surface Temperature T_s (F)	Pressure Drop with Heat Transfer Δp_{ht} (psi)
3.04	90	126	9.56
2.16	114	202	4.74
1.82	97	219	3.22
3.06	99	248	8.34
2.15	107	283	4.45

Isothermal pressure-drop date for the same tube are given in terms of the dimensionless friction coefficient $f = (\Delta p/\rho V^2)(D/2L)g_c$ and the Reynolds number based on the pipe diameter, $\mathrm{Re}_D = VD/\nu$ below.

Re_D	1.71×10^5	1.05×10^5	1.9×10^5	2.41×10^5
f	0.00472	0.00513	0.00463	0.00445

By comparing the isothermal with the nonisothermal friction coefficients at similar bulk Reynolds numbers, derive a dimensionless equation for the nonisothermal friction coefficients in the form

$$f = \text{constant} \times \mathrm{Re}_D^{\,n}(\mu_s/\mu_b)^m$$

where μ_s = viscosity at surface temperature;
μ_b = viscosity at bulk temperature;
n and m = empirical constants.

6-16. Tabulated below are some experimental data obtained by heating *n*-butyl alcohol at a bulk temperature of 60 F while flowing over a heated flat plate (1 ft long, 3 ft wide, surface temperature of 140 F). Correlate the experimental data by appropriate dimensionless numbers and compare the line which best fits the data with Eq. 6-30.

Velocity (fps)	0.26	1.0	1.6	3.74
Unit-Surface Conductance (Btu/hr sq ft F)	11.4	23	34.6	69

6-17. Tabulated below are reduced test data from measurements made to determine the heat-transfer coefficient inside tubes at Reynolds numbers only slightly above transition and at relatively high Prandtl numbers (as associated with oils). Tests were made in a double-tube exchanger with a counterflow of water to provide the cooling. The pipe used to carry the oils was $\frac{5}{8}$-in. OD, 18 BWG, 121 in. long. Correlate the data in terms of appropriate dimensionless parameters.

Test No.	Fluid	$\bar{h}_c$	ρV	c_p	k	μ_b	μ_f
11	10C oil	87.0	1,072,000	0.471	0.0779	13.7	19.5
19	10C oil	128.2	1,504,000	0.472	0.0779	13.3	19.1
21	10C oil	264.8	2,460,000	0.486	0.0776	9.60	14.0
23	10C oil	143.8	1,071,000	0.495	0.0773	7.42	9.95
24	10C oil	166.5	2,950,000	0.453	0.0784	23.9	27.3
25	10C oil	136.3	1,037,000	0.496	0.0773	7.27	11.7
36	1488 pyranol	140.7	1,795,000	0.260	0.0736	12.1	16.9
39	1488 pyranol	133.8	2,840,000	0.260	0.0740	23.0	29.2
45	1488 pyranol	181.4	1,985,000	0.260	0.0735	10.3	12.9
48	1488 pyranol	126.4	3,835,000	0.260	0.0743	40.2	53.5
49	1488 pyranol	105.8	3,235,000	0.260	0.0743	39.7	45.7

where $\bar{h}_c$ = mean surface heat-transfer coefficient, based on the mean temperature difference, Btu/hr sq ft F;
ρV = mass velocity, lb_m/hr sq ft;
c_p = specific heat, Btu/lb_m F;
k = thermal conductivity, Btu/hr ft F (based on average bulk temperature);
μ_b = viscosity, based on average bulk (mixed mean) temperature, lb_m/hr ft;
μ_f = viscosity, based on average film temperature, lb_m/hr ft.

Hint: Start by correlating $\overline{\mathrm{Nu}}$ and Re_D irrespective of the Prandtl numbers, since the influence of the Prandtl number on the Nusselt number is expected to be relatively small. By plotting $\overline{\mathrm{Nu}}$ vs. Re on log-log paper, one can guess the nature of the correlation equation, $\overline{\mathrm{Nu}} = f_1(\mathrm{Re})$. A plot of $\overline{\mathrm{Nu}}/f_1(\mathrm{Re})$ vs. Pr will then reveal the dependence upon Pr. For the final equation, the influence of the viscosity variation should also be considered.

One possible answer: $$\overline{\mathrm{Nu}}_D = 0.0067 \frac{\rho V D}{\mu_b} \left(\frac{c_p \mu_b}{k_b}\right)^{0.2} \left(\frac{\mu_b}{\mu_f}\right)^{0.3}$$

6-18. The average friction coefficient for flow over a 2-ft-long plate is 0.01. What is the value of the drag force in lb_f per foot width of the plate for the following fluids: (a) air at 60 F, (b) steam at 212F and 15 psia, (c) water at 100 F, (d) mercury at 200 F, and (e) ethyl alcohol at 212F?

6-19. The average Nusselt number for flow over a 2-ft-long plate is 100. What is the value of the average surface conductance for the following fluids: (a) air at 60 F, (b) steam at 212 F and 15 psia, (c) water at 100 F, and (d) mercury at 200 F, and (e) ethyl alcohol at 212 F.

6-20. Plot the velocity and temperature distributions in the laminar boundary layer for air at 60 F flowing over a flat plate at $Re_x = 10^4$ if the free-stream velocity is 1.0 fps and the surface temperature is 160 F using (a) the Blasius solution, (b) an assumed straight line, and (c) a cubic parabola.

6-21. Hydrogen at 60 F and at a pressure of 1 atm is flowing along a flat plate at a velocity of 10 fps. If the plate is 1 ft wide and at 160 F, calculate the following quantities at $x = 1$ ft and at the distance corresponding to the transition point, i.e., $Re_x = 5 \times 10^5$. (Take properties at 110 F.)

a) Hydrodynamic boundary layer thickness, in inches.
b) Local friction coefficient, dimensionless.
c) Average friction coefficient, dimensionless.
d) Drag force, in lb_f.
e) Thickness of thermal boundary layer, in inches.
f) Local convective-heat-transfer coefficient, in Btu/hr sq ft. F.
g) Average convective-heat-transfer coefficient, in Btu/hr sq ft F.
h) Rate of heat transfer, in Btu/hr.

6-22. Repeat Prob. 6-21 for $x = 10$ ft and $u_\infty = 200$ fps, (a) taking the laminar boundary layer into account and (b) assuming that the turbulent boundary layer starts at the leading edge.

6-23. Determine the rate of heat loss in Btu/hr from the wall of a building in a 10-mph wind blowing parallel to its surface. The wall is 80 ft long, 20 ft high, its surface temperature is 80 F, and the temperature of the ambient air is 40 F.

6-24. Plot the local heat-transfer coefficient as a function of length for air at 1000 F flowing over a 5-ft-long flat plate at 3000 F with a velocity of 100 fps.

6-25. A spacecraft heat exchanger is to operate in a nitrogen atmosphere at a pressure of about 1.5 psia and 100 F. For a flat-plate heat exchanger designed to operate on earth in a standard atmosphere of 14.7 psi and 100 F in turbulent flow, estimate the ratio of heat-transfer coefficients on the earth to that in nitrogen assuming forced circulation cooling of the plate surface at the same velocity in both cases.

6-26. A thin flat plate 6 in. square is suspended from a balance into a uniformly flowing stream of glycerin in such a way that the glycerin flows parallel to and along the top and bottom surfaces of the plate. The total drag on the plate is measured and found to be 13 lb_f. If the glycerin flows at the rate of 50 fps and is at a temperature of 112 F, what is the heat-transfer coefficient $\bar{h}_c$ in Btu/hr sq ft F?

6-27. Mercury at 60 F flows over and parallel to a flat surface at a velocity of 10 fps. Calculate the thickness of the hydrodynamic boundary layer at a distance 12 in. from the leading edge of the surface.

6-28. A thin flat plate 6 in. square is tested for drag in a wind tunnel with air at 100 fps, 14.7 psia, and 60 F flowing across and parallel to the top and bottom surfaces. The observed total drag force is 0.0150 lb. Calculate the rate of heat transfer from this plate when the surface temperature is maintained at 250 F. Neglect radiation. *Ans.* 370 Btu/hr

6-29. Mercury at 60 F flows parallel to the short side of a thin flat smooth plate with a velocity of 1 ft/sec. The plate is 6 in. wide and 1 ft long and its surface temperature is 160 F. Find:

a) the local friction coefficient at the middle point of the plate, and the total drag force on the plate
b) the temperature of the mercury at a point 4 in. from the leading edge and 0.05 in. from the surface of the plate
c) the Nusselt number at the end of the plate.

6-30. Water at a velocity of 8 ft/sec flows parallel to the surface of a 3-ft-long horizontal, smooth and thin flat plate. Determine the local thermal and hydrodynamic boundary-layer thicknesses, and the local friction coefficient, at the midpoint of the plate. What is the rate of heat transfer from the plate to the water per ft width of the plate, if the surface temperature is kept uniformly at 300 F, and the temperature of the main water stream is 60 F?

6-31. A thin flat plate is placed in an atmospheric pressure air stream flowing parallel to it at a velocity of 15 ft/sec. The temperature at the surface of the plate is maintained uniformly at 400 F, and that of the main air stream is 70 F. Calculate the temperature and horizontal velocity at a point 1 ft from the leading edge and 0.03 in. above the surface of the plate. *Ans.* 340.5 F

6-32. Find the horizontal component of the force required to hold in position in the air stream the plate of Problem 31. Consider only 1 ft length of the plate measured along the leading edge, and assume the plate to be 2 ft wide.

6-33. The surface temperature of a thin flat plate located parallel to an air stream is 196 F. The free stream velocity is 200 ft/sec and the temperature of the air is 32 F. The plate is 24 in. wide and 18 in. long in the direction of the air stream. Neglecting the end effect of the plate and assuming that the flow in the boundary layer changes abruptly from laminar to turbulent at a transition Reynolds number of $N_{\mathrm{Re}_{tr}} = 4.10^5$, find:

a) the average heat transfer coefficient in the laminar and turbulent regions
b) the rate of heat transfer for the entire plate, considering both sides
c) the average friction coefficient in the laminar and turbulent regions
d) the total drag force.

Also, plot the heat transfer coefficient and local friction coefficient as a function of the distance from the leading edge of the plate.
[*Ans.* a) 15.9, 50.4 Btu/ft^2 hr F; b) 28,340 Btu/hr; c) 0.0021, 0.0041; d) 0.934 lb$_f$]

6-34. The thickness of the laminar sublayer has been estimated to be given by $y\sqrt{\tau_s/\rho}/\nu = 5.0$. Compare this estimate with the experimental data shown in Fig. 6-20.

6-35. The boundary-layer-displacement thickness δ^* is defined as the distance by which a plane surface, past which a fluid is flowing, would have to be shifted into the stream to obtain the same flow rate with an inviscid fluid as with the real fluid. Mathematically δ^* is defined by the equation

$$\delta^* = \int_0^\infty \left(1 - \frac{u}{u_\infty}\right) dy$$

Show that $\delta^* \simeq \delta/3$ for laminar flow past a flat plate.

6-36. Assuming a linear velocity distribution and a linear temperature distribution in the boundary layer over a flat plate, derive a relation between the thermal and hydrodynamic boundary-layer thicknesses and the Prandtl number.

6-37. Derive the integral momentum boundary-layer equation for steady incompressible two-dimensional flow over a flat porous wall through which fluid is injected with a velocity v_o normal to the surface.

6-38. Assuming a velocity distribution of the type $u = a + by + cy^2$, derive by means of the integral method for flow over a flat plate a relation between the boundary-layer thickness and the Reynolds number.

6-39. Show that the energy equation (Eq. 6-21) can be expressed in the form

$$\rho u c_p \frac{\partial T}{\partial x} + \rho v c_p \frac{\partial T}{\partial y} = \frac{u}{g_c}\frac{\partial p}{\partial x} + k\frac{\partial^2 T}{\partial y^2} + \frac{\mu}{g_c}\left(\frac{\partial u}{\partial y}\right)^2$$

Hint: Multiply Eq. 6-16 by u and subtract the resulting expression from Eq. 6-21

6-40. A fluid at temperature T_∞ is flowing at a velocity u_∞ over a flat plate which is at the same temperature as the fluid for a distance x_o from the leading edge, but at a temperature T_s beyond this point. Show by means of the integral boundary-layer equations that ζ, the ratio of the thermal boundary-layer thickness to the hydrodynamic boundary-layer thickness, over the heated portion of the plate is approximately

$$\zeta \simeq \mathrm{Pr}^{-1/3}\left[1 - \left(\frac{x_o}{x}\right)^{3/4}\right]^{1/3}$$

if the flow is laminar.

Hint: Assume that the temperature distribution is a cubic parabola and use T_s as your datum to simplify the boundary conditions, i.e., let

$$T - T_s = ay + cy^3$$

Also, inspect each equation and drop those terms which are small in comparison with others. Show also that, for the partially heated plate, the Nusselt number at x, if $x > x_o$, is approximately

$$\mathrm{Nu}_x \simeq 0.33 \left(\frac{\mathrm{Pr}}{1 - (x_o/x)^{3/4}} \right)^{1/3} \mathrm{Re}_x^{1/2}$$

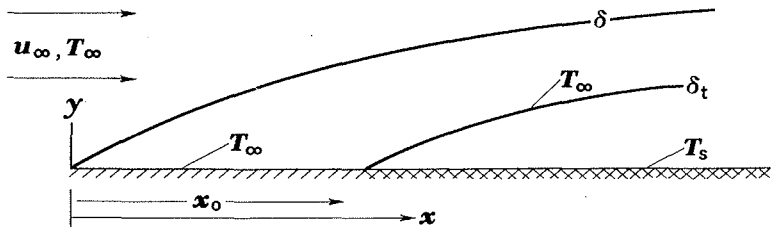

Prob. 6-40

6-41. A refrigeration truck is traveling at 50 mph on a desert highway where the air temperature is 140 F. The body of the truck may be idealized as a rectangular box, 10 ft wide, 7 ft high, and 20 ft long, at a surface temperature of 50 F. Assume that the heat transfer from the front and back of the truck may be neglected, that the stream does not separate from the surface, and that the boundary layer is turbulent over the whole surface. If, for every 12,000 Btu/hr of heat loss one ton capacity of the refrigerating unit is necessary, calculate the required tonnage of the refrigeration unit.

6-42. Wind at 50 mph is blowing in a direction parallel to the short side of the flat roof of a ranch house. The temperature at the surface of the roof is 35 F and the air temperature is −5 F. The roof measures 30 ft by 60 ft. Neglecting the end effect and assuming no separation of the air stream from the roof, calculate the heat loss through the roof.

6-43. The wing of an airplane has a polished chromium skin. At a 10,000-ft altitude it receives 200 Btu/hr sq ft by solar radiation. Assuming that the interior surface of the wing's skin is well insulated and the wing has a chord of 20-ft length, i.e., $L \simeq 20$ ft, estimate the equilibrium temperature of the wing at a flight speed of 500 fps.

6-44. A cooling fin for a heat exchanger, situated parallel to an atmospheric pressure air stream, measures 3 in. along the leading edge and 18 in. in the flow direction. Its base temperature is 190 F, and the air is at 50 F. The velocity of the air is 90 ft/sec. Determine the total drag force and the total rate of heat transfer from the fin to the air.

6-45. A 1-in.-diam, 6-in.-long transite rod (k = 0.56 Btu/hr ft F, ρ = 100 lb/cu ft, c = 0.20 Btu/lb F) on the end of a 1-in.-diam wood rod at a uniform temperature of 212 F is suddenly placed into a 60 F, 100 ft/sec air stream flowing parallel to the axis of the rod. Estimate the center line temperature of the transite rod 8 min after cooling starts. Assume radial heat conduction, but include radiation losses, based on an emissivity of 0.90, to black surroundings at air temperature.

6-46. Air at 100 fps flows between two parallel flat plates spaced 2 in. apart. Estimate the distance from the entrance where the boundary layers meet.

6-47. For Prob. 6-13 estimate the frictional pressure drop in the entrance section, taking into account the pressure drop due to the frictional drag as well as the pressure drop due to the momentum change. Assume that the velocity at the inlet is uniform and that the velocity profiles of both boundary layers can be approximated by cubic parabolas.

6-48. A preliminary design study for a nuclear moon-rocket reactor is to be made. The reactor under consideration consists of a stack of parallel flat plates which are 2 ft square, 2 in. apart, and heated to 3000 F. Gaseous hydrogen at 20-atm pressure and a temperature of 0 F enters at one end at a velocity of 200 fps and is heated as it passes between the plates. (a) Calculate the average heat-transfer coefficient assuming that transition occurs at a Reynolds number of 5×10^5. (b) Estimate the average heat-transfer coefficient assuming that a turbulence screen is placed at the entrance so that the entire boundary layer is turbulent. (c) For the turbulent flow conditions, determine the temperature of the hydrogen at the exit assuming that the surface temperature of the plate is uniformly at 3000 F. State all your assumptions clearly. (d) If the plates are $\frac{1}{10}$-in. thick and have a thermal conductivity of 10 Btu/hr ft F, determine the required rate of heat generation within the plate and the maximum temperature at the center of the plate assuming that uniform heat generation by nuclear fission occurs within the plates. (e) How many times would the hydrogen have to pass between the two plates in order to heat it to an average temperature of 2000 F?

6-49. A long plate at a uniform temperature T_1 moves at a velocity V_1 relative to a stationary insulated plate placed parallel to the moving plate at a distance h. (a) Show that the temperature of the insulated surface will exceed the temperature of the moving plate by Pr $(V_1^2/2c_p)$ if the space between the plates is filled by an ideal gas and the velocity profile of the gas is linear, and (b) derive an equation for the rate of heat transfer to each of the plates.

6-50. A flat plate is exposed to air with a temperature of 0 F, a pressure of 5 psia, and a velocity parallel to the plate of 2000 fps. How long is the laminar boundary layer, and what is the adiabatic wall temperature in the laminar region?

6-51. Air at a static temperature of 70 F and a static pressure of 0.1 psia flows at zero angle of attack over a thin electrically heated flat plate at a velocity of 800 fps. If the plate is 4-in. long in the direction of flow and 24 in. in the direction normal to the flow, determine the rate of electrical heat dissipation necessary to maintain the plate at an average temperature of 130 F.

6-52. Air at 50 F and 14.7 psia flows at 800 fps over a thermally nonconducting flat plate. What is the plate temperature 10 ft downstream from the leading edge? How much does this temperature differ from that which exists 1 in. from the leading edge?

6-53. Air at 65 F and 0.1 psia flows over a thin flat strip of metal, 1 in. long in the direction of flow, at a velocity of 900 fps. Determine (a) the surface temperature of the plate at equilibrium and (b) the rate of heat removal required per foot length if the surface temperature is to be maintained at 100 F.

6-54. An airplane model wing can be idealized as a flat plate, 2 ft long in the direction of flow and 3 ft wide. The wing is placed in an air flow at $M_\infty = 3.0$, $p_\infty = 0.05$ atm, and $T_\infty = 420$ R. Determine the temperature of this wing at a distance of 0.5 and 1.5 ft from the leading edge, if no cooling were provided, and estimate the rate at which heat must be removed from the surface of the wing to maintain its temperature at 100 F. *Ans.* 1056 and 1093 R, 5×10^4 Btu/hr

REFERENCES

1. H. Schlichting, *Boundary Layer Theory,* 6th ed. (translated by J. Kestin). (New York: McGraw-Hill Book Company, Inc., 1968.)
2. H. L. Langhaar, *Dimensional Analysis and Theory of Models.* (New York: John Wiley & Sons, Inc., 1951.)
3. E. R. Van Driest, "On Dimensional Analysis and the Presentation of Data in Fluid Flow Problems," *J. Appl. Mech.*, Vol. 13 (1940), p. A-34.
4. A. P. Colburn, "A Method of Correlating Forced Convection Heat Transfer Data and a Comparison with Fluid Friction," *Trans. Am. Inst. Chem. Engrs.*, Vol. 29 (1933), pp. 174–210.
5. W. J. King, "The Basic Laws and Data of Heat Transmission," *Mech. Eng.*, Vol. 54 (1932), pp. 410–415.
6. M. Blasius, "Grenzschichten in Flüssigkeiten mit Kleiner Reibung," *Z. Math. u. Phys.*, Vol. 56, No. 1 (1908).
7. E. Pohlhausen, "Der Wärmeaustausch zwischen festen Körpern und Flüssigkeiten mit kleiner Reibung und kleiner Wärmeleitung," *ZAMM*, Vol. 1 (1921), p. 115.
8. T. von Karman, "Über laminare und turbulente Reibung," (translation) *NACA TM* 1092, 1946.
9. E. R. G. Eckert and R. M. Drake, *Heat and Mass Transfer*, 2nd ed. (New York: McGraw-Hill Book Company, Inc., 1959.)
10. L. Prandtl, "Über die ausgebildete Turbulenz," *ZAMM*, Vol. 5 (1925), p. 136; *Proc. 2nd Int. Cong. of Appl. Mech.*, Zurich (1926).
11. S. E. Isakoff and T. B. Drew, "Heat and Momentum Transfer in Turbulent Flow of Mercury," Inst. Mech. Eng. and ASME, *Proc. General Discussion on Heat Transfer* (1951), pp. 405–409.
12. W. Forstall, Jr. and A. H. Shapiro, "Momentum and Mass Transfer in Co-axial Gas Jets," *J. Appl. Mech.*, Vol. 17 (1950), p. 399.
13. M. Hansen, "Velocity Distribution in the Boundary Layer of a Submerged Plate," *NACA TM* 585, 1930.
14. Van der Hegge-Zynen, "Measurements of the Velocity Distribution in the Boundary Layer along a Plane Surface," *Thesis*, Delft, 1924. (Delft: I. Waltman, 1924.)
15. F. Schultz-Grunow, "A New Resistance Law for Smooth Plates," *Luftfahrt Forsch.*, Vol. 17 (1940), pp. 239–246: (translation) *NACA TM* 986, 1941.
16. L. Prandtl, "Bemerkungen über den Wärmeübergang im Rohr," *Phys. Zeit.*, Vol. 29 (1928), p. 487.
17. L. Prandtl, "Eine Beziehung zwischen Wärmeaustauch and Ströhmungswiederstand der Flüssigkeiten," *Phys. Zeit.*, Vol. 10 (1910), p. 1072.
18. T. von Karman, "The Analogy between Fluid Friction and Heat Transfer," *Trans. ASME*, Vol. 61 (1939), pp. 705–711.
19. R. G. Deissler, "Investigation of Turbulent Flow and Heat Transfer in Smooth Tubes Including the Effects of Variable Properties," *Trans. ASME*, Vol. 73 (1951), pp. 101–107.

20. R. C. Martinelli, "Heat Transfer to Molten Metals," *Trans. ASME*, Vol. 69 (1947), pp. 947–959.

21. J. M. Coulson and J. V. Richardson, *Chemical Engineering*, Vol. I. (New York: McGraw-Hill Book Company, Inc., 1954).

22. K. Goldmann, "Heat Transfer to Supercritical Water and Other Fluids with Temperature Dependent Properties," *Chem. Eng. Prog. Symp. Series Nuclear Eng.*, Part 1, Vol. 50, No. 11 (1954), pp. 105–110.

23. J. G. Knudsen and D. L. Katz, "Fluid Dynamics and Heat Transfer," *Eng. Res. Bull.* 37, (Ann Arbor: Univ. of Michigan, 1953).

24. A. H. Davis, "Convective Cooling of Wires in Streams of Viscous Liquids," *Phil. Mag.*, Vol. 47 (1924), pp. 1057–1091.

25. E. L. Diret, W. James, and M. Stracy, "Heat Transmission from Fine Wires to Water," *Ind. Eng. Chem.*, Vol. 39 (1947), pp. 1098–1103.

26. R. Hilpert, "Wärmeabgabe von geheizten Drähten und Rohren," *Forsch. Gebiete Ingenieurw.*, Vol. 4 (1933), pp. 215–224.

27. D. Coles, "The Law of the Wake in the Turbulent Boundary Layer," *J. Fluid Mech.*, Vol. 1, Part 2 (1956), pp. 191–225.

28. E. R. Van Driest, "Calculation of the Stability of the Laminar Boundary Layer in a Compressible Fluid on a Flat Plate with Heat Transfer," *J. Aero. Sci.*, Vol. 19 (1952), pp. 801–813.

29. A. H. Shapiro, *The Dynamics and Thermodynamics of Compressible Fluid Flow*, Vol. 1. (New York: The Ronald Press Co., 1954).

30. S. V. Pantakar and D. B. Spalding, *Heat and Mass Transfer in Boundary Layers*, 2nd ed. London: International Textbook Co., 1970).

31. J. Kaye, "Survey of Friction Coefficients, Recovery Factors, and Heat Transfer Coefficients for Supersonic Flow," *J. Aeronautical Sci.*, Vol. 21, No. 2 (1954), pp. 117–129.

32. E. R. A. Eckert, "Engineering Relations for Heat Transfer and Friction in High-Velocity Laminar and Turbulent Boundary Layer Flow over Surface with Constant Pressure and Temperature," *Trans. ASME*, Vol. 78 (1956), pp. 1273–1284.

33. E. R. Van Driest, "Turbulent Boundary Layer in Compressible Fluids," *J. Aeronautical Sci.*, Vol. 18, No. 3 (1951), pp. 145–161.

34. A. K. Oppenheim, "Generalized Theory of Convective Heat Transfer in a Free-Molecule Flow," *J. of the Aero. Sci.*, Vol. 20 (1953), pp. 49–57.

35. W. D. Hayes and R. F. Probstein, *Hypersonic Flow Theory.* (New York, N.Y.: Academic Press, Inc., 1959.)

36. B. Gebhart, Heat Transfer (New York, N.Y.: McGraw-Hill Book Company, Inc., 2d ed., 1971.)

7
Free convection

7-1. Introduction

Free-convection heat transfer occurs whenever a body is placed in a fluid at a higher or a lower temperature than that of the body. As a result of the temperature difference, heat flows between the fluid and the body and causes a change in the density of the fluid layers in the vicinity of the surface. The difference in density leads to downward flow of the heavier fluid and upward flow of the lighter. If the motion of the fluid is caused solely by differences in density resulting from temperature gradients, without the aid of a pump or a fan, the associated heat-transfer mechanism is called *natural* or *free convection.* Free-convection currents transfer internal energy stored in the fluid in essentially the same manner as forced-convection current. However, the intensity of the mixing motion is generally less in free convection, and consequently the heat-transfer coefficients are lower than in forced convection.

Although free-convection heat-transfer coefficients are relatively low, many devices depend largely on this mode of heat transfer for cooling. In the electrical-engineering field, transmission lines, transformers, rectifiers, and electrically heated wires such as the filament of an incandescent lamp or the heating elements of an electric furnace are cooled by free convection. As a result of the heat generated internally, the temperature of these bodies rises above that of the surroundings. As the temperature difference increases, the rate of heat flow also increases until a state of

equilibrium is reached where the rate of heat generation is equal to the rate of heat dissipation.

Free convection is the dominant heat-flow mechanism from steam radiators, walls of a building, or the stationary human body in a quiescent atmosphere. The determination of the heat load on air-conditioning or refrigeration equipment requires, therefore, a knowledge of free-convection heat-transfer coefficients. Free convection is also responsible for heat losses from pipes carrying steam or other heated fluids. Recently natural convection has been proposed in nuclear-power applications to cool the surfaces of bodies in which heat is generated by fission (1).

In all of the aforementioned examples the body force responsible for the convection currents is the gravitational attraction. Gravity, however, is not the only body force which can produce free convection. In certain aircraft applications there are components such as the blades of gas turbines and helicopter ramjets which rotate at high speeds. Associated with these rotative speeds are large centrifugal forces whose magnitudes, like the gravitational force, are also proportional to the fluid density and hence can generate strong free-convection currents. Cooling of rotating components by free convection is therefore feasible even at high heat fluxes.

The fluid velocities in free-convection currents, especially those generated by gravity, are generally low, but the characteristics of the flow in the vicinity of the heat-transfer surface are similar to those in forced convection. A boundary layer forms near the surface and the fluid velocity at the interface is zero. Figure 7-1 shows the velocity and temperature distributions near a heated flat plate placed in a vertical position in air (3). At a given distance from the bottom of the plate, the local upward velocity increases with increasing distance from the surface to reach a maximum value at a distance between 0.1 and 0.2 in., then decreases and approaches zero again about 1 to 2 in. from the surface. Although the velocity profile is different from that observed in forced convection over a flat plate where the velocity approaches the free-stream velocity asymptotically, in the vicinity of the surface the characteristics of both types of boundary layer are similar. In free convection, as in forced convection, the flow may be laminar or turbulent, depending on the distance from the leading edge, the fluid properties, the body force, and the temperature difference between the surface and the fluid.

The temperature field in free convection (Fig. 7-1) is similar to that observed in forced convection. Hence, the physical interpretation of the Nusselt number presented in Sec. 6-4 applies. For practical application however, Newton's equation (Eq. 1-13)

$$dq = h_c dA\,(T_s - T_\infty)$$

is generally used. The reason for writing the equation for a differential area dA is that, in free convection, the heat-transfer coefficient h_c is not

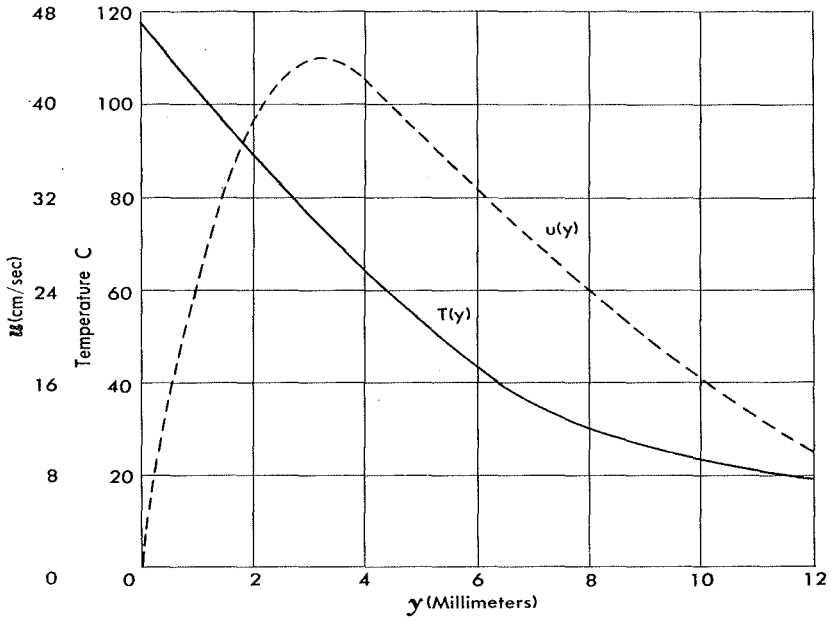

Fig. 7-1. Temperature and velocity distributions in the vicinity of a heated flat plate placed vertically in still air. (After E. Schmidt and W. Beckman, Ref. 3).

uniform over a surface. As in forced convection over a flat plate, we shall therefore distinguish between a local value of h_c and an average value $\bar{h}_c$ obtained by averaging h_c over the entire surface. The temperature T_∞ refers to a point in the fluid sufficiently removed from the body that the temperature of the fluid is not affected by the presence of a heating (or cooling) source.

An exact evaluation of the heat-transfer coefficient for free convection from the boundary layer is very difficult. The problem has only been solved for simple geometries, such as a vertical flat plate and a horizontal cylinder (3,4,19). We shall not discuss these specialized solutions here. Instead, we shall set up the differential equations for free convection from a vertical flat plate using only fundamental physical principles. From these equations, without actually solving them, we shall determine the similarity conditions and associated dimensionless moduli which correlate experimental data. In Sec. 7-3 pertinent experimental data for various shapes of practical interest will be presented in terms of these dimensionless moduli, and their physical significance will be discussed.

7-2. Similarity parameters for free convection

In the analysis of free convection we shall make use of a phenomenon observed by the Greeks over 2000 years ago and phrased by Archi-

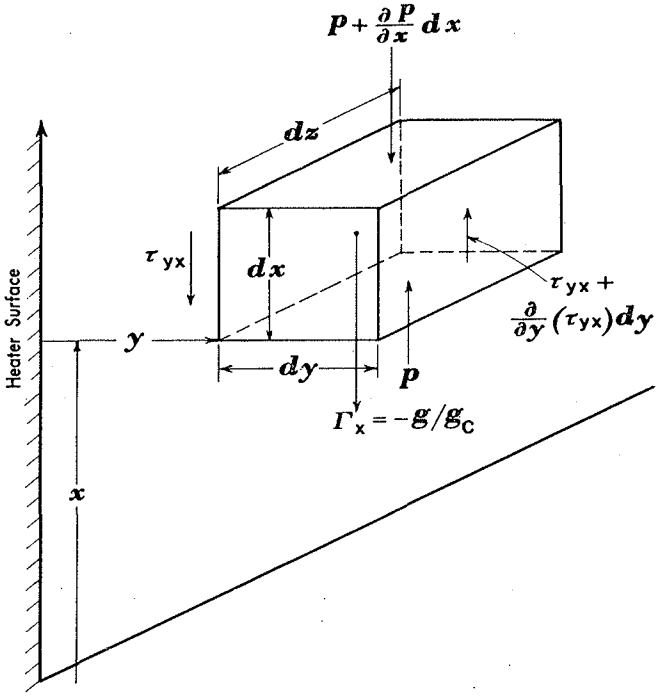

Fig. 7-2. Sketch illustrating forces acting on a fluid element in free-convection flow.

medes somewhat as follows: A body immersed in a fluid experiences a buoyant or lifting force equal to the mass of the displaced fluid. Hence, a submerged body rises when its density is less than that of the surrounding fluid and sinks when its density is greater. The buoyant effect is the driving force in free convection.

For the purpose of analysis, consider a domestic heating panel which can be idealized by a vertical flat plate, very long and wide in the plane perpendicular to the floor so that the flow is two-dimensional (Fig. 7-2). When the heater is turned off, the panel is at the same temperature as the surrounding air. The gravitational or body force acting on each fluid element is in equilibrium with the hydrostatic pressure gradient, and the air is motionless. When the heater is turned on, the fluid in the vicinity of the panel will be heated and its density will decrease. Hence, the body force (defined as the force per unit mass) on a unit volume in the heated portion of the fluid is less than in the unheated fluid. This imbalance causes the heated fluid to rise, a phenomenon which is well-known from experience. In addition to the buoyant force, there are pressure forces and also frictional forces acting when the air is in motion. Once steady-state conditions have been established, the total force on a volume element, $dxdydz$ in the positive x direction perpendicular to the floor consists of the following:

1. The force due to the pressure gradient

$$pdydz - \left(p + \frac{\partial p}{\partial x}\, dx\right) dydz = -\frac{\partial p}{\partial x}\,(dxdydz)$$

2. The body force $\Gamma_x \rho\ (dxdydz)$, where $\Gamma_x = -g/g_c$, since gravity alone is active.
3. The frictional shearing forces due to the velocity gradient

$$(-\tau_{yx})\, dxdz + \left(\tau_{yx} + \frac{\partial \tau_{yx}}{\partial y}\, dy\right) dxdz$$

Since $\tau_{yx} = \mu\,(\partial u/\partial y)/g_c$ in laminar flow, the net frictional force is

$$\left(\frac{\mu}{g_c}\,\frac{\partial^2 u}{\partial y^2}\right) dxdydz$$

Forces due to the deformation of the fluid element will be neglected in view of the low velocity.[1]

The rate of change of momentum of the fluid element is $\rho dxdydz$ $[u\,(\partial u/\partial x) + v\,(\partial u/\partial y)]$ as shown in Sec. 6-7. Applying Newton's second law to the elemental volume yields

$$\rho\left(u\,\frac{\partial u}{\partial x} + v\,\frac{\partial u}{\partial y}\right) = -g_c\,\frac{\partial p}{\partial x} - \rho g + \mu\,\frac{\partial^2 u}{\partial y^2} \qquad (7\text{-}1)$$

after canceling $dxdydz$. The unheated fluid far removed from the plate is in hydrostatic equilibrium, or $g_c(\partial p_e/\partial x) = -\rho_e g$ where the subscript e denotes equilibrium conditions. At any elevation the pressure is uniform and therefore $\partial p/\partial x = \partial p_e/\partial x$. Substituting $\rho_e g$ for $-(\partial p/\partial x)$ in Eq. 7-1 gives

$$\rho\left(u\,\frac{\partial u}{\partial x} + v\,\frac{\partial u}{\partial y}\right) = (\rho_e - \rho)g + \mu\,\frac{\partial^2 u}{\partial y^2} \qquad (7\text{-}2)$$

A further simplification can be made by assuming that the density ρ depends only on the temperature, and not on the pressure. For an incompressible fluid this is self-evident, but for a gas it implies that the vertical dimension of the body is small enough that the hydrostatic density ρ_e is

---

[1] The effects of the compression work and frictional heating are discussed in Reference 1.

constant. With these assumptions the buoyant term can be written

$$g(\rho_e - \rho) = g(\rho_\infty - \rho) = -g\rho\beta(T_\infty - T) \tag{7-3}$$

where β is the coefficient of thermal expansion, defined as

$$\beta = \frac{\rho_\infty - \rho}{\rho(T - T_\infty)} \tag{7-4}$$

For an *ideal gas* (i.e., $\rho = p/\mathcal{R}T$) the coefficient of expansion is

$$\beta = \frac{\rho_\infty/\rho - 1}{T - T_\infty} = \frac{T/T_\infty - 1}{T - T_\infty} = \frac{1}{T_\infty} \tag{7-5}$$

and

$$g\rho\beta(T_\infty - T) = -g\rho\left(\frac{T}{T_\infty} - 1\right)$$

The equation of motion for free convection is obtained finally by substituting the buoyant term as expressed by Eq. 7-3 into Eq. 7-2 and we get

$$\rho\left(u\frac{\partial u}{\partial x} + v\frac{\partial u}{\partial y}\right) = g\rho\beta(T - T_\infty) + \mu\frac{\partial^2 u}{\partial y^2} \tag{7-6}$$

Equation 7-6 is identical to the boundary-layer equation for forced convection over a flat plate except for the term $g\rho\beta(T - T_\infty)$, which appears as a result of the body force which was ignored in forced convection.

The problem now is to determine the conditions for which the velocity field in one free-convection system is similar to the velocity field in another. The boundary conditions are the same for all free-convection systems, that is the velocity is zero both at the surface and a distance far removed from the surface. Hence, dynamic similarity for different systems exists if Eq. 7-6 applies.

Let us first write Eq. 7-6 for system A as

$$\rho_A\left(u_A\frac{\partial u_A}{\partial x_A} + v_A\frac{\partial u_A}{\partial y_A}\right) = \rho_A g_A \beta_A (T - T_\infty)_A + \mu_A\frac{\partial^2 u_A}{\partial {y_A}^2} \tag{7-7}$$

Now consider another system, B, related to system A by the equations

$$u_B = C_V u_A \qquad \beta_B = C_\beta \beta_A$$
$$v_B = C_V v_A \qquad (T - T_\infty)_B = C_T(T - T_\infty)_A$$
$$x_B = C_L x_A \qquad \mu_B = C_\mu \mu_A$$
$$y_B = C_L y_A \qquad \rho_B = C_\rho \rho_A$$
$$g_B = C_g g_A$$

These equations state that a velocity in system B is equal to C_V, a velocity constant or reference quantity, times the velocity in system A; the viscosity in system B is equal to a constant C_μ times the viscosity in system A; etc. Equation 7-6 applies also to system B, or

$$\rho_B\left(u_B\frac{\partial u_B}{\partial x_B}+v_B\frac{\partial u_B}{\partial y_B}\right)=\rho_B g_B\beta_B(T-T_\infty)_B+\mu_B\frac{\partial^2 u_B}{\partial {y_B}^2} \tag{7-7a}$$

We can express the equation of motion for system B in terms of the quantities pertaining to system A by inserting the relations previously listed. Then Eq. 7-7a becomes

$$\frac{C_\rho {C_V}^2}{C_L}\left[\rho_A\left(u_A\frac{\partial u_A}{\partial x_A}+v_A\frac{\partial u_A}{\partial y_A}\right)\right]$$

$$=C_\tau C_\rho C_g C_\beta[\rho_A g_A\beta_A(T-T_\infty)_A]+\frac{C_\mu C_V}{{C_L}^2}\left[\mu_A\frac{\partial^2 u_A}{\partial {y_A}^2}\right] \tag{7-8}$$

The next step is crucial in this type of analysis and should be noted carefully. Equation 7-8, the equation of motion for system B, is identical to the equation of motion of system A if the coefficients of each of the terms in square brackets are identical. Then, the solutions of the equations of motion for both systems (the boundary conditions being similar) will be the same and the systems are said to be dynamically similar. Therefore, the dynamic similarity requirements are that

$$\frac{C_\rho {C_V}^2}{C_L}=C_T C_\rho C_g C_\beta=\frac{C_\mu C_V}{{C_L}^2} \tag{7-9}$$

To see the physical significance of Eq. 7-9, we substitute for the reference quantities (i.e., the C's), the equalities relating systems A and B in the tabulation (for instance $C_\beta=\beta_B/\beta_A$, $C_\mu=\mu_B/\mu_A$, etc.). To simplify the relationships we shall use the symbol V for the significant velocity and L for the significant length. Then we have

$$\frac{\rho_B {V_B}^2/L_B}{\rho_A {V_A}^2/L_A}=\frac{\rho_B g_B\beta_B(T-T_\infty)_B}{\rho_A g_A\beta_A(T-T_\infty)_A}=\frac{\mu_B V_B/{L_B}^2}{\mu_A V_A/{L_A}^2} \tag{7-10}$$

Any combination of terms in the above similarity equation is permissible, but only those combinations which have some physical significance are of practical use. However, it is not always obvious which of the many possibilities is most convenient and significant. Often a trial-and-error approach, with some experimental data as a guide, is required to find the right combination.

If we combine the first and the last term of Eq. 7-10 we get

$$\frac{\rho_B V_B L_B}{\mu_B} = \frac{\rho_A V_A L_A}{\mu_A} \tag{7-11}$$

which are equivalent expressions of the Reynolds number. The equality of the Reynolds numbers means that the ratios of inertia forces to frictional forces are identical at corresponding points.

Combining the second and the third term of Eq. 7-10 we obtain

$$\frac{\rho_B g_B \beta_B (T - T_\infty)_B L_B^2}{\mu_B V_B} = \frac{\rho_A g_A \beta_A (T - T_\infty)_A L_A^2}{\mu_A V_A} \tag{7-12}$$

that is, the ratios of buoyant to frictional forces are equal.

From the physical aspects of the problem we recall that the velocity of the fluid is not an independent quantity, but depends upon the buoyant driving force. Hence, we can eliminate V from Eq. 7-12 by substituting its value from the Reynolds number. We then obtain

$$\frac{\rho_B^2 g_B \beta_B (T - T_\infty)_B L_B^3}{\mu_B^2} = \frac{\rho_A^2 g_A \beta_A (T - T_\infty)_A L_A^3}{\mu_A^2} \tag{7-13}$$

The dimensionless modulus $\rho^2 g\beta(T - T_\infty)L^3/\mu^2$ *is called the Grashof number*, Gr, *and represents the ratio of buoyant to viscous forces.*[2] Consistent units are:

Engineering System				SI System			
ρ	lb_m/cu ft	L	ft	ρ	kg/cu m	L	m
μ	lb_m/sec ft	$(T - T_\infty)$	F	μ	kg/m sec	$(T - T_\infty)$	K
β	1/R	g	ft/sec^2	β	1/K	g	m/sec^2

When the buoyancy is the only driving force, the fluid velocity is determined entirely by the quantities contained in the Grashof modulus. Therefore, the Reynolds number is superfluous for free convection, and *equality of the Grashof numbers establishes dynamic similarity.*

The equation (6-23) describing the temperature field in free convection is

$$\rho c_p \left(u \frac{\partial T}{\partial x} + v \frac{\partial T}{\partial y} \right) = k \frac{\partial^2 T}{\partial y^2}$$

This equation is identical to the heat-transfer equation for forced convec-

[2]In Table A-3 the combination $\rho^2 g\beta/\mu^2$ is listed to facilitate numerical computations.

tion over a flat plate, and its derivation has been presented previously (Sec. 6-7). For similarity of temperature fields in forced convection, we found that the Prandtl numbers, $c_p\mu/k$, must be equal. This applies also to free convection. Therefore, when geometrically similar bodies are cooled or heated by free convection, both the velocity and temperature fields are similar provided Gr and Pr are equal at corresponding points. It follows also from the same arguments used in the case of forced convection that, when the Grashof and Prandtl numbers are equal, the Nusselt numbers for the bodies are the same. Hence, experimental results for free-convection heat transfer can be correlated by an equation of the type

$$\mathrm{Nu} = \phi(\mathrm{Gr})\,\psi(\mathrm{Pr}) \tag{7-14}$$

where ϕ and ψ denote functional relationships.

The Prandtl number of gases having the same number of atoms per molecule is nearly constant. For a group of gases having the same number of atoms, Eq. 7-14 can therefore be reduced to

$$\mathrm{Nu} = \phi(\mathrm{Gr}) \tag{7-15}$$

As a first approximation, data for different fluids can also be correlated on a single curve. If the velocities are sufficiently small that inertia forces can be neglected in comparison with the forces of friction and buoyancy, the left-hand side of Eq. 7-9, which represents the inertia forces, can be discarded (see Prob. 7-15). Then, the similarity condition is

$$C_\rho C_g C_\beta C_T = \frac{C_\mu C_V}{C_L^{\,2}} \tag{7-16}$$

By substituting the equality relations for systems A and B it can easily be verified that the dimensional similarity parameter is (Gr Pr). The product of Gr and Pr is called the Rayleigh number, Ra. Hence, when the inertia forces are negligible, the Nusselt number becomes a function of a single variable and we have

$$\mathrm{Nu} = \phi(\mathrm{Gr\ Pr}) \tag{7-17}$$

Using an equation of this type, experimental data from various sources for free convection from horizontal wires and tubes are correlated in Fig. 7-3 by plotting $\bar{h}_c D/k$, the average Nusselt number, against $c_p\rho^2 g\beta\Delta T D^3/\mu k$, the product of the Grashof and Prandtl numbers. The physical properties are evaluated at the arithmetic mean temperature. We observe that data for fluids as different as air, glycerine, and water are well correlated over a range of Grashof numbers from 10^{-5} to 10^7 for

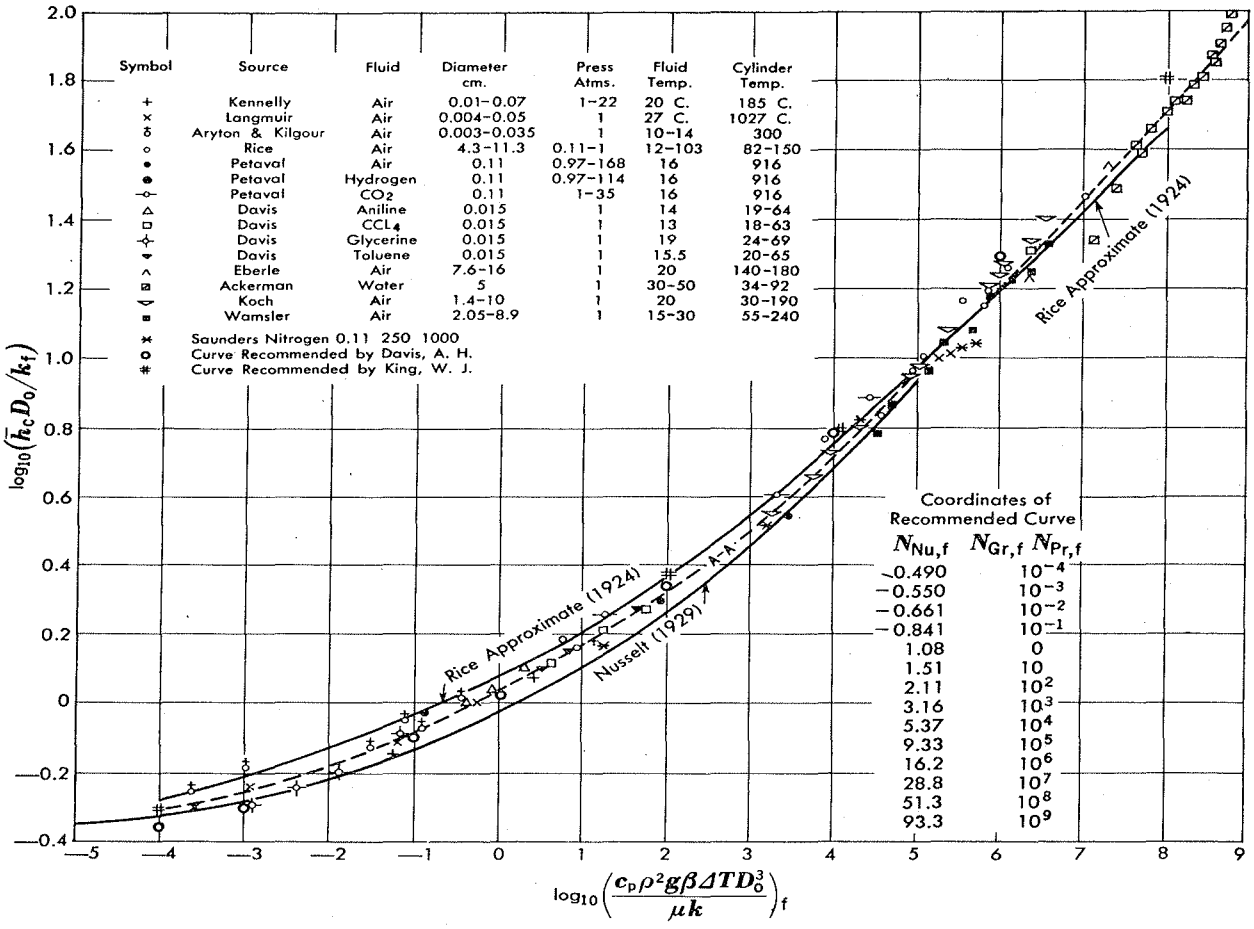

Fig. 7-3. Correlation of data for free-convection heat transfer from horizontal cylinders in gases and liquids. (By permission from W. H. McAdams, *Heat Transmission*, 3d ed., New York: McGraw-Hill Book Company Inc., 1954).

cylinders ranging from small wires to large pipes. King (9) has shown that the correlation in Fig. 7-3 gives approximate results also for three-dimensional shapes such as short cylinders and blocks if the characteristic length dimension is determined by the equation

$$\frac{1}{L} = \frac{1}{L_{\text{hor}}} + \frac{1}{L_{\text{vert}}}$$

where L_{vert} is the height and L_{hor} the average horizontal dimension of the body.

A similar correlation for free convection from vertical plates and vertical cylinders is shown in Fig. 7-4.[3] The ordinate is $\bar{h}_c L/k$, the average

[3] According to Ref. 31, a vertical cylinder of diameter D may be treated as a flat plate of height L when $D/L > 35\,\text{Gr}_L^{-1/4}$.

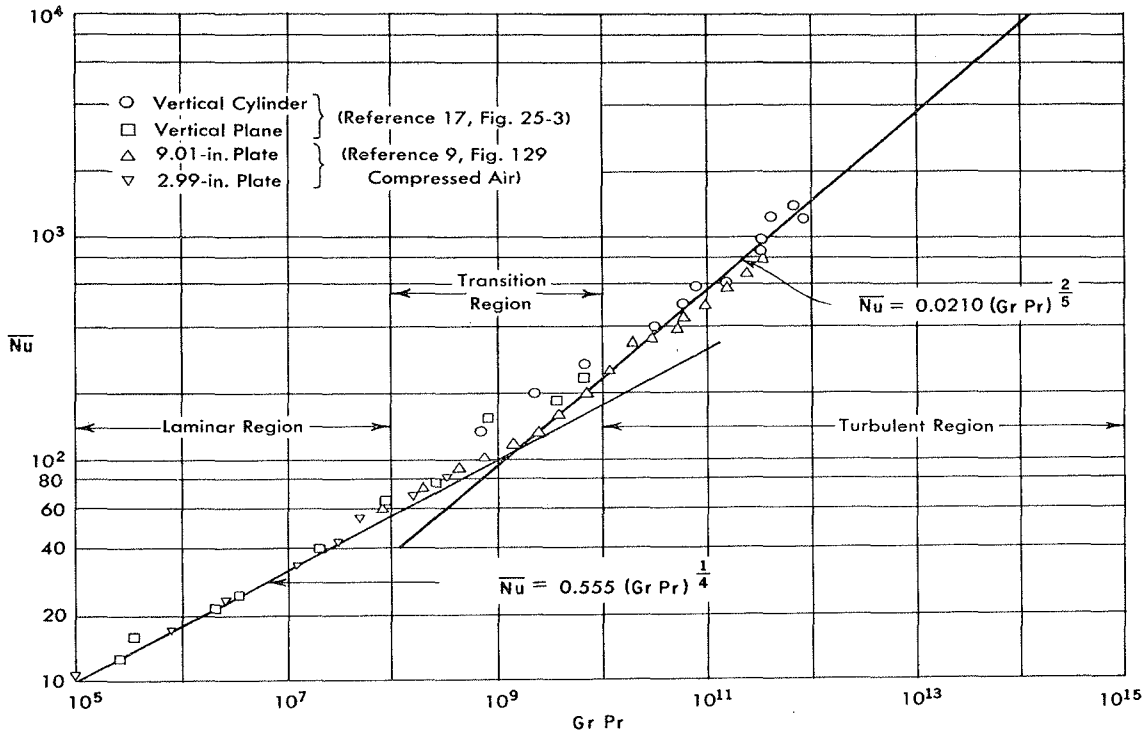

Fig. 7-4. Correlation of data for free-convection heat transfer from vertical plates and cylinders.

Nusselt number based on the height of the body, and the abscissa is the product of Gr and Pr, i.e., $c_p\rho^2\beta g\Delta TL^3/\mu k$. We note that there is a change in the slope of the line correlating the experimental data at a Grashof Number of 10^9. The reason for the change in slope is that the flow is laminar up to a Grashof number of about 10^8, passes through a transition regime between 10^8 and 10^{10}, and becomes fully turbulent at Grashof numbers above 10^{10}. This behavior of the flow is illustrated in the photographs of Fig. 7-5. These pictures show lines of constant density in free convection from a vertical flat plate to air at atmospheric pressure obtained with a *Mach-Zehnder* (6, 7) optical interferometer. This instrument produces interference fringes which are recorded by a camera. The fringes are the result of density gradients caused by temperature gradients in gases. The spacing of the fringes is a direct measure of the density distribution, which is related to the temperature distribution. Figure 7-5 shows the fringe pattern observed near a heated vertical flat plate in air, 3 ft. high and 1.5 ft. wide. We observe that the flow is laminar for about 20 in. from the bottom of the plate. Transition to turbulent flow begins at 21 in., corresponding to a critical Grashof number of about 4×10^8. Near the top of the plate, turbulent flow is approached. This type of behavior is typical of free convection on vertical surfaces, and under normal conditions the critical value of Grashof number is usually taken at 10^9.

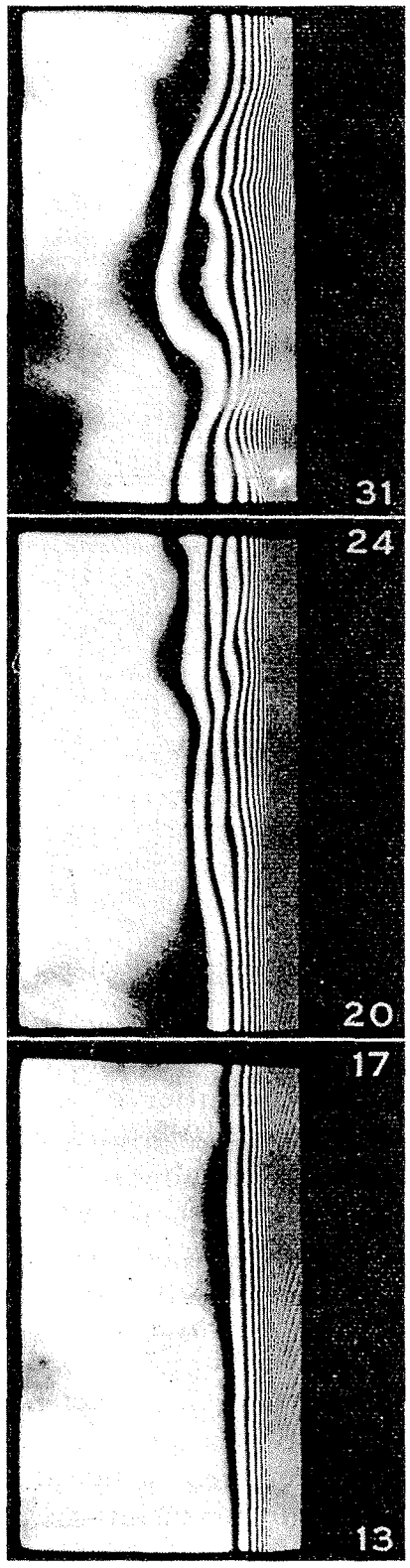

Fig. 7-5. Interference photograph illustrating laminar and turbulent free-convection flow of air along a vertical flat plate. (Courtesy of Professor E. R. G. Eckert).

When the physical properties of the fluid vary considerably with temperature and the temperature difference between the body surface T_s and the surrounding medium T_∞ is large, satisfactory results can be obtained by evaluating the physical properties in Eq. 7-14 at the mean temperature $(T_s + T_\infty)/2$. However, when the surface temperature is not known, a value must be assumed initially. It can then be used to calculate the unit-surface conductance to a first approximation. The surface temperature is then recalculated with this value of the surface conductance and if there is a discrepancy between the assumed and the calculated value of T_s, the latter is used to recalculate the heat-transfer coefficient for the second approximation.

7-3. Evaluation of unit-surface conductance

After experimental data have been correlated by dimensional analysis, it is general practice to write an equation for the line faired through the data and to compare the experimental results with those obtained by analytic means. In this section the results of some experimental studies on free convection for a number of geometric shapes of practical interest are presented. Each shape is identified by a characteristic dimension, such as its distance from the leading edge x, length L, diameter D, etc. The characteristic dimension is attached as a suffix to the dimensionless parameters Nu and Gr. Average values of the Nusselt number for a given surface are identified by a bar, i.e., $\overline{\text{Nu}}$; local values are without a bar. All physical properties are to be evaluated at the arithmetic mean between the surface temperature T_s and the temperature of the undisturbed fluid T_∞. The temperature difference in the Grashof number ΔT represents the absolute value of the difference between the temperatures T_s and T_∞. All of the equations to be discussed apply strictly to bodies immersed in an effectively infinite medium in which the flow pattern is influenced only by the body transferring the heat. The accuracy with which in practice the unit-surface conductance can be predicted from any of the equations is generally no better than 20 percent, because most experimental data scatter by as much as ± 15 percent or more and in a majority of engineering applications stray currents due to some interaction with surfaces other than the one transferring the heat are unavoidable.

Vertical planes and cylinders. The local value of the heat-transfer coefficient for laminar free convection from an isothermal vertical plate or cylinder at a distance x from the leading edge is

$$h_{cx} = 0.41 \frac{k}{x} (\text{Pr} \cdot \text{Gr}_x)^{1/4} \tag{7-18}$$

Eq. 7-18 shows that the heat transfer coefficient decreases with the distance from the leading edge to the 1/4 power. The leading edge is the lower edge for a heated surface and the upper edge for a surface cooler than the surrounding fluid. The average value of the heat-transfer coefficient for a height L is obtained by integrating Eq. 7-18 and dividing by L, or

$$\bar{h}_{cL} = \frac{1}{L}\int_0^L h_{cx}dx = 0.555_L{}^k(\mathrm{Gr}_L \cdot \mathrm{Pr})^{1/4} \qquad (7\text{-}19a)$$

In dimensionless form, the *average Nusselt number is*

$$\overline{\mathrm{Nu}}_L = \frac{\bar{h}_c L}{k} = 0.555\,(\mathrm{Gr}_L \cdot \mathrm{Pr})^{1/4} \qquad (7\text{-}19b)$$

in the range $10 < \mathrm{Gr}_L\,\mathrm{Pr} < 10^9$ (30). For a vertical plane submerged in a liquid metal ($\mathrm{Pr} < 0.03$), the average Nusselt number in laminar flow is (28)

$$\overline{\mathrm{Nu}}_L = \frac{\bar{h}_{cL} L}{k} = 0.68\,(\mathrm{Gr}_L \cdot \mathrm{Pr}^2)^{1/4} \qquad (7\text{-}19c)$$

In the turbulent region, the value of h_{cx}, the local heat-transfer coefficient, is nearly constant over the surface. In fact, McAdams (9) recommends for $\mathrm{Gr} > 10^9$ the equation

$$\overline{\mathrm{Nu}}_L = \frac{\bar{h}_c L}{k} = 0.10\,(\mathrm{Gr}_L \mathrm{Pr})^{1/3} \qquad (7\text{-}20)$$

according to which the heat-transfer coefficient is independent of the length L.

A theoretical analysis by Sparrow and Gregg (10), supported by experimental data by Dotson (11), indicates that the equations for laminar free convection from a vertical flat plate apply to a constant surface temperature as well as to a uniform heat flux over the surface. In the latter case the surface temperature T_s is to be taken at one-half of the total height of the plate. Other types of correlations for constant heat flux are presented in Refs. (33) and (34).

If a heated plane is inclined somewhat from the vertical, as shown in Fig. 7-6, the body force along the x-axis is $[g\beta(T - T_\infty)\cos\alpha]$ and the average Nusselt number for the upper surface can be obtained by using an effective Grashof number $(\rho^2 g\beta\Delta T\cos\alpha L^3/\mu^2)$ in Eqs. 7-19 or 7-20.

EXAMPLE 7-1. The maximum allowable surface temperature at the center of an electrically heated vertical plate, 6 in. high and 4 in. wide, is 270 F. Esti-

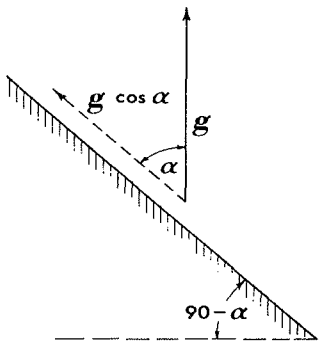

Fig. 7-6. Sketch illustrating body force acting on a fluid on or near an inclined surface.

mate the maximum rate of heat dissipation from both sides of the plate in 70 F atmospheric air if the unit-surface conductance for radiation $\bar{h}_r$ is 1.5 Btu/hr sq ft F for the specified maximum surface temperature.

Solution: The arithmetic mean temperature is 170 F and the corresponding value of Gr_L is found to be $1.2 \times 10^6 L^3 (T_s - T_\infty)$, from the last column in Table A-3 by interpolation. For the specified conditions we get

$$\mathrm{Gr}_L = (1.2 \times 10^6)(6/12)^3(200) = 3 \times 10^7$$

Since the Grashof number is less than 10^9, the flow is laminar. For air at 170 F the Prandtl number is 0.71 and GrPr is therefore 2.1×10^7. From Fig. 7-4 the average Nusselt number is 38 at GrPr of 2.1×10^7 and therefore

$$\bar{h}_c = 38 \times k_f/L = 38 \frac{0.0172}{0.5} \frac{\text{Btu/hr ft F}}{\text{ft}} = 1.31 \text{ Btu/hr sq ft F}$$

The maximum total heat-dissipation rate is therefore

$$q = A(\bar{h}_c + \bar{h}_r)(T_s - T_\infty)$$

$$= \left[\frac{(2)(6)(4)}{144} \text{ sq ft}\right] [(1.31 + 1.5) \text{ Btu/hr sq ft F}] (200 \text{ F})$$

$$= 187 \text{ Btu/hr} \qquad \textit{Ans.}$$

Note that more than half of the heat is transferred by radiation.

Horizontal plates. For square plates with a surface warmer than the surrounding medium facing upward or a cooler surface facing downward, McAdams (9) recommends the equation

$$\overline{\mathrm{Nu}}_L = \frac{\bar{h}_c L}{k} = 0.14(\mathrm{Gr}_L \mathrm{Pr})^{1/3} \qquad (7\text{-}21)$$

in the turbulent range, Gr_L from 2×10^7 to 3×10^{10}, and

$$\overline{Nu}_L = \frac{\bar{h}_c L}{k} = 0.54 (Gr_L Pr)^{1/4} \tag{7-22}$$

in the laminar range, Gr_L from 10^5 to 2×10^7, where L is length of the side of the square. For heated plates facing downward and cooled plates facing upward, the equation

$$\overline{Nu}_L = \frac{\bar{h}_c L}{k} = 0.27 (Gr_L Pr)^{1/4} \tag{7-23a}$$

is recommended (9) in the laminar range, (i.e., Gr from 3×10^5 to 3×10^{10}). Data in the turbulent range are lacking. As a first approximation, the foregoing three equations can be applied to horizontal circular disks if L is replaced by 0.9 D, where D is the diameter of the disk, and to rectangular surfaces if L is taken as the mean between the two sides.

Experimental data for a cooled circular horizontal plate facing down in a liquid metal are correlated by the relation (29)

$$\overline{Nu}_D = \frac{\bar{h}_c D}{k} = 0.26 (Gr_D Pr^2)^{0.35} \tag{7-23b}$$

Horizontal cylinders, spheres, and cones. The temperature field around a horizontal cylinder heated in air is illustrated in Fig. 7-7, which shows interference fringes photographed by Eckert and Soehnghen (7). The flow is laminar over the entire surface. The closer spacing of the interference fringes over the lower portion of the cylinder indicates a steeper temperature gradient and consequently a larger local unit-surface conductance than over the top portion. The variation of the surface conductance with angular position α is shown in Fig. 7-8 for two Grashof numbers. The experimental results do not differ appreciably from the theoretical calculations of Herman (4) who derived the equation

$$Nu_{D\alpha} = 0.604 Gr_D^{1/4} \phi(\alpha) \tag{7-24}$$

for air, i.e., Pr = 0.74. The angle α is measured from the horizontal position and numerical values of the function $\phi(\alpha)$ are as follows:

α	−90	−60	−30	0	30	60	75	90
$\phi(\alpha)$	0.76	0.75	0.72	0.66	0.58	0.46	0.36	0
	Bottom half			Top half				

An equation for the average heat-transfer coefficient from single horizontal wires or pipes in free convection, recommended by McAdams (9)

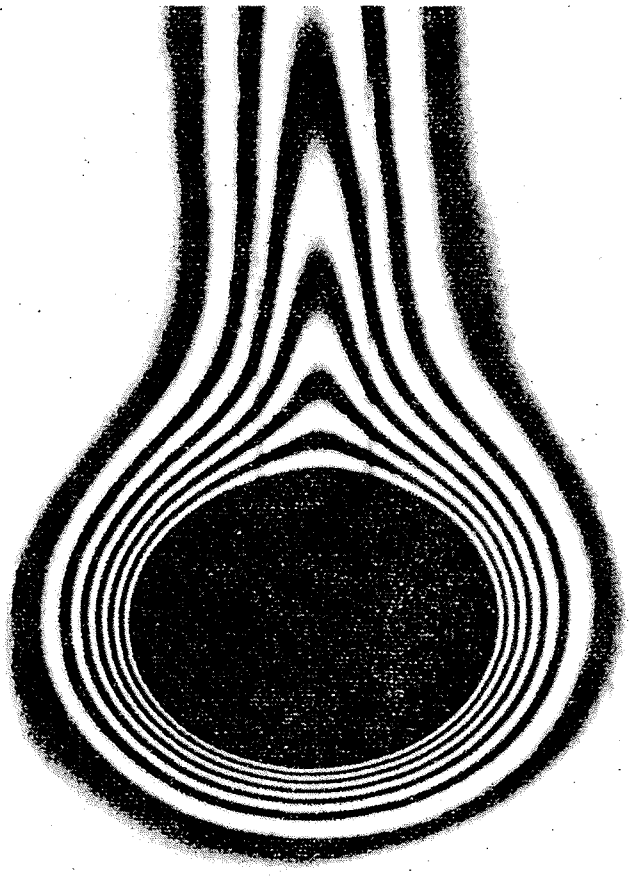

Fig. 7-7. Interference photograph illustrating temperature field around a horizontal cylinder in laminar flow. (Courtesy of Professor E. R. G. Eckert).

on the basis of the experimental data in Fig. 7-3, is

$$\overline{\mathrm{Nu}}_D = 0.53\,(\mathrm{Gr}_D\,\mathrm{Pr})^{1/4} \tag{7-25}$$

This equation is valid for Prandtl numbers larger than 0.5 and Grashof numbers ranging from 10^3 to 10^9. For very small diameters, Langmuir has shown that the rate of heat dissipation per unit length is nearly independent of the wire diameter, a phenomenon he applied in his invention of the coiled filaments in gas-filled incandescent lamps. The average unit-surface conductance for Gr_D less than 10^3 is most conveniently evaluated from the curve A–A drawn through the experimental points in Fig. 7-3 in the low Grashof-number range.

The onset of turbulence in free-convection flow over horizontal cylinders for fluids other than liquid metals occurs at a value of $\mathrm{Gr}_D\,\mathrm{Pr}/D^3$ of about 10^{11} (12). In turbulent flow it has been observed (12) that the heat flux can be increased substantially without a corresponding

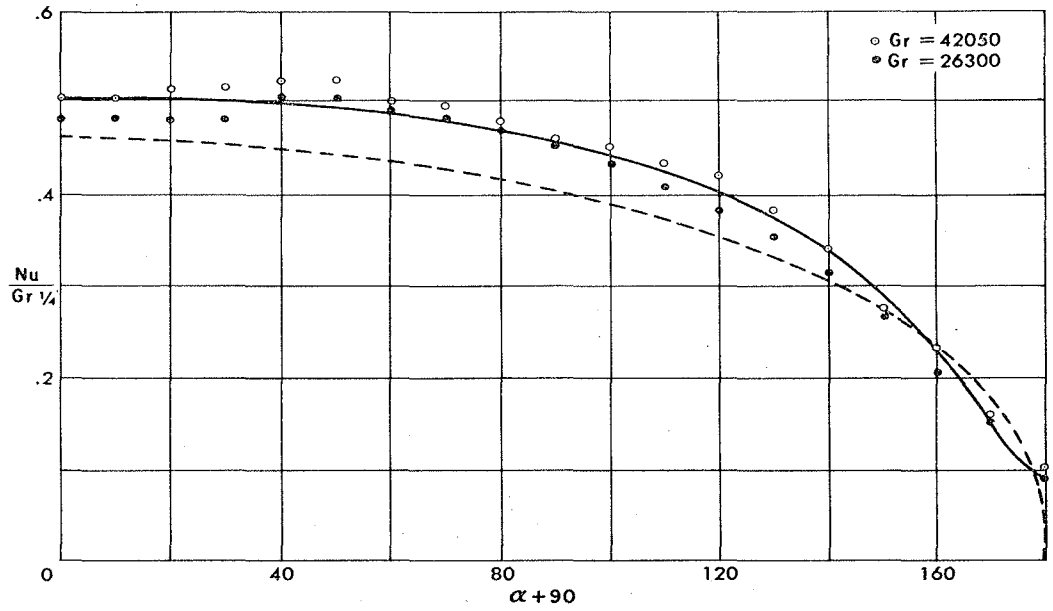

Fig. 7-8. Local dimensionless unit-surface conductance along the circumference of a horizontal cylinder in laminar free convection (dashed line according to Ref. 4). (Courtesy of U.S. Air Force, from "Studies on Heat Transfer in Laminar Free Convection with the Zehnder-Mach Interferometer," by E. R. G. Eckert and E. E. Soehngen, Ref. 7).

increase in the surface temperature. It appears that in free convection the turbulent-exchange mechanism increases in intensity as the rate of heat flow is increased and thereby reduces the thermal resistance.

Simplified equations for horizontal cylinders at moderate surface temperatures are given in Reference 9 *for air* at atmospheric pressure. They are

$$\bar{h}_c = 0.18\,\Delta T^{1/3} \tag{7-26}$$

for Gr_D from 10^9 to 10^{12}, and

$$\bar{h}_c = 0.27\left(\frac{\Delta T}{D}\right)^{1/4} \tag{7-27}$$

for Gr_D from 10^3 to 10^9, where $\bar{h}_c$ is in Btu/hr sq ft F and ΔT is in F.

For *liquid metals* in laminar flow the equation

$$\overline{\mathrm{Nu}}_D = 0.53\,(\mathrm{Gr}_D\,\mathrm{Pr}^2)^{1/4} \tag{7-28}$$

correlates the available data (12) for horizontal cylinders.

For *free convection to or from spheres* of diameter D the empirical equation

$$\overline{\mathrm{Nu}}_D = 2 + 0.45(\mathrm{Gr}_D \cdot \mathrm{Pr})^{1/4} \tag{7-29}$$

is recommended (35). For very small spheres, as the Grashof number approaches zero, the Nusselt number approaches a value of 2, i.e. $(\bar{h}_c D/k) \rightarrow 2$. This condition corresponds to pure conduction through a stagnant layer of fluid surrounding the sphere.

EXAMPLE 7-2. A $1\frac{1}{2}$-in. OD pipe carrying slightly wet steam at 15 psig is installed in a location where it is covered by water after a heavy rain but is exposed to air under normal conditions. Compare the rate of heat transfer to air with the rate of heat transfer to water, assuming that both fluids are at 50 F.

Solution: From steam tables we find that the temperature of the steam at 15 psig is 250 F. Assuming that the pipe temperature equals the steam temperature because the heat-transfer coefficient inside the pipe is large (Table 1-2), the mean film temperature is 150 F. From Table A-3, the product of the Grashof and Prandtl numbers is

$$\mathrm{Gr}_D\mathrm{Pr} = (1.2 \times 10^9)(200)\left(\frac{1.50}{12}\right)^3 = 4.7 \times 10^8 \qquad \text{for water}$$

$$\mathrm{Gr}_D\mathrm{Pr} = (0.85 \times 10^6)(200)\left(\frac{1.5}{12}\right)^3 = 3.3 \times 10^5 \qquad \text{for air}$$

From Fig. 7-3 the respective Nusselt numbers are therefore

$$\overline{\mathrm{Nu}}_D = 77 \qquad \text{for water}$$

$$\overline{\mathrm{Nu}}_D = 12.6 \qquad \text{for air}$$

The respective heat-transfer coefficients are therefore

$$\bar{h}_c = \mathrm{Nu}\,\frac{k}{D} = 77\,\frac{0.384\ \mathrm{Btu/hr\ ft\ F}}{1.5/12\ \mathrm{ft}} = 23.6\ \mathrm{Btu/hr\ sq\ ft\ F} \qquad \text{for water}$$

$$\bar{h}_c = 12.6\,\frac{0.0164}{1.5/12} = 1.66\ \mathrm{Btu/hr\ sq\ ft\ F} \qquad \text{for air}$$

The rate of heat loss by convection per foot length of pipe is therefore

$$q_c = \bar{h}_c A(T_s - T_\infty) = (236)\,\pi\,(1.5/12)(200) = 18{,}500\ \mathrm{Btu/hr\ ft} \qquad \text{in water}$$

$$q_c = (1.66)\,\pi\,(1.5/12)(200) = 130\ \mathrm{Btu/hr\ ft} \qquad \text{in air}$$

There is no appreciable radiation in water, but in air the heat transfer by radiation is from Eq. 1-7.

$$q_r = (0.171)(0.9)\,\pi\,(1.5/12)\,[(7.10)^4 - (5.10)^4] = 115\ \mathrm{Btu/hr\ ft}$$

if the emissivity of the pipe is 0.9. The total heat-transfer rate in air is therefore 245 Btu/hr ft, which is only a small fraction of the heat-transfer rate when the pipe is covered by water. *Ans.*

Experimental data for free convection from vertical cones with vertex angles between 3 and 12 degrees have been correlated (36) by the equation

$$\overline{\mathrm{Nu}}_L = 0.63(1 + 0.72\epsilon)\,\mathrm{Gr}_L^{1/4}$$

where $\epsilon = \dfrac{2}{\mathrm{Gr}_L^{1/4}\tan(\phi/2)}$

ϕ = vertex angle

L = slant height of the cone.

An extensive treatment of transition and stability in natural convection systems is presented in Ref. 31.

Free convection in enclosed spaces. Empirical formulas for calculation of free-convection heat transfer in an enclosed air space between vertical walls can be presented in the following form (14):

$$\overline{\mathrm{Nu}}_\delta = \begin{cases} 0.18\,\mathrm{Gr}_\delta^{1/4}\left(\dfrac{L}{\delta}\right)^{-1/9} & \text{for } 2000 < \mathrm{Gr}_\delta < 20{,}000 \quad (7\text{-}30) \\ 0.065\,\mathrm{Gr}_\delta^{1/3}\left(\dfrac{L}{\delta}\right)^{-1/9} & \text{for } 20{,}000 < \mathrm{Gr}_\delta < 11 \times 10^6 \quad (7\text{-}31) \end{cases}$$

where Gr_δ is defined by

$$\mathrm{Gr}_\delta = \frac{\rho^2 g \beta (T_1 - T_2)\delta^3}{\mu^2} \qquad (7\text{-}32)$$

where T_1 and T_2 are the temperatures of the walls on either side of the enclosed space and δ is the thickness of the air space as shown in Fig. 7-9. The height of the air space is designated by L. It should be noted that the length in the Grashof number is the thickness of the air space. For Grashof numbers below 2000, the heat transfer is essentially all conduction, so that $\overline{\mathrm{Nu}}_\delta = 1.0$ for this region.

For free convection in horizontal air spaces the following relations are recommended (14):

$$\overline{\mathrm{Nu}}_\delta = \begin{cases} 0.195\,\mathrm{Gr}_\delta^{1/4} & \text{for } 10^4 < \mathrm{Gr}_\delta < 4 \times 10^5 \quad (7\text{-}33) \\ 0.068\,\mathrm{Gr}_\delta^{1/3} & \text{for } 4 \times 10^5 < \mathrm{Gr}_\delta \quad (7\text{-}34) \end{cases}$$

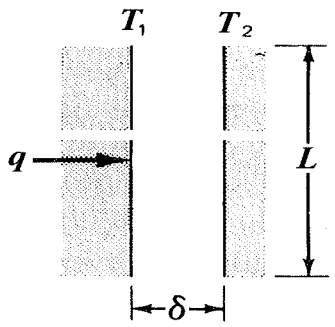

Fig. 7-9. Nomenclature for free convection in enclosed vertical spaces.

The experiments of Globe and Dropkin (27) are useful for calculation of free convection through liquids in horizontal spaces. The results of their work indicate that

$$\overline{\mathrm{Nu}}_\delta = 0.069\,\mathrm{Gr}_\delta^{1/3}\,\mathrm{Pr}^{0.407} \qquad \text{for } 3 \times 10^5 < \mathrm{Gr}_\delta \mathrm{Pr} < 7 \times 10^9 \qquad (7\text{-}35)$$

For free convection inside spherical cavities of diameter D the relation (13)

$$\frac{D\bar{h}_c}{k} = C(\mathrm{Gr}_D \cdot \mathrm{Pr})^n \qquad (7\text{-}36)$$

is recommended with the constants C and n selected from the tabulation below

$\mathrm{Gr}_D \cdot \mathrm{Pr}$	C	n
$10^4 - 10^9$	0.59	1/4
$10^9 - 10^{12}$	0.13	1/3

7-4. Convection from rotating cylinders, disks, and spheres

Heat transfer by convection between a rotating body and a surrounding fluid is of importance in the thermal analysis of shafting, flywheels, turbine rotors, and other rotating components of various machines. Convection from a heated rotating horizontal cylinder to ambient air has been studied by Anderson and Saunders (15). Turbulence begins to appear at a critical *peripheral-speed Reynolds number*, $\mathrm{Re}_\omega = \omega\pi D^2/\nu$,

of about 50, where ω is the rotational speed in rad/sec. With heat transfer the critical speed is reached when the circumferential speed of the cylinder surface becomes approximately equal to upward free-convection velocity at the side of a heated stationary cylinder.

Below the critical velocity simple free convection, characterized by the conventional Grashof number $\beta g(T_s - T_\infty) D^3/\nu^2$, controls the rate of heat transfer. At speeds greater than critical ($\mathrm{Re}_\omega > 8000$ in air) the peripheral speed Reynolds number $\pi D^2 \omega/\nu$ becomes the controlling parameter. The combined effects of the Reynolds, Prandtl, and Grashof numbers on the average Nusselt number for a horizontal cylinder rotating in air above the critical velocity can be expressed by the empirical equation (16)

$$\overline{\mathrm{Nu}}_D = \frac{\bar{h}D}{k} = 0.11\,[0.5\,\mathrm{Re}_\omega{}^2 + \mathrm{Gr}_D)\,\mathrm{Pr}]^{0.35} \tag{7-37}$$

Heat transfer from a rotating disk has been investigated experimentally by Cobb and Saunders (17) and theoretically, among others, by Millsaps and Pohlhausen (18) and Kreith and Taylor (19). The boundary layer on the disk is laminar and of uniform thickness at rotational Reynolds numbers $\omega D^2/\nu$ below about 10^6. At higher Reynolds numbers the flow becomes turbulent and the boundary layer thickens with increasing radius (see Fig. 7-10). The average Nusselt number for a disk rotating in air is (17, 20)

$$\overline{\mathrm{Nu}}_D = \frac{\bar{h}_c D}{k} = 0.35 \left(\frac{\omega r_o{}^2}{\nu}\right)^{1/2} \tag{7-38}$$

for $\mathrm{Re}_D < 5 \times 10^5$.

In the turbulent flow regime of a disk rotating in air (17), the local value of the Nusselt number at a radius r is approximately given by

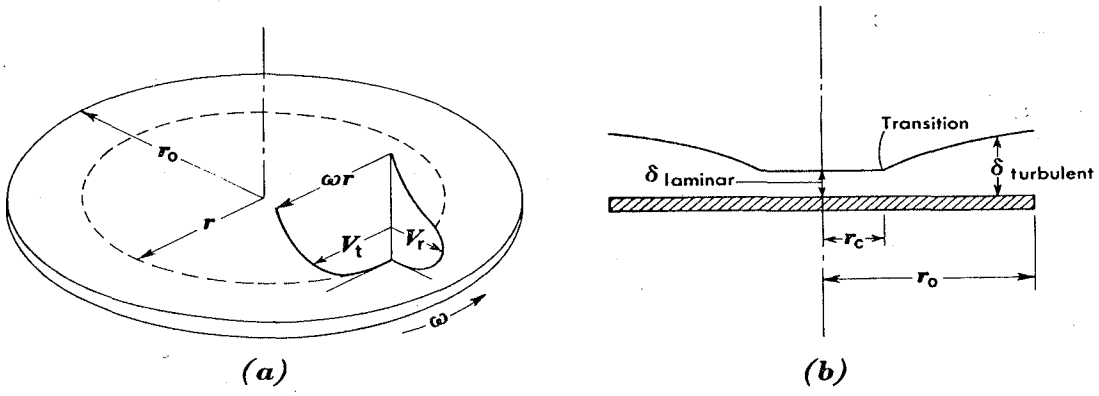

Fig. 7-10. Velocity and boundary layer profiles for a disk rotating in an infinite environment.

$$\mathrm{Nu}_r = \frac{h_c r}{k} = 0.0195\,(\omega r^2/\nu)^{0.8} \tag{7-39}$$

and the average value of the Nusselt number for laminar flow between $r = 0$ and r_c, and turbulent flow in the outer ring between $r = r_c$ and r_o is approximately

$$\overline{\mathrm{Nu}}_{r_o} = \frac{\bar{h}_c r_o}{k} = 0.015\left(\frac{\omega r_o^2}{\nu}\right)^{0.8} - 100\left(\frac{r_c}{r_o}\right)^2 \tag{7-40}$$

For a disk rotating in a fluid having a Prandtl number larger than unity, the local Nusselt number can be obtained according to Reference 21 from the equation

$$\overline{\mathrm{Nu}}_r = \frac{\mathrm{Re}_r \mathrm{Pr}\,(\sqrt{C_{Dr}/2})}{5\,\mathrm{Pr} + 5\ln(5\,\mathrm{Pr} + 1) + (\sqrt{2/C_{Dr}}) - 14} \tag{7-41}$$

where C_{Dr} is the local drag coefficient at radius r which, according to Reference 22, is given by the relation

$$\frac{1}{\sqrt{C_{Dr}}} = -2.05 + 4.07 \log_{10} \mathrm{Re}_r \sqrt{C_{Dr}} \tag{7-42}$$

For a sphere of diameter D rotating in an infinite environment with $\mathrm{Pr} > 0.7$ in the laminar flow regime ($\mathrm{Re}_D = \omega D^2/\nu < 5 \times 10^4$) the average Nusselt number ($\bar{h}_c D/k$) can be obtained from the equation

$$\overline{\mathrm{Nu}}_D = 0.43\,\mathrm{Re}_D^{0.5}\,\mathrm{Pr}^{0.4} \tag{7-43}$$

while in the Reynolds-number range between 5×10^4 and 7×10^5 the equation

$$\overline{\mathrm{Nu}}_D = 0.066\,\mathrm{Re}^{0.67}\,\mathrm{Pr}^{0.4} \tag{7-44}$$

correlates the available experimental data.

7-5. Combined forced and free convection

In Chapter 6 forced convection in flow over a flat surface was treated, and the preceding sections of this chapter dealt with heat transfer in natural-convection systems. In this section the interaction between free- and forced-convection processes will be considered.

In any heat-transfer process density gradients occur and in the presence of a force field natural-convection currents arise. If the forced-convection effects are very large, the influence of natural-convection currents may be negligible and, similarly, when the natural-convection forces are very strong, the forced-convection effects may be negligible. The questions we wish to consider now are under what circumstances can either forced or free convection be neglected and what are the conditions when both effects are of the same order of magnitude.

To obtain an indication of the relative magnitudes of free- and forced-convection effects, we consider the differential equation describing the uniform flow over a vertical flat plate with the buoyancy effect and the free-stream velocity U_∞ going in the same direction. This would be the case when the plate is heated and the flow is upward, or when the plate is cooled and the flow is downward. Taking the flow direction as x and assuming that the physical properties are uniform except for the temperature effect on the density, the Navier-Stokes boundary-layer equation for uni-dimensional flow with free convection is

$$u\frac{\partial u}{\partial x} + v\frac{\partial u}{\partial y} = -\frac{1}{\rho}\frac{\partial p}{\partial x} + \frac{\mu}{\rho}\frac{\partial\, u}{\partial y^2} + g\beta\,(T - T_\infty) \tag{7-45}$$

This equation can be generalized by a method similar to that outlined in Sec. 7-2. Substituting X for x/L, Y for y/L, Θ for $(T - T_\infty)/(T_o - T_\infty)$, P for $(p - p_\infty)/\rho U_\infty{}^2/2g_c)$, U for u/U_∞ and V for v/U_∞ in Eq. 7-45 gives

$$U\frac{\partial U}{\partial X} + V\frac{\partial U}{\partial Y} = -\frac{1}{2}\frac{\partial P}{\partial X} + \left(\frac{\mu}{\rho U_\infty L}\right)\frac{\partial^2 U}{\partial Y^2} + \left(\frac{g\beta L^3(T_o - T_\infty)}{\nu^2}\right)\frac{\nu^2}{U_\infty{}^2 L^2}\Theta \tag{7-46}$$

In the region near the surface, i.e., in the boundary layer, $\partial U/\partial X$ and U are of the order of unity. Since U changes from 1 at $x = 0$ to a very small value at $x = 1$, and u is of the same order of magnitude as U_∞, the left-hand side of Eq. 7-46 is of the order of unity. Similar reasoning indicates that the first two terms on the right-hand side as well as Θ are of the order of unity. Consequently, the buoyancy effect will influence the velocity distribution, on which, in turn, the temperature distribution depends, if the coefficient of Θ is of the order of 1 or larger, i.e., if

$$\frac{[g\beta L^3(T_o - T_\infty)]/\nu^2}{(U_\infty L/\nu)^2} = \frac{\mathrm{Gr}_L}{\mathrm{Re}_L{}^2} \simeq 1 \tag{7-47}$$

In other words, the ratio of $\mathrm{Gr}/\mathrm{Re}^2$ gives a qualitative indication of the influence of buoyancy on forced convection, and when the Grashof num-

ber is of the same order of magnitude or larger than the square of the Reynolds number, free convection effects cannot be ignored, compared to forced convection. Similarly, in a natural-convection process the influence of forced convection becomes significant when the square of the Reynolds number is of the same order of magnitude as the Grashof number.

Several special cases have been treated in the literature (24, 25, 26). For example, for laminar forced convection over a vertical flat plate Sparrow and Gregg (24) showed that for Prandtl numbers between 0.01 and 10 the effect of buoyancy on the average heat-transfer coefficient for pure forced convection will be less than 5 per cent if $\mathrm{Gr}_L \leq 0.225\,\mathrm{Re}_L{}^2$.

Acrivos (26) showed that for Prandtl numbers between 0.07 and 10, forced convection has negligible effects on natural convection from a vertical flat plate if the Grashof number is at least ten times larger than the square of the Reynolds number. In the region where both free- and forced-convection effects are of the same order of magnitude, heat transfer is increased by buoyancy effects acting in the direction of flow and decreased when acting in the opposite direction.

PROBLEMS

7-1. An empirical equation proposed by Heilman (*Trans. ASME*, Vol. 51, 1929, p. 287) for the unit-surface conductance in free convection from long horizontal cylinders to air is

$$\bar{h}_c = \frac{1.016\,(T_s - T_\infty)^{0.266}}{D^{0.2}\mathrm{T}_f{}^{0.181}}$$

The corresponding equation in dimensionless form is

$$\frac{h_c D}{k_f} = C\mathrm{Gr}_f{}^m\mathrm{Pr}_f{}^n$$

By comparing the two equations, determine those values of the constants C, m, and n in the latter equation which will give the same results as the first equation.

7-2. Consider a design for a nuclear reactor using free-convection heating of liquid bismuth. The reactor core is to be constructed of parallel vertical plates, 6 ft tall and 4 ft wide, in which heat is generated uniformly. Estimate the maximum possible heat-dissipation rate from each plate if the surface temperature of the plate is not to exceed 1600 F and the lowest allowable bismuth temperature is 600 F.

7-3. A 10-gal tank full of water at 60 F is to be heated to 120 F by means of a $\frac{3}{8}$-in. OD copper steam coil having 10 turns of 12 in. diameter. The steam is at atmospheric pressure, and its thermal resistance is negligibly small. Neglecting heat losses from the tank, estimate the heating time required.

7-4. An 8-in. diameter sphere containing liquid air (−220 F) is covered with 2-in.-thick glass wool. Estimate the rate of heat transfer to the liquid air from the surrounding air at 70 F by convection and radiation. How would you reduce the heat transfer?

7-5. A horizontal $2\frac{3}{8}$-in. OD, $2\frac{1}{16}$-in. ID steam pipe carrying saturated steam at 50 psia is covered by 1-in.-thick molded-asbestos insulation. Estimate the rate of heat loss to surrounding air at 70 F for a 100-ft length. What would be the quality of the steam at the outlet if it is saturated at the inlet? The unit-surface conductance at the steam side is 2000 Btu/hr sq ft F and the average velocity is 10 fps.

7-6. Calculate the rate of heat transfer from a 10-in. diameter sphere suspended from a fine wire in air at 70 F if the sphere is rotating at 2000 rpm and has a surface temperature of 300 F.

7-7. Estimate the rate of heat transfer by free convection and radiation across a $\frac{1}{2}$-in. air space formed between two horizontal 24-ST aluminum sheets, the upper one of which is maintained at 300 F while the lower one remains at 70 F.

7-8. Repeat Prob. 7-7 for the case in which the air space is divided in half by a very thin sheet of bright aluminum foil, placed parallel to the surface.

7-9. A vertical isothermal plate 1 ft high is suspended in an atmospheric air stream flowing at 6 fps in a vertical direction. If the air is at 60 F, estimate the plate temperature for which the free-convection effect on the heat-transfer coefficient will be less than 5 percent. *Ans.* 250 F

7-10. If the plate in Example 7-9 is at a surface temperature of 100 F, determine the maximum air velocity for which forced-convection effects on the heat-transfer coefficient are negligible. *Ans.* 0.5 fps

7-11. Starting with the equation

$$\mathrm{Nu}_D = 0.53 \left(\frac{\mathrm{Pr}^2}{0.452 + \mathrm{Pr}} \mathrm{Gr} \right)^{1/4}$$

show that, if Pr is much larger than unity,

$$\mathrm{Nu} \simeq (\mathrm{Gr}\ \mathrm{Pr})^{1/4}$$

and when Pr is much less than unity (e.g., liquid metals)

$$\mathrm{Nu} \simeq (\mathrm{Gr}\ \mathrm{Pr}^2)^{1/4}$$

7-12. Consider a thin vertical flat plate L feet high and 1 ft wide at a temperature difference between surrounding medium (Pr = 1) and plate surface of ΔT. If heat exchange is taking place by free convection in laminar flow, derive an

expression for the lifting force acting on the plate as a result of the temperature difference ΔT.

7-13. A light oil is maintained at 150 F in a 2-ft-square sump tank by ten 2-ft-long, $\frac{1}{2}$-in. OD tubes which are widely spaced and arranged horizontally in the lower third of the 6 ft tank depth. The tube surface temperature is maintained at 50 F by cooling water circulated at a high rate through the tubes. Estimate the oil cooling rate in Btu/hr if the heat-transfer area is 2.62 sq ft.

Ans. ~6500 Btu/hr

7-14. A thermocouple ($\frac{1}{32}$-in. OD) is located horizontally in a large enclosure whose walls are at 100 F. The enclosure is filled with a transparent quiescent gas which has the same properties as air. The electromotive force (emf) of the thermocouple indicates a temperature of 450 F. Estimate the true gas temperature if the emissivity of the thermocouple is 0.8.

7-15. Starting with Eqs. 7-2 and 7-6 verify the validity of Eq. 7-16 under the assumption that inertia forces are negligible.

7-16. Show from Eq. 7-39 that if $V_r = 0.162\omega r(y/\delta)^{1/7}\,[1 - (y/\delta)]$, $\delta = 0.526r(r^2\omega/\nu)^{-1/5}$ (see *ZAMM*, Vol. 1, 1921, p. 231), and $(T - T_\infty) = (T_s - T_\infty)\,[1 - (y/\delta)^{\frac{1}{7}}]$, the average Stanton number for turbulent flow of a fluid with Pr = 1 on a rotating disk of radius r_o is given by

$$\overline{\mathrm{St}} = \frac{\bar{h}_c}{c_p \rho \omega r_o} = 0.0116\,(\nu/r_o^2\omega)^{1/5}$$

7-17. A mild steel, 1-in. OD shaft, rotating in 70 F air at 20,000 rpm, is attached to two bearings, 2 ft apart. If the temperature at the bearings is 200 F, determine the temperature distribution along the shaft. HINT: Show that for high rotational speeds Eq. 7-38 approaches $\mathrm{Nu}_D = 0.076\,(\pi D^2\omega/\nu)^{0.7}$.

7-18. Estimate the rate of heat transfer from one side of a 6-ft-diameter disk rotating at 600 rpm in 70 F air, if its surface temperature is 120 F.

7-19. A 4 ft by 4 ft flat, chromeplated plate, supported horizontally on 6-ft legs, is exposed to the sun at 12 o'clock noon on May 1. If the air temperature is 80 F, (a) determine the equilibrium temperature on an average day; (b) determine the equilibrium temperature for an irradiation of 350 Btu/sq ft hr.

7-20. Estimate the equilibrium temperature of a polished aluminum plate mounted on an insulating pad when exposed on a clear day to the noon sun. The irradiation is 255 Btu/sq ft hr and the ambient temperature is 80 F. Assume that the effective sky temperature is also 80 F.

7-21. A cubical furnace having external dimensions of 20 ft on a side rests on a concrete floor. If the sides and the top are at 200 F and the surrounding air is 70 F, find the total rate of heat loss from the furnace neglecting any losses from the base to the concrete. Assume that the emissivity of the surface is 0.9.

7-22. A 1-in. OD electrical transmission line carrying 5000 amp and having a resistance of 1×10^{-6} ohms per foot of length is placed horizontally in still air at 95 F. Determine the surface temperature of the line in the steady state (a) if radiation is neglected, and (b) if radiation is taken into account. *Ans.* (a) 290 F

7-23. A flat metal plate 4 in. square is mounted in a vertical position in a milling machine. While a rotating cutter is shaping the plate, a coolant coil at 90 F (Pr = 450, $\mu = 700 \times 10^{-7}$ lb/ft sec, $\rho = 50$ lb/cu ft, $\beta = 0.38 \times 10^{-3} F^{-1}$, $k = 0.7$ Btu hr ft F) is flowing down over both sides of the plate at a velocity of 0.2 fps. If under these conditions the plate temperature is 140 F, determine the rate of heat generation due to friction by the cutting tool.

7-24. A thin sheet of galvanized iron 2 ft square is placed vertically in air at 40 F on a clear day. If the solar irradiation is 100 Btu/hr sq ft, estimate the equilibrium temperature of the plate.

7-25. The needles of conifers may be idealized as small horizontal cylinders. If a conifer needle has an average diameter of $\frac{1}{32}$ in. and is at a temperature of 90 F, estimate its rate of heat loss by free convection to air at 60 F per inch length of needle. Express your answer in calories per second.

7-26. Assuming a temperature distribution given by $(T - T_\infty)/(T_w - T_\infty) = (1 - y/\delta)^2$ and a velocity distribution given by $u/u_\infty = (y/\delta)(1 - y/\delta)^2$, show by means of the integral momentum equation that for a vertical wall at a uniform temperature of T_w, the ratio of the boundary-layer thickness to the distance from the leading edge can be expressed in the form

$$\delta/x = 3.93\,\mathrm{Pr}^{-1/2}(0.952 + \mathrm{Pr})^{1/4}\,\mathrm{Gr}_x^{-1/4}$$

and that the Nusselt number at a given distance x from the leading edge is given by the equation

$$\mathrm{Nu}_x = 0.508\,\mathrm{Pr}^{1/2}(0.952 + \mathrm{Pr})^{-1/4}\,\mathrm{Gr}_x^{1/4}$$

7-27. A 1000-watt tungsten heating element is mounted inside a 1-ft-diameter polished copper container having a spherical shape. The container is filled with argon under 2 atm pressure and is suspended in a large room filled with atmospheric air at 70 F. Estimate the temperature of the surface of the container for steady-state conditions.

7-28. An 8- by 8-ft steel sheet $\frac{1}{16}$ in. thick is removed from an annealing oven at a uniform temperature of 800 F and placed into a large room at 70 F in a horizontal position. (a) Calculate the rate of heat transfer from the steel sheet immediately after its removal from the furnace, considering both radiation and convection. (b) Determine the time required for the steel sheet to cool to a temperature of 100 F. HINT: This will require numerical integration.
Ans. (a) About 625,000 Btu/hr; (b) About 17 min

7-29. A so-called swimming-pool nuclear reactor consists of 20 parallel

vertical plates 1 ft wide and 2 ft high, spaced a distance of 2 in. apart. Calculate the power level at which the reactor may operate safely in 80 F water if the plate surface is not to exceed a temperature of 200 F. State all your assumptions.

7-30. Find the temperature at the center of a horizontal brass rod 4 in. long and $\frac{1}{4}$ in. in diameter. One end of the rod is at 100 F and the other end protrudes into air at 60 F. The total unit-surface conductance by free convection and by radiation may be assumed to be uniform over the entire surface of the rod, and the emissivity of the surface may be taken as 0.9. *Ans.* 89 F

7-31. The maximum allowable surface temperature at the center of an electrically heated vertical plate, 6 in. high and 4 in. wide, is 270 F. Estimate maximum rate of heat dissipation from both sides of the plate in 70 F atmospheric air if the unit-surface conductance for radiation heat transfer is 1.5 Btu/hr sq ft F at the maximum specified temperature.

REFERENCES

1. S. Ostrach, "New Aspects of Natural-Convection Heat Transfer," *Trans. ASME*, Vol. 75 (1953), pp. 1287–1290.
2. E. Griffith and A. H. Davis, "The Transmission of Heat by Radiation and Convection," *Special Report* 9, Food Investigation Board, British Dept. of Sci. and Ind. Res., 1922.
3. E. Schmidt and W. Beckman, "Das Temperatur und Geschwindigkeits-feld vor einer wärmeabgebenden senkrechten Platte bei natürlicher Konvection," *Tech. Mech. u. Thermodynamic*, Bd. 1, No. 10 (October, 1930), pp. 341–349; cont. Bd. 1, No. 11 (November, 1930), pp. 391–406.
4. R. Herman, "Wärmeübergang bei freier Ströhmung am wagrechten Zylinder in zwei-atomic Gasen," *VDI—Forschungsheft*, No. 379 (1936); translated in *NACA TM* 1366, November, 1954.
5. E. R. G. Eckert and T. W. Jackson, "Analysis of Turbulent Free Convection Boundary Layer on Flat Plate," *NACA Report* 1015, July, 1950.
6. E. R. G. Eckert and E. Soehnghen, "Interferometric Studies on the Stability and Transition to Turbulence of a Free-Convection Boundary Layer," *Proc. of the General Discussion on Heat Transfer* (London: ASME-IME, 1951), pp. 321–323.
7. E. R. G. Eckert and E. Soehnghen, "Studies on Heat Transfer in Laminar Free Convection with the Zehnder-Mach Interferometer," *USAF Tech. Report* 5747, December, 1948.
8. E. R. G. Eckert, *Introduction to the Transfer of Heat and Mass.* (New York: McGraw-Hill Book Company, Inc., 1951.)
9. W. H. McAdams, *Heat Transmission*, 3d ed. (New York: McGraw-Hill Book Company, Inc., 1954.)
10. E. M. Sparrow and J. L. Gregg, "Laminar Free Convection from a Vertical Flat Plate," *Trans. ASME*, Vol. 78 (1956), pp. 435–440.
11. J. P. Dotson, *Heat Transfer from a Vertical Flat Plate by Free Convection*, M. S. Thesis, Purdue University, May, 1954.
12. S. C. Hyman, C. F. Bonilla, and S. W. Ehrlich, "Heat Transfer to Liquid Metals and Non-metals at Horizontal Cylinders," *AIChE Symposium on Heat Transfer*, Atlantic City, 1953, pp. 21–33.

13. F. Kreith, "Thermal Design of High Altitude Balloons and Instrument Packages", *J. Heat Trans.*, Vol. 92 (1970), pp. 307–332.

14. M. Jacob, *Heat Transfer*, Vol. I (New York: John Wiley & Sons, Inc., 1949).

15. J. T. Anderson and O. A. Saunders, "Convection from an Isolated Heated Horizontal Cylinder Rotating About its Axis," Proc. Roy. Soc., A., Vol. 217 (1953), pp. 555–562.

16. W. M. Kays and I. S. Bjorklund, "Heat Transfer from a Rotating Cylinder with and without Cross Flow," *Trans. ASME*, ser. C, Vol. 80 (1958), pp. 70–78.

17. E. C. Cobb and O. A. Saunders, "Heat Transfer from a Rotating Disk," Proc. Roy. Soc., A., Vol. 220 (1956), pp. 343–351.

18. K. Millsap and K. Pohlhausen, "Heat Transfer by Laminar Flow from a Rotating Plate," *J. of the Aero. Sci.*, Vol. 19 (1952), pp. 120–126.

19. F. Kreith and J. H. Taylor, Jr., "Heat Transfer from a Rotating Disk in Turbulent Flow," *ASME Paper* No. 56-A-146, 1956.

20. C. Wagner, "Heat Transfer from a Rotating Disk to Ambient Air," *J. of Appl. Phys.*, Vol. 19 (1948), pp. 837–841.

21. F. Kreith, J. H. Taylor, and J. P. Chang, "Heat and Mass Transfer from a Rotating Disk," *Trans. ASME*, ser. C, Vol. 81 (1959), pp. 95–105.

22. T. Theodorsen and A. Regier, "Experiments on Drag of Revolving Disks, Cylinders, and Streamlined Rods at High Speeds," *NACA Rep.* No. 793, Washington, D.C., 1944.

23. F. Kreith, L. G. Roberts, J. A. Sullivan, and S. N. Sinha, "Convection Heat Transfer and Flow Phenomena of Rotating Spheres," *International Journal of Heat and Mass Transfer*, Vol. 6 (1963), pp. 881–895.

24. E. M. Sparrow and J. L. Gregg, "Buoyancy Effects in Forced Convection Flow and Heat Transfer," *Trans. ASME, Journal of Applied Mechanics*, Sec. E, Vol. 81 (1959), pp. 133–135.

25. Y. Mori, "Buoyancy Effects in Forced Laminar Convection Flow Over a Horizontal Flat Plate," *Trans. ASME, Journal of Heat Transfer*, Sec. C, Vol. 83 (1961), pp. 479–482.

26. A. Acrivos, "Combined Laminar Free- and Forced-Convection Heat Transfer in External Flows," *AIChE Journal*, Vol. 4 (1958), pp. 285–289.

27. S. Globe and D. Dropkin, "Natural Convection Heat Transfer in Liquids Confined by Two Horizontal Plates and Heated From Below." *Trans. ASME,* ser. C, Vol. 81 (1959), pp. 24–28.

28. O. E. Dwyer, "Liquid-Metal Heat Transfer," Chapt. 5, Sodium and NaK Supplement to the *Liquid Metals Handbook*, 1970 ed., (Washington D.C.: Atomic Energy Commission.)

29. J. S. McDonald and T. J. Connally, "Investigation of Natural Convection Heat Transfer in Liquid Sodium," *Nucl. Sci. Eng.* Vol. 8 (1960), pp. 369–377.

30. J. Gryzagoridis, "Natural Convection from a Vertical Flat Plate in the Low Grashof Number Range," *Int. J. Heat Mass Transfer*, Vol. 14 (1971), pp. 162–164.

31. B. Gebhart, *Heat Transfer, 2nd ed.*, Chapt. 8. (New York: McGraw Hill Book Co., 1970).

32. C. Y. Warner and V. S. Arpaci, "An Experimental Investigation of Turbulent Natural Convection in Air at Low Pressure along a Vertical Heated Flat Plate," *Int. J. Heat and Mass Trans.*, Vol. 11 (1968), p. 397.

33. G. C. Vliet, "Natural Convection Local Heat Transfer on Constant

Heat Flux Inclined Surfaces," *ASME Trans.*, ser. *C, J. Heat Transfer*, vol. 91 (1969), pp. 511–516.

34. G. C. Vliet and C. K. Lin, "An Experimental Study of Turbulent Natural Convection Boundary Layers,' *ASME Trans.*, ser. *C, J. Heat Transfer*, Vol. 91 (1969), pp. 517–531.

35. T. Yuge, "Experiments on Heat Transfer from Spheres Including Combined Natural and Forced Convection," *ASME Trans.*, ser. *C, J. Heat Transfer*, Vol. 82 (1960), pp. 214–220.

36. P. H. Oosthuizen and E. Donaldson, "Free Convection Heat Transfer from Vertical Cones," *Trans. ASME*, ser. *C, J. Heat Transfer*, Vol. 94 (1972), pp. 330–331.